The Role of Matrix Properties in Directing Valvular Interstitial Cell Phenotype

by

Kelly Marie Pollock Mabry

B.S., Cornell University, 2010

M.S., University of Colorado at Boulder, 2013

A thesis submitted to the

Faculty of the Graduate School of the

University of Colorado in partial fulfillment

of the requirement for the degree of

Doctor of Philosophy

Department of Chemical and Biological Engineering

2015

This thesis entitled:
The Role of Matrix Properties in Directing Valvular Interstitial Cell Phenotype
written by Kelly Marie Pollock Mabry
has been approved for the Department of Chemical and Biological Engineering

_____
Kristi S. Anseth

_____
Leslie Leinwand

Date_____

The final copy of this thesis has been examined by the signatories, and we
Find that both the content and the form meet acceptable presentation standards
Of scholarly work in the above mentioned discipline.

Abstract

Mabry, Kelly M. (Ph.D., Chemical Engineering)
Department of Chemical and Biological Engineering, University of Colorado

The Role of Matrix Properties in Directing Valvular Interstitial Cell Phenotype

Thesis directed by Professor Kristi S. Anseth

This thesis presents the development of hydrogel platforms to study the fibroblast-to-myofibroblast transition in valvular interstitial cells (VICs). These systems were used to characterize the effects of extracellular matrix cues on VICs, as well as the synergies between mechanical and biochemical signals. First, the impact of culture platform on VIC phenotype was assessed by culturing VICs in peptide-functionalized poly(ethylene glycol) hydrogels (2D and 3D) and comparing them to those cultured on tissue culture polystyrene (TCPS). Expression of the myofibroblast marker α-smooth muscle actin (αSMA), as well as by a global analysis of the transcriptional profiles[1] demonstrated that TCPS caused significant perturbations in gene expression from the native VIC phenotype. The dimensionality of the hydrogel (2D vs 3D) was particularly influential in the regulation of genes related to cell structure and motility, developmental processes, proliferation and differentiation, and transport; these findings motivated the use of 3D cultures for the following experiments.

The effect of matrix modulus, particularly matrix stiffening, on encapsulated VICs was investigated[2]. To vary the matrix modulus without dramatic changes in VIC morphology, a method was developed for in situ stiffening of cell-laden hydrogels using

sequential gelation steps. In contrast with prior findings in 2D, increased stiffness resulted in lower levels of myofibroblast activation, and suggested that stiffness alone was not sufficient to cause pathological activation of VICs to the myofibroblast phenotype in 3D. To facilitate the investigation of additional stimuli in a physiologically-relevant context, a high-throughput technique to encapsulate VICs within 3D hydrogels was developed and used to study VIC response to dynamic changes in matricellular signals[3]. A thiol-ene photoclick reaction provided temporal control over the presentation of peptide ligands to study their effects on VIC morphology and myofibroblast properties. Collectively, these studies demonstrate the ability to study and direct VIC phenotype through the temporal presentation of mechanical and biochemical cues in 3D polymer matrices.

References

1. Mabry, K. M., Payne, S. Z. & Anseth, K. S. Microarray analyses to quantify advantages of 2D and 3D hydrogel culture systems in maintaining the native valvular interstitial cell phenotype. Submitted.

2. Mabry, K. M., Lawrence, R. L. & Anseth, K. S. Dynamic stiffening of poly(ethylene glycol)-based hydrogels to direct valvular interstitial cell phenotype in a three-dimensional environment. *Biomaterials* **49,** 47–56 (2015).

3. Mabry, K. M., Schroeder, M. E., Payne, S. Z. & Anseth, K. S. Three-dimensional high-throughput cell encapsulation platform to study dynamic changes to the extracellular environment. In preparation.

Acknowledgements

I would like to thank my advisor, Kristi Anseth, for all of her help and support throughout my doctoral research. It was a great privilege to be able to learn from her these past five years. I would also like to thank my committee members, Leslie Leinwand, Stephanie Bryant, Andrew Goodwin, and Jennifer Cha for their guidance and suggestions.

Throughout the course of this work, I have had the pleasure of working with a number of talented post-doctoral researchers, graduate students, undergraduates, and high school students. I would like to acknowledge my talented collaborators, Adrianne Rosales and Megan Schroeder. Caitlin Jones, Samuel Payne, and Rosa Lawrence were also a pleasure to work with and made many contributions to the research presented in this thesis. Sharon Wang and Sarah Gould introduced me to the heart valve project and helped me get started in the lab. I am also grateful to all of the other Anseth lab members for their help and encouragement, especially Emi Tokuda, Kelly Shekiro, Jen Leight, Katie Lewis, William Wan, and Joe Grim.

Finally, I would like to thank my family for all of their support, especially my husband, Josh Mabry, and my parents, Bill and Tresa Pollock. I would not have made it here without your love and encouragement.

Contents

Tables

Table

Figures

Chapter 1

Introduction

Aortic valve disease is an important clinical problem, with aortic sclerosis affecting as many as 25% of adults over 65 years old[1]. About 2% of adults over 60 years old exhibit progression to aortic stenosis and require surgical valve replacement[2]. While aortic stenosis was originally viewed as a passive, degenerative process, it is now known that the disease is actively regulated by cells within the valve[3]. Valvular interstitial cells (VICs) are found throughout the valve and are important regulators of valve homeostasis; however, they are also responsible for much of the fibrosis that leads to aortic stenosis. While VICs are able to remodel their environment, they also receive cues from the environment, leading to complex interactions that make it difficult to elucidate the critical mechanisms of disease progression. Currently, the only treatment for aortic stenosis is the surgical replacement of the valve, which motivates this thesis research. Specifically, experiments are designed to study how VICs interact with and respond to signals in their local microenvironment with the goal of better understanding the molecular mechanisms that contribute to the pathological behavior of VICs. Ultimately, such an understanding may lead to the identification of better therapeutic targets to slow or reverse the progression of valve disease.

1.1. Aortic stenosis

Aortic stenosis is a fibrotic disease characterized by stiffened valve leaflets, obstructed blood flow, and compromised cardiac function[4]. Diagnosis of this disease is based on multiple measurements of valve function: increased peak ejection velocity, reduced effective valve orifice area, and increased mean transvalvular pressure gradient[5]. While the mitral, pulmonary, and tricuspid valves can also become dysfunctional, here we focus on the aortic valve because aortic valve disorders have a much higher mortality rate than all of the other valves combined[6]. Once a patient presents with symptoms of aortic stenosis, the average survival time without treatment is only 3-5 years[7]. Surgical replacement of the valve is the only proven treatment option, and two standard types of replacement valves exist. Mechanical valves are very durable but require the use of anticoagulants for the rest of the patient's life, while bioprosthetic valves composed of decellularized porcine, bovine, or human valves have a limited durability due to the lack of cells to maintain the extracellular matrix (ECM, Figure 1.1)[5]. Alternatively, the Ross procedure replaces the dysfunctional aortic valve with the pulmonary valve, which is in a less hemodynamically demanding position, and then a bioprosthetic valve is used to replace the pulmonary valve[8]. Improvements in minimally invasive surgery have reduced the mortality of valve replacement. Inoperable or high-risk patients can even receive transcatheter valve replacement; however, this procedure results in somewhat higher risk of aortic regurgitation[9]. Additional complications also arise in young patients, as accelerated calcification of bioprosthetic valves is associated with low recipient age[10].

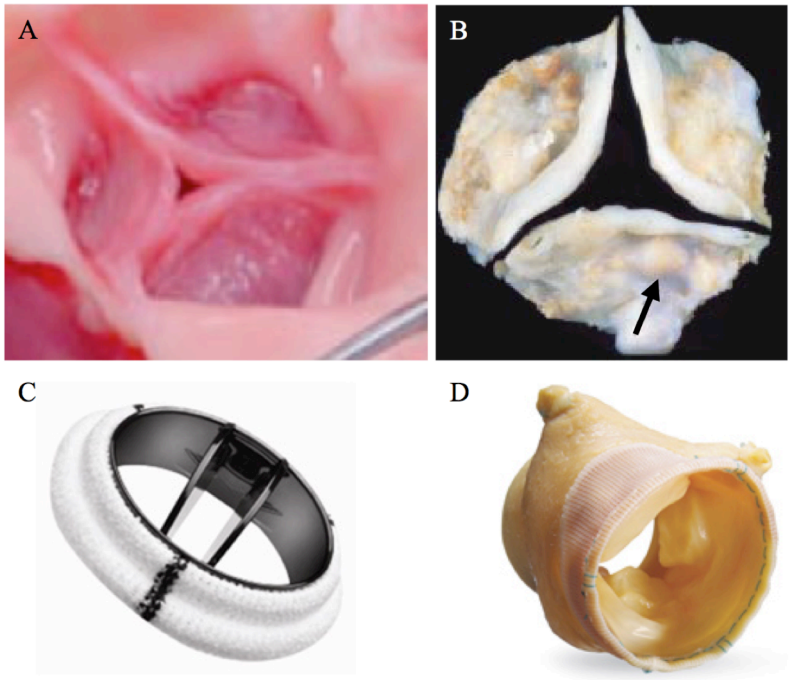

Figure 1.1. A) Healthy porcine aortic valve. B) Calcified aortic valve explanted during surgical valve replacement. Arrow indicates a calcified nodule. C) The Medtronic Open Pivot Valve, a mechanical valve replacement. D) The Medtronic Freestyle Valve, a bioprosthetic valve replacement derived from decellularized porcine tissue. Adapted from Benton, 2009[103] (A), Rajamannan *et al.*, 2003[104] (B), and www.medtronic.com (C, D).

The invasive nature of valve replacement surgery and the medical costs of around $14 billion in the US annually provide a significant incentive for the development of pharmacological treatments for aortic stenosis[5]. Unfortunately, once aortic stenosis has been diagnosed, there are no non-surgical methods to stop or slow progression of the disease. Aortic stenosis has many risk factors in common with atherosclerosis, including advanced age, hypertension, and hypercholesterolemia[11]. While only about half of patients with aortic valve disease have significant atherosclerosis, the overlap in risk factors has prompted the exploration of adapting treatments that have proven effective for atherosclerosis to the treatment of aortic stenosis[1].

Statins, or HMG-CoA reductase inhibitors, reduce plasma lipid levels and showed promise for treating aortic stenosis in *in vitro* experiments, animal studies, and retrospective clinical studies; however, prospective randomized trials did not show a benefit[12,13]. Angiotensin converting enzyme inhibitors have also been of interest due to success in treating cardiovascular diseases, but were not successful in slowing the progression of aortic stenosis in humans[14,15]. The disappointing lack of efficacy of these pharmaceutical therapeutics demonstrate the necessity of expanding our knowledge of valve biology and disease progression.

1.2. Valve structure and composition

The aortic valve is a semilunar valve composed of three cusps that helps maintain blood flow from the heart to the aorta with minimal obstruction and no regurgitation[16]. These thin, pliable cusps must open and close fully (Figure 1.2A) ~40 million times per year[16]. Each cusp has three distinct layers that together impart unique mechanical properties to the valve, as well as the durability and pliability required to maintain this functionality despite the mechanical stresses in this dynamic environment (Figure 1.2B). On the aortic side of the valve, the fibrosa provides strength with an extracellular matrix (ECM) enriched in fibrous collagen. The ventricularis is the layer on the ventricle (inflow) side of the valve and is enriched in elastin, which is organized into fibrils and oriented radially[16,17]. These layers are connected by the spongiosa, which permits the ventricularis and fibrosa to bend and deform during the opening and closing of the valve, and which is composed primarily of proteoglycans[17]. The valve also contains other ECM proteins, such as the adhesive proteins laminin and fibronectin[17].

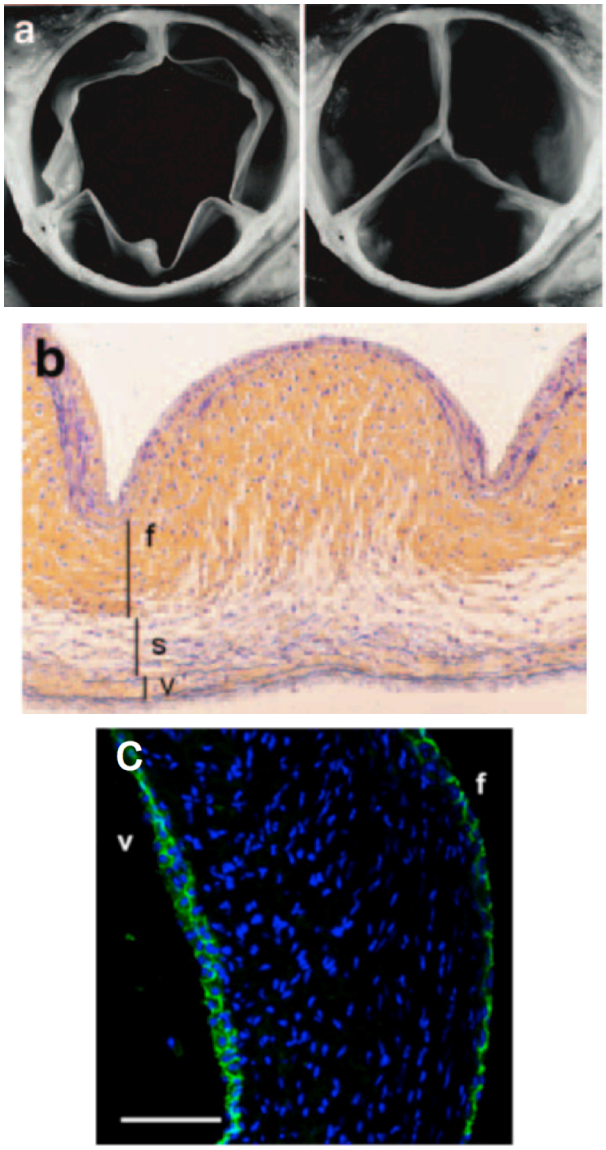

Figure 1.2. Aortic valve structure. A) The aortic valve is comprised of 3 pliable cusps that open (systole) and close (diastole) to maintain unidirection blood flow from the heart to the aorta. B) Photomicrograph of aortic valve cross-section. Each leaflet consists of 3 distinct layers: the elastin-rich ventricularis (v) on the ventricle side of the valve, the GAG-enriched spongiosa (s) in the center, and the collagen-enriched fibrosa (f) on the outflow side of the valve. Movat pentachrome stain (collagen - yellow; proteoglycan - blue; elastin and nuclei - black; cytoplasm and muscle – red), 100x magnification. C) Staining for CD31, and endothelial cell marker, shows that VICs are found throughout the valve (nuclei only), and a monolayer of VECs coat the blood-contacting surfaces (green). Scale bar = 200 μm. Images from Schoen, 2008[16] and Wang *et al.*, 2013[20].

Valvular interstitial cells (VICs) are found throughout all three layers of the valve, while the blood-contacting surfaces of the valve are covered by a layer of valvular endothelial cells (VECs)[16] (Figure 1.2C). Note that the valve cusps are largely avascular, as oxygen requirements are met by diffusion through this relatively thin (~500 μm) tissue[18]. The valve ECM is actively maintained by the resident VICs[19]. VICs are a heterogeneous population of cells consisting mostly of fibroblasts, but also containing small populations of cells that are positive for myofibroblast or progenitor cell markers[20]. VECs align perpendicularly to the direction of flow and contribute to regulation of inflammation and thromboresistance[10,21]. Additionally, VECs influence the phenotype of the VICs through paracrine signaling regulated by several mediators, including nitric oxide, endothelin, and natriuretic peptides[21–23].

1.3. The fibroblast-to-myofibroblast transition

1.3.1. The role of myofibroblasts in the body

Myofibroblasts play a critical role in remodeling and repair of numerous tissues and organs throughout the body, including skin, lung, liver, kidney, and heart. In general, the fibroblast-to-myofibroblast transition results in increased cell contractility (due to the formation of bundles containing actin and myosin), increased proliferation, and increased secretion of extracellular matrix (ECM) proteins[24]. This myofibroblast phenotype promotes wound healing, as the myofibroblasts contract the tissue and generate new ECM. Once the wound has healed, the myofibroblast population is reduced[25]. If instead the myofibroblast population persists, this pathological activation can lead to tissue fibrosis (Figure 1.3). One example of pathological fibrosis is hypertrophic scarring after a skin wound; however, persistent activation to the

myofibroblast phenotype is also associated with a wide range of fibrotic diseases, including pulmonary fibrosis, scleroderma, cirrhosis, and cardiovascular disease[26].

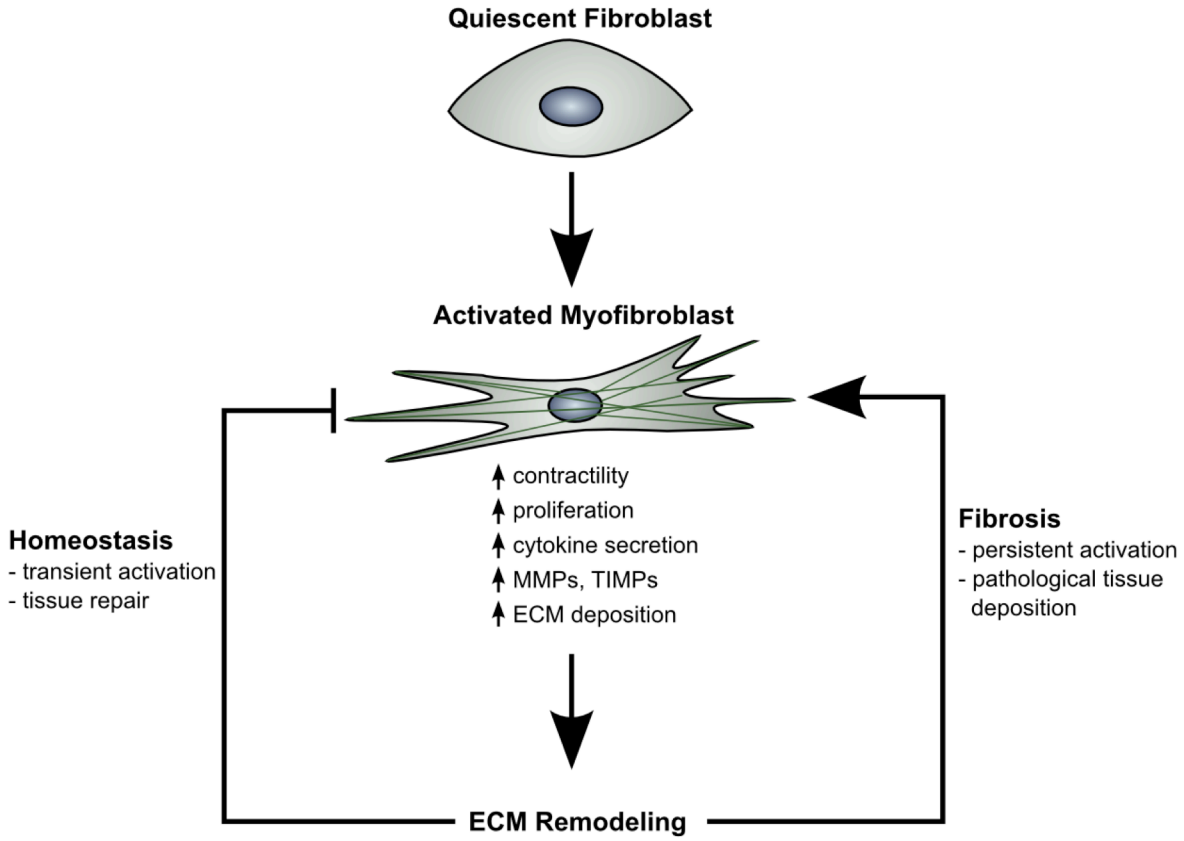

Figure 1.3. VIC activation. When VICs become activated to the myofibroblast phenotype, they exhibit increased contractility with αSMA+ stress fibers, proliferation, cytokine secretion, MMPs, TIMPs, and ECM deposition. This change in phenotype results in remodeling of the ECM. These changes initiate feedback loops, with negative feedback leading to tissue homeostasis; however, positive feedback leads to persistent VIC activation and fibrosis.

1.3.2. The fibroblast-to-myofibroblast transition in the aortic valve

VICs are a heterogeneous cell population, consisting largely of fibroblasts that reside in the leaflets of healthy adult valves[27]. Interestingly, the phenotype of the VIC population shifts

significantly throughout development, adulthood, and disease. During fetal development, there is a large population of activated myofibroblasts (>50%), as myofibroblasts play a critical role in valve development and tissue deposition[16,28]. By adulthood, VIC myofibroblasts exist at relatively low levels in healthy valves (<5%), but play an important role in maintaining valve homeostasis[29]. While these myofibroblasts are necessary for the generation and maintenance of healthy valve tissue, the persistent activation of VICs to the myofibroblast phenotype can lead to aortic valvular stenosis[30]. High levels of VIC activation correspond to stiffening of the valve ECM in both development and disease[29]. These changes in VIC activation levels and valve stiffness are illustrated in Figure 1.4.

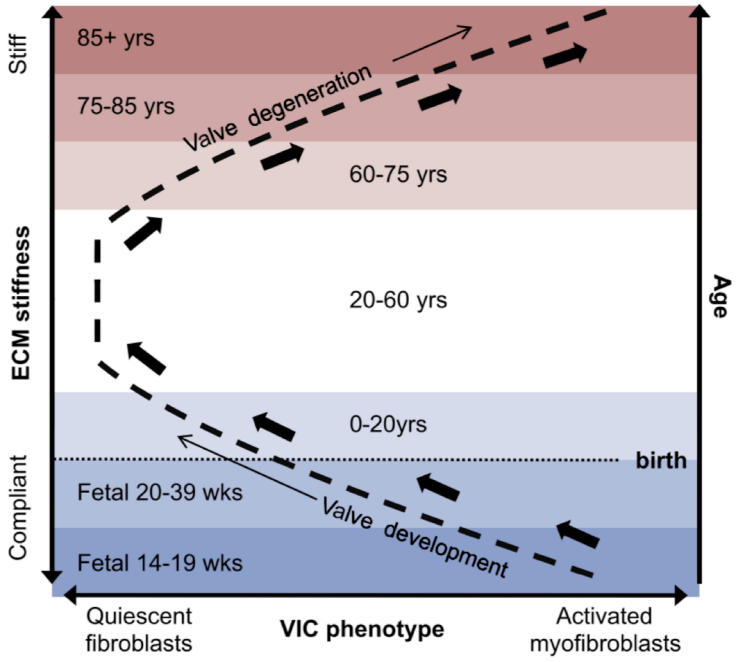

Figure 1.4. Changes in VIC activation and ECM stiffness with increasing age. In utero, the VIC population is highly activated and remodeling the very compliant tissue in order to develop a functional aortic valve. The phenotype shifts slowly during childhood to quiescence as stiffness increases. During adulthood, valve modulus and percentage of activated myofibroblasts are largely constant. Many people over 60 exhibit signs of aortic valve disease, with a higher percentage of VIC myofibroblasts and increasing valve stiffness. Image from Merryman, 2010[29].

1.3.3. Molecular mechanisms in myofibroblast activation and valve disease progression

There are a number of stimuli that can play a role in VIC activation and in the initiation and progression of aortic stenosis (Figure 1.5). Mechanical signals caused by the deformation of the valve in response to hemodynamic forces can influence both VIC and VEC phenotype. *In vitro*, valves exposed to elevated cyclic stretch had higher expression levels of matrix remodeling genes, consistent with changes observed in stenotic valves[31]. A co-culture model demonstrated that VECs reduce VIC proliferation in a shear stress-dependent manner[21]. Patients with a congenital bicuspid aortic valve tend to develop aortic stenosis much earlier than people with tricuspid valves, likely as a result of the increased stresses exerted on bicuspid valves and dysregulated molecular mechanisms[32,33]. VICs also receive mechanical signals by generating force on the surrounding ECM and sensing the local matrix modulus. *In vivo*, VIC activation correlates with a higher valve modulus[29], and corresponding *in vitro* experiments have demonstrated that higher substrate stiffness leads to the activated myofibroblast phenotype[34].

Endothelial integrity is important to valve homeostasis and the suppression of the myofibroblast phenotype. The disruption of the endothelium in hypercholesterolemic rabbits led to increased VIC activation, as well as macrophage accumulation, demonstrating the importance of the endothelium in regulating VIC phenotype[35]. Inflammation is also associated with valve disease, with stenotic valves exhibiting infiltration by macrophages and lymphocytes[36]. Inflammatory cytokines, such as TGF-β1, increase VIC activation, and can be secreted by inflammatory cells or by the VICs themselves[37,38]. TGF-β1 has been recognized as a key cytokine capable of inducing the myofibroblast differentiation in VICs and other fibroblasts[25,37,39,40]. Treatment of VICs with TGF-β1 increases αSMA expression and

contractility[37] through a SMAD-dependent mechanism[41]. The importance of TGF-β1 is also demonstrated by the finding that calcified aortic valves contain much higher levels of TGF-β1, as well as increased levels of the receptor TGF-βRI[42]. Interestingly, the influence of this soluble factor is dependent on the extracellular matrix mechanics, as cells must be able to generate enough force to convert the latent TGF-β1 complex to its active form[43]. The level of VIC activation in response to TGF-β1 is further influenced by the type of extracellular matrix proteins present[44]. Eventually, persistent activation of VICs to the myofibroblast phenotype and extensive fibrosis in the valve can lead to calcification, which occurs through either osteogenic differentiation of resident cells or by mineralization within apoptotic nodules (Figures 1.1B, 1.6C)[5].

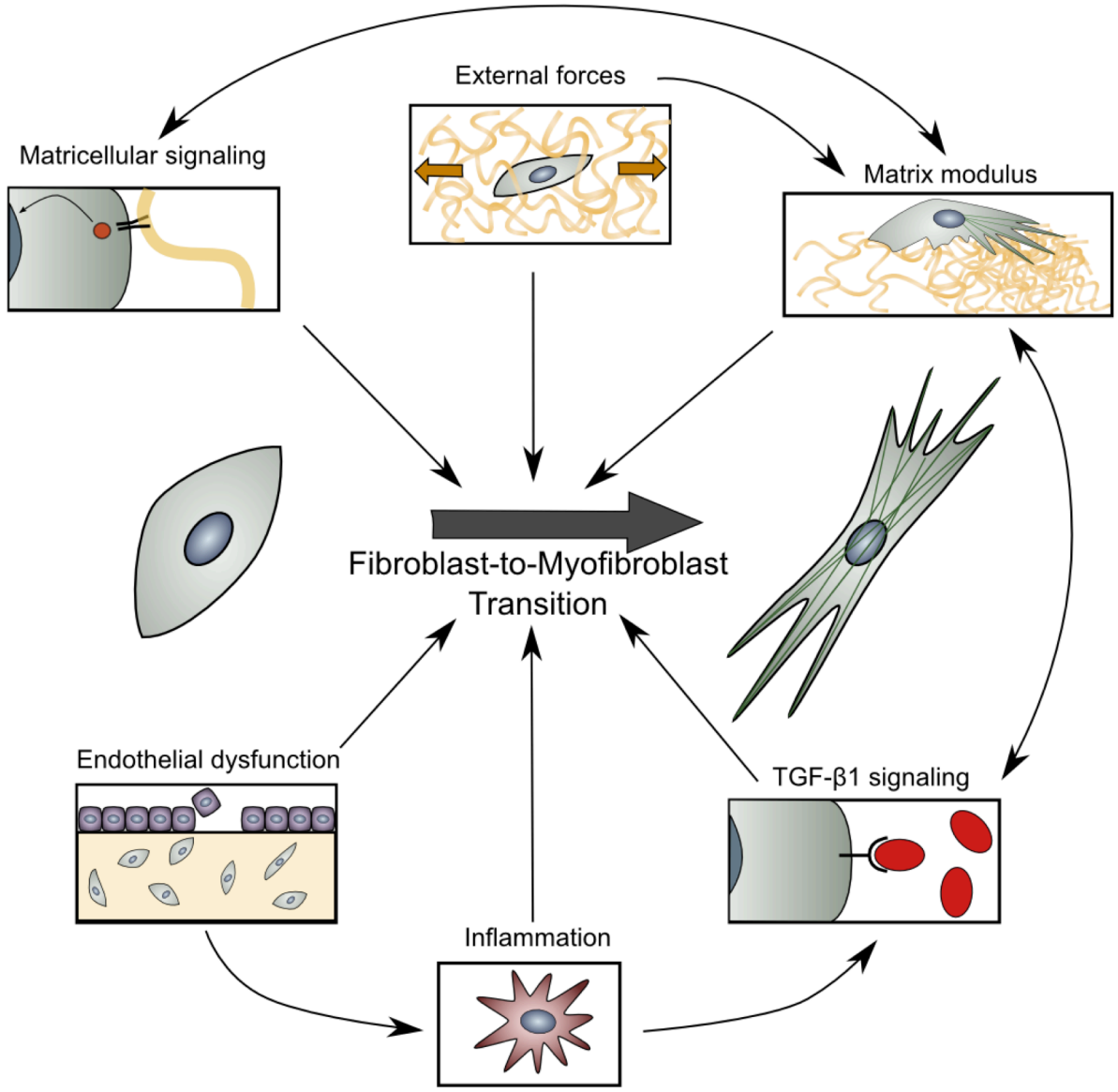

Figure 1.5. VIC activation to the myofibroblast phenotype. A number of stimuli have been identified, both *in vivo* and *in vitro*, that activate quiescent VIC fibroblasts to the myofibroblast phenotype. Some of these stimuli include matrix modulus, matricellular signaling, external forces, TGF-β1 signaling, endothelial dysfunction, and inflammation. Interactions between these stimuli complicate the understanding of the mechanisms leading to the fibroblast-to-myofibroblast transition. Additionally, many of these signals involve feedback loops, where the activated myofibroblasts amplify the original cue, further complicating the study of the fibroblast-to-myofibroblast transition. Persistent activation of the myofibroblast phenotype eventually leads to fibrotic stiffening and thickening of the valve, which causes stenosis.

1.3.4. Matrix remodeling in aortic stenosis

In patients with aortic stenosis, resident valve cells secrete increased levels of both ECM proteins and enzymes that degrade the ECM and disrupt the trilaminar structure of the valve (Figure 1.6)[32]. Much of the fibrotic thickening of diseased valves is due to increased proteoglycan content[32] (Figure 1.6B). Increases in proteoglycans may exacerbate fibrosis, as these proteins are involved in collagen fibrillogenesis, sequestration of growth factors, and lipid binding[45]. Additionally, diseased valves contain some ECM proteins, such as collagen types II and X, that are not found in healthy adult valves[46]. The myofibroblast VICs also secrete increased levels of collagen types I and III; however, due to large increases in total protein content, collagen makes up only 50% of the protein in non-calcified regions of diseased valves, compared to 90% in healthy valves[47]. Shifts in collagen content and type influence cell phenotype through multiple mechanisms. Deposition of collagen changes the mechanical properties of the valve, which is detected by the cells through mechanotransduction. Collagen structure is dependent on the isoform, and shifts in collagen composition can change the mechanics and therefore function of the valve. Type I collagen assembles into fibers, while type X is a short chain collagen that assembles into hexagonal matrices[48]. Growth factor sequestration depends on collagen type as well, with type IIA binding to TGF-β1 and BMP2[49], and potentially causing a feed-forward loop to exacerbate valve fibrosis. Additionally, matricellular signaling is affected by collagen type, as different receptors bind to the various isoforms[50].

Beyond changes in the composition of deposited ECM, increases in matrix metalloproteinases (MMP), specifically MMP3, MMP9, and MMP12[51,52], are also observed in valve disease, leading to the disruption and fragmentation of collagen and elastin fibers[32]. Tissue inhibitors of MMPs (TIMPs) also regulate ECM remodeling. In stenotic valves, there is an

increase in TIMP1, while TIMP2 is constitutively active[51]. Overall, this shift in the regulation of ECM remodeling proteins changes the structure of the valve matrix and causes a thickening and stiffening of the valve tissue[36]. This change in the ECM leads not only to mechanical changes in the valve, but also influences biological signaling cascades through matricellular signaling initiated by integrin binding to adhesive sites in the ECM[17].

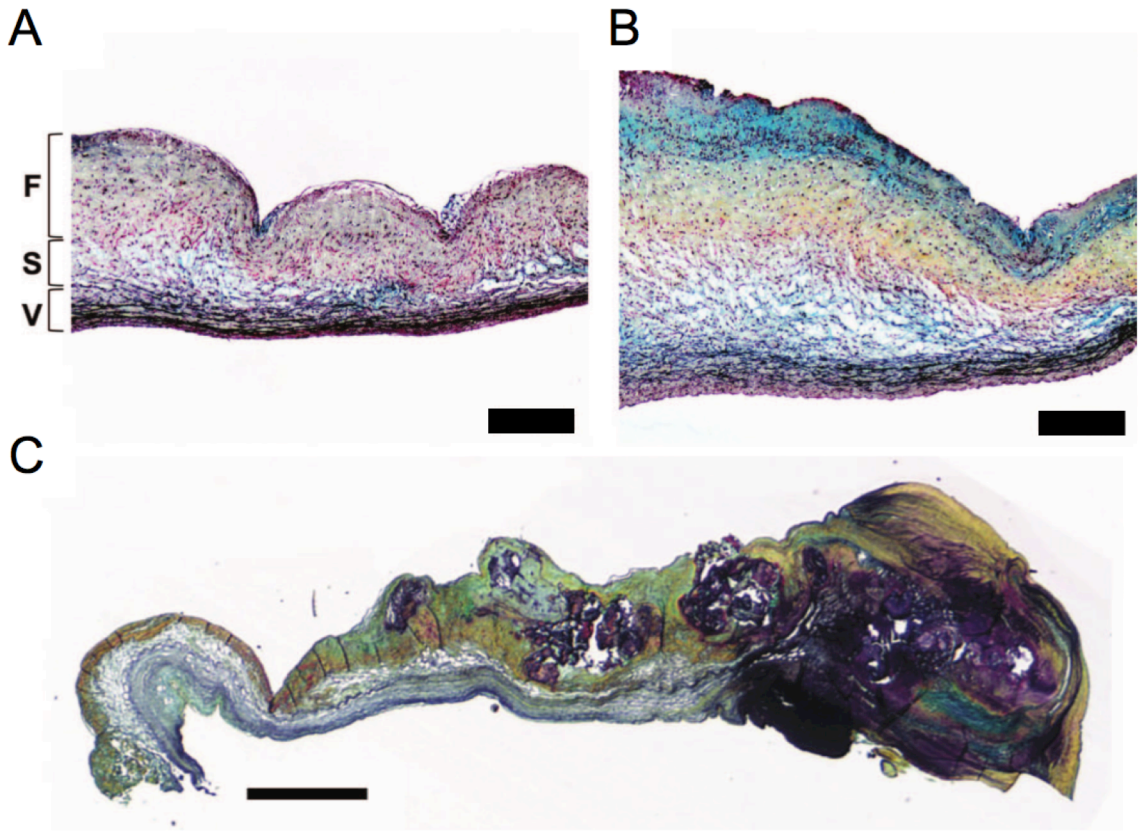

Figure 1.6. Matrix remodeling in aortic stenosis. Movat's pentachrome stain (collagen - yellow; proteoglycan - blue; elastin and nuclei - black; cytoplasm and muscle – red) of A) a healthy porcine aortic valve, B) a porcine valve exhibiting early signs of valve disease, and C) a calcified human valve. Initially disease progression includes thickening, increased ECM deposition (most notably a proteoglycan-rich region (blue) laid on the fibrosa), and fragmentation of elastin fibers (black). Further disease progression results in additional ECM remodeling and frequently results in the formation of calcified nodules (purple). Scale bar = 200 μm (A & B) or 1 mm (C). Adapted from Chen *et al.*, 2011[17].

1.3.5. Fibrotic and calcific contributions to aortic stenosis

While the valves of patients with severe aortic stenosis typically exhibit calcification and contain calcific nodules, there is some debate as to whether this calcification is a critical contributor to regurgitation or reduced valve function[53]. Although calcification is present in most patients that require aortic valve surgery, children that have developed symptoms due to a bicuspid or unicuspid valve typically have minimal or no calcification even when suffering from severe stenosis[54–56]. The importance of fibrosis rather than calcification has also been demonstrated in animal models. Activin Receptor Type 1 (Alk2) knockout mice develop aortic stenosis without calcification or inflammation[57]. Further, the elimination of calcification does not necessarily improve valve function. The reversa mouse model ($Ldlr^{-/-}Apob^{100/100}/Mttp^{fl/fl}$ $Mx1Cre^{+/+}$) gives the experimenter the ability to reverse hypercholesterolemia, a risk factor for aortic stenosis, using a genetic switch[58]. After these reversa mice develop aortic stenosis, reversal of hypercholesterolemia reduces calcification by up to 70%, but profibrotic signaling remains elevated and function is not recovered[59]. These findings emphasize the importance of the underlying fibrosis in the development of disease and in strategies to potentially reverse aortic stenosis.

1.4. The extracellular matrix directs VIC phenotype

VIC phenotype is influenced not only by soluble biochemical cues, like TGF-β1, but also by mechanical cues from the ECM. Cells bind to ECM proteins using transmembrane receptors called integrins (Figure 1.7)[60]. Integrins are heterodimeric proteins, and the combination of subunits determine which peptide sequences the integrin is able to bind. Inside the cell, integrins bind to a number of proteins, such as vinculin, talin, and α-actinin, which connect the integrins to

the actin cytoskeleton. Signaling molecules such as focal adhesion kinase (FAK) and p130CAS are known to interact with these integrins[61]. These signaling events are upstream of many pathways, including the PI3K/AKT, MAPK, ERK, and Rho pathways, which ultimately influence cell proliferation, contractility, transcriptional regulation, and other cell functions[62].

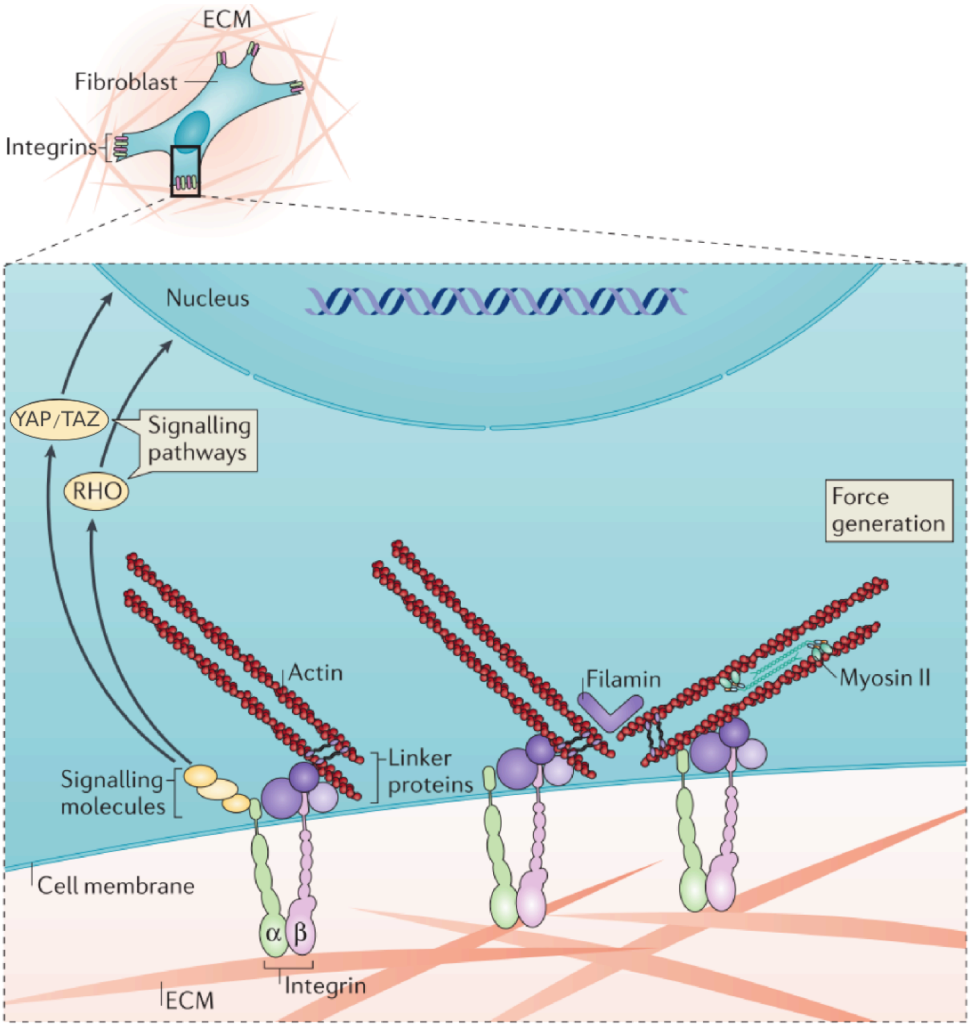

Figure 1.7. Cells sense, respond to, and remodel the ECM. A) Schematic showing fibroblast attachment to ECM proteins through integrins. The integrins connect to the actin cytoskeleton via linker proteins and initiate intracellular signaling cascades, including the RHO pathway and YAP/TAZ translocation. These integrin-ECM linkages enable cells to generate force by pulling on the ECM proteins. Image modified from Humphrey *et al.*, 2014[62].

Rho signaling is of particular interest, as Rho-mediated contractility is necessary for cells to sense their mechanical environment and drives stress fiber formation[63–65]. The MAPK/ERK signaling pathway has been implicated in VIC calcification and likely plays an important role in valve disease[66]. Further downstream, yes-associated protein (YAP) and transcriptional co-activator with PDZ-binding motif (TAZ) have been identified as key transducers of mechanical signals to nuclear transcription[67]. On soft substrates, YAP/TAZ remain in the cytoplasm and are subject to proteosomal degradation, but on stiff substrates, these transcriptional co-activators translocate to the nucleus. Nuclear localization directs cell phenotype, leading to increased proliferation[68], fibroblast activation, ECM deposition, and contractility[69].

These examples illustrate that mechanical cues from the ECM can direct cell phenotype, but the cells also alter their mechanical environment, which can result in complex feedback loops. Tissue homeostasis requires negative feedback loops, in which cells respond to a stiffened environment by preventing further stiffening; in contrast, positive feedback leads to pathological cell behavior and fibrosis (Figure 1.3). Further elucidation of the molecular mechanisms controlling these feedback loops would be valuable towards the identification of targets that could be leveraged to prevent valve disease.

Biomaterial matrices allow controlled *in vitro* experiments to study specific interactions between VICs and the ECM. For example, fibronectin-coated TCPS reduced αSMA expression and calcification markers, while fibrin-coated TCPS increased both αSMA and calcification[70]. Effects of matricellular signaling are observed even when a short peptide sequence from a protein is used rather than the full protein. Gould *et al.* found that a collagen-derived peptide, P15, increases VIC αSMA expression on hydrogels compared to substrates that contain RGDS, a fibronectin-derived peptide, with or without VGVAPG, an elastin-derived peptide[71]. Further,

these effects are context-dependent, as in 3D hydrogel cultures, VGVAPG resulted in higher VIC activation than either RGDS or P15[72].

ECM remodeling during fibrosis results in a shift in both the biochemical composition of the matrix, as well as the valve modulus[29]. While correlations have been developed to relate ECM stiffness or composition to VIC phenotype for valves *in vivo*, the precise cause-and-effect relationships within this cascade of changes in the valve are difficult to elucidate in humans because metrics such as cell phenotype, infiltration of inflammatory cells, and characterization of ECM components can only be characterized after the valve has been explanted. Typically, these valves can only be acquired during surgical replacement, which generally occurs at late stages of the disease. Thus, animal models provide a way to examine these changes at earlier time points in the progression of valve disease. Mice with genetic or dietary modifications are the most common model for aortic stenosis[1], but rabbit[73] and porcine[74] models have also been developed. Unfortunately, each of these animal models has its drawbacks: mice lack the trilaminar valve structure found in humans, while rabbit and porcine models have only been able to recapitulate the early stages of valve disease[1]. The ability of the VICs to remodel their local environment and influence the behavior of other cell types further complicates the elucidation of the impact of specific cues on VIC activation, necessitating the development of methods to investigate specific variables. This thesis work aims to improve our understanding of the VIC fibroblast-to-myofibroblast transition through the development of culture platforms to recapitulate specific cues and isolate the effects of these cues on VIC phenotype.

1.5. Hydrogels as matrices to study and quantify VIC phenotype *in vitro*

To isolate the effects of specific stimuli on VICs, the number of variables influencing cell phenotype can be reduced through the use of *in vitro* experiments. Many culture platforms have also been implemented to study VIC phenotype. Valve explants can be cultured *ex vivo*[75,76]; bioreactors have been used to control mechanical stretching[31,77]; and natural and synthetic hydrogels have been used to recapitulate the valve matrix *in vitro*. The most common approach, however, is to isolate the cells and culture them on tissue culture polystyrene (TCPS) plates. The use of traditional cell culture methods, in which cells are isolated from their complex, 3D environment and expanded on TCPS, leads to pathological activation of VICs[37]. Because of this high level of background activation, progress towards elucidating some of the biochemical signaling cascades that are important in valve disease has been limited. As shown in Figure 1.8, when VICs that have been removed from the valve (P0) are plated on TCPS, dramatic changes in gene expression levels occur[78]. Specifically, 2173 gene probes are up-regulated and 1926 are down-regulated by simply plating the VICs, but even more interestingly, these changes are orders of magnitude greater than the differences induced by treatment with TGF-β1, a potent activator of the myofibroblast phenotype. It is also important to note that this persistent activation makes it difficult, if not impossible, to study the fibroblast-to-myofibroblast transition, especially its reversal. Collectively, this is just one example that supports the hypothesis that the VIC microenvironment has a dramatic influence on its phenotype, and motivates the application of biomaterials matrices when studying VICs *in vitro*.

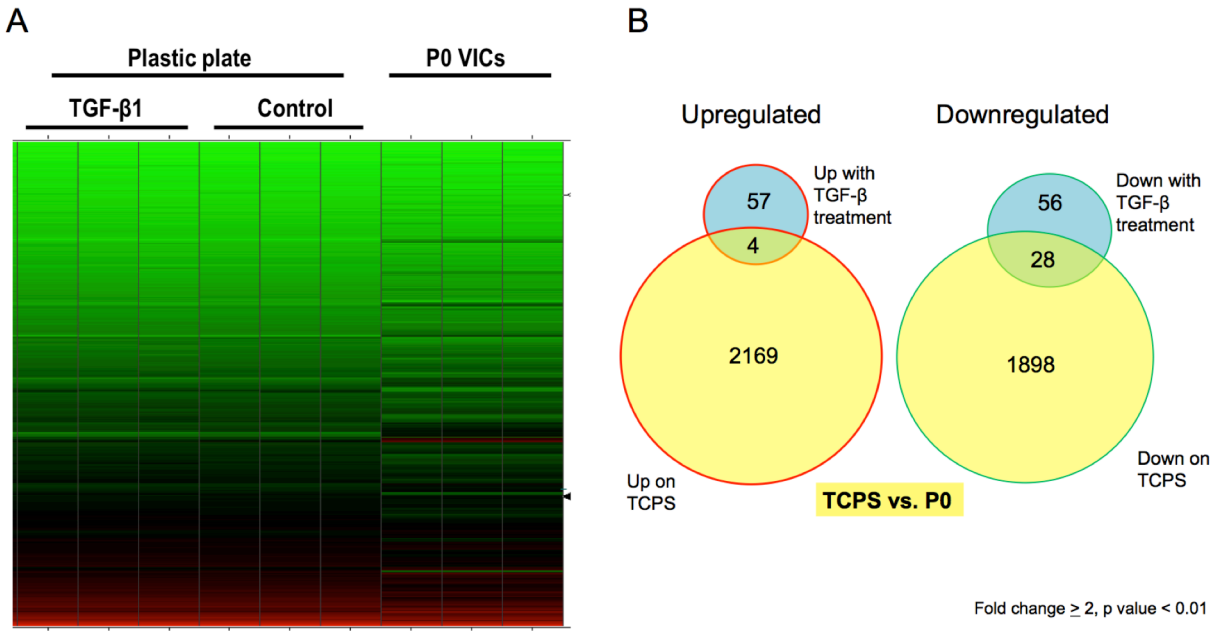

Figure 1.8. Culture on TCPS dramatically alters VIC phenotype. A) Microarray data show that culturing VICs on TCPS results in many changes in gene expression compared to freshly isolated (P0) VICs, with each row representing a different gene probe and the color representing the expression level. B) 2173 gene probes were upregulated and 1926 gene probes were downregulated on TCPS. In comparison, treatment with TGF-β1, a potent inducer of the myofibroblast phenotype, resulted in much fewer differences in the transcriptional profile. Additionally, many of the genes upregulated by TGF-β1 treatment did not overlap with genes upregulated by TCPS culture. Adapted from Wang *et al.*, 2013[78] to include unpublished data.

To better understand how matrix mechanical signaling influences VIC expression, VICs have been seeded on soft hydrogels of physiologically relevant moduli instead of TCPS, which is more than 5 orders of magnitude stiffer than the aortic valve. Wang *et al*. noted that when VICs were cultured on softer (~7 kPa) hydrogel substrates, the quiescent fibroblast phenotype could be maintained, indicating the importance of substrate modulus in the determination of VIC phenotype (Figure 1.9)[78].

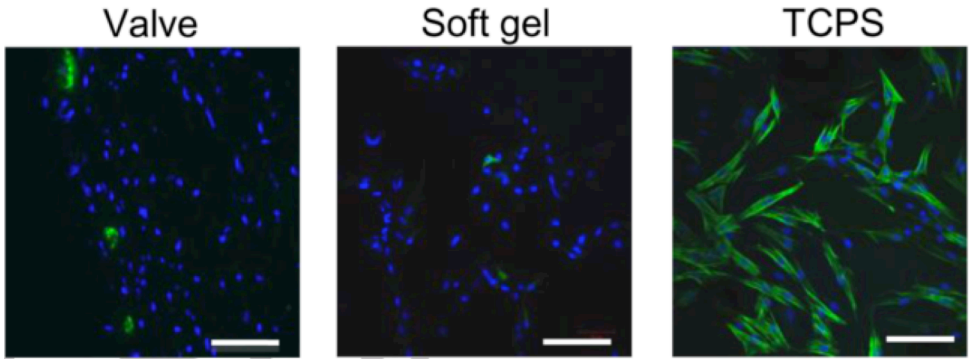

Figure 1.9. Soft gels recapitulate activation levels in aortic valve. Immunostaining for αSMA shows that healthy valves contain <5% activated myofibroblasts. Culture on TCPS leads to the activation of nearly all of the VICs to the myofibroblast phenotype. When VICs are instead cultured on a soft hydrogel, activation levels are very low, similar to those found *in vivo*. Green: αSMA, Blue: nuclei. Scale bar: 100 μm. Adapted from Wang *et al.*, 2013[78].

A wide range of biomaterials with more physiologically-relevant moduli have been implemented for the culture of cells in both two and three dimensions, as reviewed by Peppas *et al.*[79] and Tibbitt *et al.*[80]. Of these, hydrogels are a particularly attractive culture platform for VICs not only because of their soft moduli, but also because of their favorable mass transport properties and high water content, which mimics the water content in many soft tissues, such as the valve. Natural protein matrices, such as collagen or fibrin, form soft hydrogels relevant for the culture of VICs[81,82]. These protein-based hydrogels inherently contain numerous biological signals that promote VIC survival and spreading, permit local degradation of the matrix, and initiate signaling cascades that can influence VIC function; however, they are typically too soft to study the effects of mechanical signaling, and VICs can rapidly contract these matrices[13]. This motivated our interest in synthetic matrices with more tunable moduli, but which allow incorporation of some of the key biological functionalities. For example, the glycosaminoglycan hyaluronic acid has been covalently crosslinked to form hydrogels with improved mechanical properties while retaining the ability to promote VIC survival and ECM deposition[83].

Alternatively, peptide-fuctionalized PEG hydrogels can promote cellular interactions with the matrix while maintaining precise control over the mechanical and biochemical properties. These PEG-peptide hydrogels will be the focus of this thesis work.

Poly(ethylene glycol) (PEG) is a common choice for synthetic hydrogels due to its hydrophilicity and low levels of protein adsorption[84]. PEG polymers can be functionalized with a variety of reactive endgroups, such acrylates, vinyl sulfones, or norbornenes, that can be utilized for the formation of a covalently crosslinked network. Of particular interest for the formation of cytocompatible cell culture platforms are thiol-ene chemistries due to their high yields, lack of oxygen inhibition, aqueous reaction conditions, and biological orthogonality[85]. The step-growth networks formed by thiol-ene reactions have more homogeneous network structures than chain-growth networks[86]. Additionally, thiol-ene chemistries also allow for the simple incorporation of any cysteine-containing biomacromolecule (e.g., peptides, proteins) without any additional modifications. These cues can be presented in a controlled manner to promote cell attachment[87] or to incorporate enzymatically-cleavable sites[88]. Thiol-ene hydrogels can be formed through a photo-initiated polymerization, which results in cytocompatible reaction conditions that can be spatially and temporally controlled[89].

2D *in vitro* experiments comparing VIC phenotype when cultured on a range of substrate elasticities using PEG hydrogels generally show that lower moduli ($E < \sim 5$ kPa) lead to a mostly quiescent VIC phenotype, while higher substrate moduli ($E > \sim 25$ kPa) activate most VICs to myofibroblasts. A range of activation levels are observed at intermediate elasticities[34,90]. These trends recapitulate aspects of valve disease, with the stiffer, disease-like substrates leading to the myofibroblast phenotype that is more prevalent in diseased valves. Interestingly, this activation has been observed to be reversible, at least over short times scales (<1 week), in response to changes in the local environmental mechanics, when *in situ* softening hydrogels were used to study VIC

deactivation[91]. Substrate elasticity has also been shown to influence VIC morphology and calcification, with stiffer substrates leading to a more spread, elongated morphology and higher levels of calcium deposition[90,92]. While there has been much progress in understanding how VICs respond to mechanical and biochemical cues in two dimensions, less is known about how these factors may influence phenotype in a three-dimensional environment.

Peptide-functionalized PEG hydrogels formed via the thiol-ene photoclick reaction can be used to further recapitulate the native cellular microenvironment through the encapsulation of cells within a 3D matrix (Figure 1.10A)[80]. The dimensionality in which matrix cues are presented is important because the dimensionality of a cell's microenvironment can influence many cellular characteristics, including polarity, morphology, motility, focal adhesion distribution, contractility, cell-cell interactions, diffusion of cell-secreted factors, and matrix remodeling[93–99]. Benton *et al.* demonstrated high viability of VICs encapsulated within enzymatically-degradable PEG-based hydrogels formed by the photopolymerization of a 4-arm PEG-norbornene with dithiol peptide crosslinks. Results showed that the addition of the adhesive peptide sequence RGDS led to VIC elongation within the gel (Figure 1.10B)[100]. Immediately after encapsulation, VICs exhibited high levels of αSMA mRNA, likely due to the recent removal from TCPS. After two days, αSMA levels were dramatically lower; however, increasing αSMA was observed over time as the VICs continued to interact with and remodel the matrix. These findings demonstrate that the microenvironmental mechanical properties are critical to the VIC function, but also suggest that dynamic alterations in the environment lead to differences in phenotype over time.

A

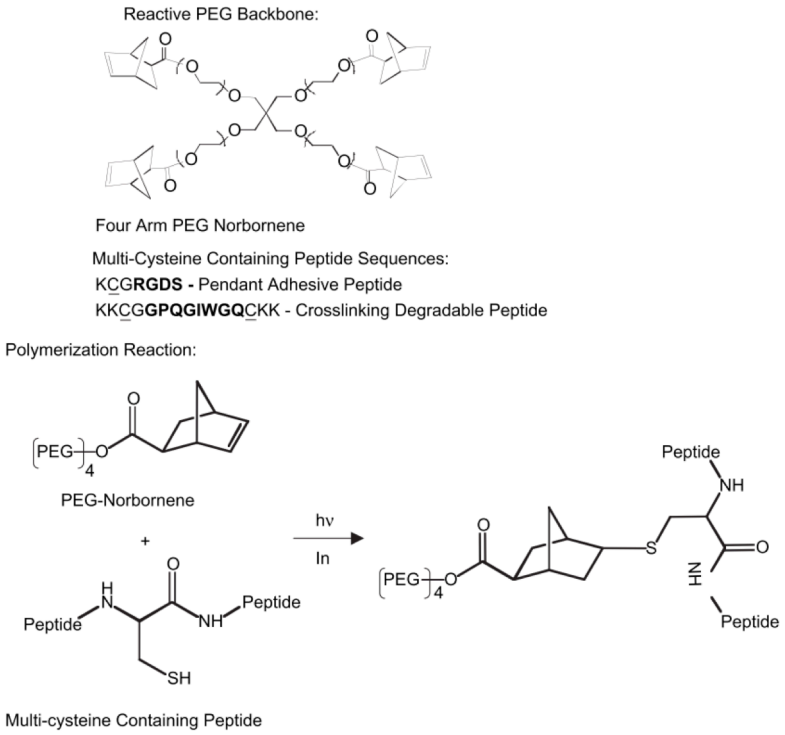

B

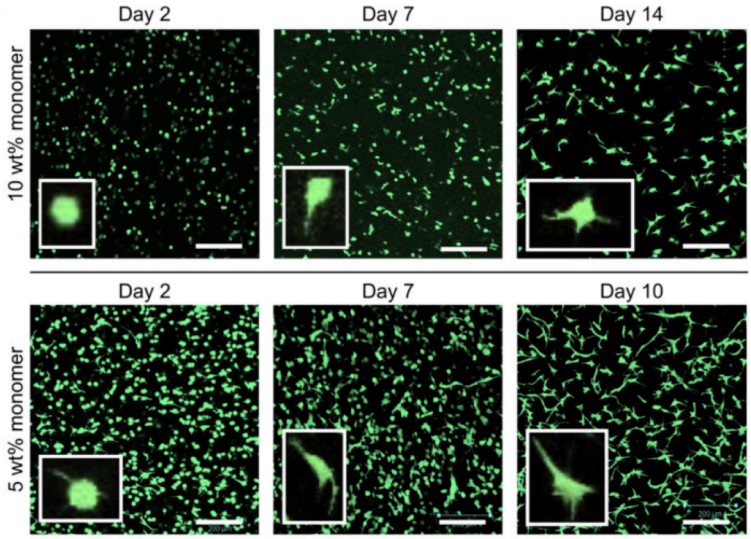

Figure 1.10. PEG hydrogels to study VICs *in vitro*. A) Multi-arm PEG molecules are functionalized with norbornene to undergo a thiol-ene "click" reaction with thiols on cysteine-containing peptides to form a step-growth network. An MMP-degradable peptide sequence flanked by cysteines is incorporated within the network to permit cell-mediated local degradation. The adhesive peptide facilitates cell-matrix interactions and is incorporated pendantly. B) Live/dead staining of VICs encapsulated within PEG hydrogels shows local degradation and cell spreading in a manner that is dependent on the crosslinking density (wt% monomer). Scale bar = 200 μm. Adapted from Benton, *et al.*, 2009[100].

The valve microenvironment is in a state of constant turnover, with the VICs replacing ECM that has been damaged by the mechanical stresses exerted on the valve. In a diseased state, this environment becomes even more dynamic, with dramatic changes in the tissue mechanical properties and biochemical composition. To understand how VIC phenotype is influenced by these changes, culture platforms have been developed to recapitulate some of these dynamic changes. Figure 1.11A shows the change in modulus of a photoresponsive material that contains nitrobenzyl ether-derived groups that were cleaved by light[101]. The final modulus of the material is controlled by the dose of light applied to the hydrogel. This platform was implemented to study how activated VICs cultured on a stiff (32 kPa) substrate respond to a reduction in modulus and demonstrated that a reduction in substrate modulus was sufficient to reduce VIC activation (Figure 1.11B)[34]. Further investigation revealed that the reduction in the percentage of myofibroblasts was in fact due to deactivation of myofibroblasts and not a result of apoptosis of the activated VICs[91]. The PI3K/AKT pathway has been implicated in this response to substrate stiffness. VICs seeded on TCPS and treated with a PI3K inhibitor do not exhibit αSMA stress fibers, and softening of a 32 kPa activating substrate to 7 kPa caused a reduction in pAKT in VICs[78].

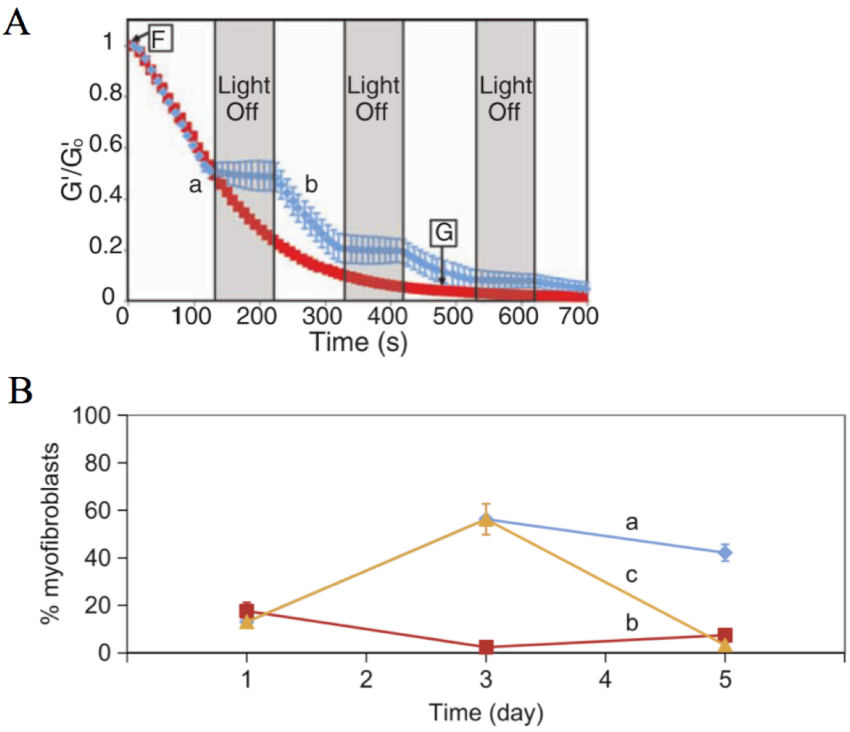

Figure 1.11. Dynamic hydrogel substrates to study VIC phenotype. A) PEG hydrogel modulus was reduced by photodegradation by 365 nm light. Adapted from Kloxin *et al.*, 2009[101]. B) VICs were seeded on 32 kPa (a) or 7 kPa (b) substrates, which resulted in high or low activation, respectively, after 3 days. When the 32 kPa substrate was reduced to 7 kPa on day 3, nearly all of the VICs deactivated to the level seen on 7 kPa by day 5. Adapted from Kloxin *et al.*, 2010[34].

This photodegradable platform permits the study of a reduction in matrix modulus; however, the ability to cyclically stiffen and soften may be more relevant to the continuous injury and repair that occurs in valve homeostasis. To recapitulate these dynamic changes in matrix mechanics, VICs were encapsulated in a photoresponsive hydrogel in which exposure to either 365 nm or 405 nm light would reversibly change the conformation of an azobenzene group incorporated within the network, thereby decreasing or increasing the matrix modulus[102].

1.5. Thesis approach

The objective of this thesis is to understand how cell-matrix interactions direct VIC phenotype using tunable PEG hydrogels as synthetic ECM mimics. An improved understanding of how VICs become persistently activated to a myofibroblast phenotype is critical to the elucidation of the biomolecular mechanisms that contribute to fibrosis and progression of aortic stenosis. Insight into the regulation of VIC phenotype would help identify strategies that could be leveraged to prevent or reverse valve disease.

We hypothesize that VIC interactions with the ECM direct critical cell functions, such as ECM remodeling, contractility, and cytokine secretion, and that VIC phenotype can be actively regulated by the presentation of specific matrix cues. The principal objectives and rationale of this thesis are outlined in Chapter 2. The first aim in this thesis research is to characterize the influence of dimensionality on VIC phenotype, as the 2D geometry of traditional *in vitro* studies is diametrically opposed to the natural 3D environment of these cells. In addition to the standard method of characterizing VIC phenotype by counting the percentage of VICs with αSMA stress fibers, a hallmark of the myofibroblast phenotype, a global transcriptional analysis was performed to more fully describe the VIC myofibroblast phenotype and changes that occur in this phenotype during culture in different matrix microenvironments. Chapter 3 reports on the results of this analysis.

Chapter 4 describes a method for *in situ* stiffening of cell-laden hydrogels using sequential gelation steps to study the influence of increasing modulus on VIC phenotype in 3D. This approach makes possible the deconvolution of two variables that are typically interdependent in 3D studies: morphology and matrix modulus. The ability to separately

investigate these variables is important, as both morphology and substrate modulus have been shown to direct cell phenotype in 2D experiments.

The vast collection of changes that occur in the dynamic VIC microenvironment during valve disease progression present a number of potentially important cues in the determination of VIC phenotype. To better understand which of these many cues are critical to directing VIC phenotype, high-throughput approaches that recapitulate the dynamic nature of the cellular microenvironment during disease progression are needed. Building on the PEG-peptide matrices that are useful for VIC culture, Chapter 5 focuses on the development of a dynamic, high-throughput cell encapsulation platform in which both soluble and matrix cues can be added *in situ* to represent the changing VIC microenvironment in disease progression. Finally, Chapter 6 presents the conclusions of this thesis work and discusses recommendations for future studies.

1.6. References

1. Miller, J. D., Weiss, R. M. & Heistad, D. D. Calcific aortic valve stenosis: methods, models, and mechanisms. *Circ. Res.* **108,** 1392–412 (2011).

2. Towler, D. A. Molecular and cellular aspects of calcific aortic valve disease. *Circ. Res.* **113,** 198–208 (2013).

3. Carabello, B. A. Introduction to aortic stenosis. *Circ. Res.* **113,** 179–85 (2013).

4. Stewart, B. F. *et al.* Clinical Factors Associated With Calcific Aortic Valve Disease. *J. Am. Coll. Cardiol.* **29,** 630–634 (1997).

5. Butcher, J. T., Mahler, G. J. & Hockaday, L. A. Aortic valve disease and treatment: the need for naturally engineered solutions. *Adv. Drug Deliv. Rev.* **63,** 242–68 (2011).

6. Go, A. S. *et al. Heart Disease and Stroke Statistics - 2014 Update: A report from the American Heart Association*. *Circulation* **129,** (2014).

7. Lindman, B. R., Bonow, R. O. & Otto, C. M. Current management of calcific aortic stenosis. *Circ. Res.* **113,** 223–37 (2013).

8. El-Hamamsy, I. *et al.* Long-term outcomes after autograft versus homograft aortic root replacement in adults with aortic valve disease: a randomised controlled trial. *Lancet* **376,** 524–531 (2010).

9. Mack, M. J. *et al.* 5-year outcomes of transcatheter aortic valve replacement or surgical aortic valve replacement for high surgical risk patients with aortic stenosis (PARTNER 1): a randomised controlled trial. *Lancet* **385,** 2477–2484 (2015).

10. Schoen, F. J. Mechanisms of function and disease of natural and replacement heart valves. *Annu. Rev. Pathol.* **7,** 161–83 (2012).

11. Messika-Zeitoun, D. *et al.* Aortic valve calcification: determinants and progression in the population. *Arterioscler. Thromb. Vasc. Biol.* **27,** 642–8 (2007).

12. Hermans, H. *et al.* Statins for calcific aortic valve stenosis: into oblivion after SALTIRE and SEAS? An extensive review from bench to bedside. *Curr. Probl. Cardiol.* **35,** 284–306 (2010).

13. Benton, J. A., Kern, H. B., Leinwand, L. A., Mariner, P. D. & Anseth, K. S. Statins Block Calcific Nodule Formation of Valvular Interstitial Cells by Inhibiting α -Smooth Muscle Actin Expression. *Arter. Thromb Vasc Biol* 1950–1957 (2009). doi:10.1161/ATVBAHA.109.195271

14. Shafi, S. Role of ACE Inhibitors in Atherosclerosis. *Int. J. Biomed. Adv. Res.* **4,** 849–856 (2013).

15. Rosenhek, R. *et al.* Statins but not angiotensin-converting enzyme inhibitors delay progression of aortic stenosis. *Circulation* **110,** 1291–1295 (2004).

16. Schoen, F. J. Evolving concepts of cardiac valve dynamics: the continuum of development, functional structure, pathobiology, and tissue engineering. *Circulation* **118,** 1864–80 (2008).

17. Chen, J. H. & Simmons, C. A. Cell-matrix interactions in the pathobiology of calcific aortic valve disease: critical roles for matricellular, matricrine, and matrix mechanics cues. *Circ. Res.* **108,** 1510–24 (2011).

18. Weind, K. L., Ellis, C. G. & Boughner, D. R. Aortic valve cusp vessel density: Relationship with tissue thickness. *J. Thorac. Cardiovasc. Surg.* **123,** 333–340 (2002).

19. Liu, A. C., Joag, V. R. & Gotlieb, A. I. The emerging role of valve interstitial cell phenotypes in regulating heart valve pathobiology. *Am. J. Pathol.* **171,** 1407–18 (2007).

20. Wang, H., Sridhar, B., Leinwand, L. A. & Anseth, K. S. Characterization of cell subpopulations expressing progenitor cell markers in porcine cardiac valves. *PLoS One* **8,** e69667 (2013).

21. Butcher, J. T. & Nerem, R. M. Valvular endothelial cells regulate the phenotype of interstitial cells in co-culture: effects of steady shear stress. *Tissue Eng.* **12,** 905–15 (2006).

22. Gould, S. T., Matherly, E. E., Smith, J. N., Heistad, D. D. & Anseth, K. S. The role of valvular endothelial cell paracrine signaling and matrix elasticity on valvular interstitial cell activation. *Biomaterials* **35,** 3596–3606 (2014).

23. Simmons, C. A. Aortic Valve Mechanics. An Emerging Role for the Endothelium. *J. Am. Coll. Cardiol.* **53,** 1456–1458 (2009).

24. Hinz, B. The myofibroblast: paradigm for a mechanically active cell. *J. Biomech.* **43,** 146–55 (2010).

25. Hinz, B. Formation and function of the myofibroblast during tissue repair. *J. Invest. Dermatol.* **127,** 526–37 (2007).

26. Cox, T. R. & Erler, J. T. Remodeling and homeostasis of the extracellular matrix: implications for fibrotic diseases and cancer. *Dis. Model. Mech.* **4,** 165–178 (2011).

27. Rajamannan, N. M. *et al.* Calcific Aortic Valve Disease: Not Simply a Degenerative Process: A Review and Agenda for Research From the National Heart and Lung and

Blood Institute Aortic Stenosis Working Group * Executive Summary: Calcific Aortic Valve Disease - 2011 Update. *Circulation* **124,** 1783–1791 (2011).

28. Aikawa, E. *et al.* Human semilunar cardiac valve remodeling by activated cells from fetus to adult: implications for postnatal adaptation, pathology, and tissue engineering. *Circulation* **113,** 1344–52 (2006).

29. Merryman, W. D. Mechano-potential etiologies of aortic valve disease. *J. Biomech.* **43,** 87–92 (2010).

30. Rabkin-Aikawa, E., Farber, M., Aikawa, M. & Schoen, F. J. Dynamic and reversible changes of interstitial cell phenotype during remodeling of cardiac valves. *J. Heart Valve Dis.* **13,** 841–7 (2004).

31. Balachandran, K., Sucosky, P., Jo, H. & Yoganathan, A. P. Elevated cyclic stretch alters matrix remodeling in aortic valve cusps: implications for degenerative aortic valve disease. *Am. J. Physiol. Heart Circ. Physiol.* **296,** H756–H764 (2009).

32. Hinton, R. B. *et al.* Extracellular matrix remodeling and organization in developing and diseased aortic valves. *Circ. Res.* **98,** 1431–1438 (2006).

33. Bouchareb, R. *et al.* Mechanical strain induces the production of spheroid mineralized microparticles in the aortic valve through a RhoA/ROCK-dependent mechanism. *J. Mol. Cell. Cardiol.* (2013). doi:10.1016/j.yjmcc.2013.12.009

34. Kloxin, A. M., Benton, J. A. & Anseth, K. S. In situ elasticity modulation with dynamic substrates to direct cell phenotype. *Biomaterials* **31,** 1–8 (2010).

35. Arishiro, K. *et al.* Angiotensin Receptor-1 Blocker Inhibits Atherosclerotic Changes and Endothelial Disruption of the Aortic Valve in Hypercholesterolemic Rabbits. *J. Am. Coll. Cardiol.* **49,** 1482–1489 (2007).

36. Otto, C. M., Kuusisto, J., Reichenbach, D. D., Gown, a M. & O'Brien, K. D. Characterization of the early lesion of 'degenerative' valvular aortic stenosis. Histological and immunohistochemical studies. *Circulation* **90,** 844–853 (1994).

37. Walker, G. A., Masters, K. S., Shah, D. N., Anseth, K. S. & Leinwand, L. A. Valvular myofibroblast activation by transforming growth factor-beta: implications for pathological extracellular matrix remodeling in heart valve disease. *Circ. Res.* **95,** 253–60 (2004).

38. Gu, X. & Masters, K. S. Regulation of valvular interstitial cell calcification by adhesive peptide sequences. *J. Biomed. Mater. Res. A* **93,** 1620–30 (2010).

39. Gu, L. *et al.* Effect of TGF-beta/Smad signaling pathway on lung myofibroblast differentiation. *Acta Pharmacol. Sin.* **28,** 382–91 (2007).

40. Desmoulière, A., Geinoz, A., Gabbiani, F. & Gabbiani, G. Transforming growth factor-beta 1 induces alpha-smooth muscle actin expression in granulation tissue myofibroblasts and in quiescent and growing cultured fibroblasts. *J. Cell Biol.* **122,** 103–111 (1993).

41. Frangogiannis, N. G. Targeting the Transforming Growth Factor (TGF)-β cascade in the remodeling heart: Benefits and perils. *J. Mol. Cell. Cardiol.* (2014). doi:10.1016/j.yjmcc.2014.09.001

42. Jian, B. *et al.* Progression of aortic valve stenosis: TGF-B1 is present in calcified aortic valve cusps and promotes aortic valve interstitial cell calcification via apoptosis. *Ann. Thorac. Surgery,* 457–465 (2003).

43. Wipff, P.-J., Rifkin, D. B., Meister, J.-J. & Hinz, B. Myofibroblast contraction activates latent TGF-beta1 from the extracellular matrix. *J. Cell Biol.* **179,** 1311–23 (2007).

44. Cushing, M. C., Liao, J.-T. & Anseth, K. S. Activation of valvular interstitial cells is mediated by transforming growth factor-beta1 interactions with matrix molecules. *Matrix Biol.* **24,** 428–37 (2005).

45. Stephens, E. H. *et al.* Differential proteoglycan and hyaluronan distribution in calcified aortic valves. *Cardiovasc. Pathol.* **20,** 334–342 (2011).

46. Wirrig, E. E., Hinton, R. B. & Yutzey, K. E. Differential expression of cartilage and bone-related proteins in pediatric and adult diseased aortic valves. *J. Mol. Cell. Cardiol.* **50,** 561–569 (2011).

47. Eriksen, H. a. *et al.* Type I and type III collagen synthesis and composition in the valve matrix in aortic valve stenosis. *Atherosclerosis* **189,** 91–98 (2006).

48. Kwan, A. P. L., Cummings, C. E., Chapman, J. A. & Grant, M. E. Macromolecular organization of chicken type X collagen in vitro. *J. Cell Biol.* **114,** 597–604 (1991).

49. Zhu, Y., Oganesian, A., Keene, D. R. & Sandell, L. J. Type IIA procollagen containing the cysteine-rich amino propeptide is deposited in the extracellular matrix of prechondrogenic tissue and binds to TGF-β1 and BMP-2. *J. Cell Biol.* **144,** 1069–1080 (1999).

50. Gelse, K., Pöschl, E. & Aigner, T. Collagens - Structure, function, and biosynthesis. *Adv. Drug Deliv. Rev.* **55,** 1531–1546 (2003).

51. Fondard, O. *et al.* Extracellular matrix remodelling in human aortic valve disease: The role of matrix metalloproteinases and their tissue inhibitors. *Eur. Heart J.* **26,** 1333–1341 (2005).

52. Bossé, Y. *et al.* Refining molecular pathways leading to calcific aortic valve stenosis by studying gene expression profile of normal and calcified stenotic human aortic valves. *Circ. Cardiovasc. Genet.* **2,** 489–98 (2009).

53. Weiss, R. M., Miller, J. D. & Heistad, D. D. Fibrocalcific aortic valve disease: Opportunity to understand disease mechanisms using mouse models. *Circ. Res.* **113,** 209–222 (2013).

54. Baker, C. G. & Campbell, M. The results of valvotomy for aortic stenosis. *Lancet* **267,** 171–175 (1956).

55. Fealey, M. E., Edwards, W. D., Miller, D. V. & Maleszewski, J. J. Unicommissural aortic valves: Gross, histological, and immunohistochemical analysis of 52 cases (1978-2008). *Cardiovasc. Pathol.* **21,** 324–333 (2012).

56. Keane, J. F., Bernhard, W. F. & Nadas, A. S. Aortic Stenosis in Infancy. *Circulation* **52,** 1138–1145 (1975).

57. Thomas, P. S., Sridurongrit, S., Ruiz-Lozano, P. & Kaartinen, V. Deficient signaling via Alk2 (Acvr1) leads to Bicuspid aortic valve development. *PLoS One* **7,** (2012).

58. Lieu, H. D. *et al.* Eliminating atherogenesis in mice by switching off hepatic lipoprotein secretion. *Circulation* **107,** 1315–1321 (2003).

59. Miller, J. D. *et al.* Evidence for active regulation of pro-osteogenic signaling in advanced aortic valve disease. *Arterioscler. Thromb. Vasc. Biol.* **30,** 2482–6 (2010).

60. Tomasek, J. J., Gabbiani, G., Hinz, B., Chaponnier, C. & Brown, R. a. Myofibroblasts and mechano-regulation of connective tissue remodelling. *Nat. Rev. Mol. Cell Biol.* **3,** 349–63 (2002).

61. Iskratsch, T., Wolfenson, H. & Sheetz, M. P. Appreciating force and shape — the rise of mechanotransduction in cell biology. *Nat. Rev. Mol. Cell Biol.* **15,** 825–833 (2014).

62. Humphrey, J. D., Dufresne, E. R. & Schwartz, M. a. Mechanotransduction and extracellular matrix homeostasis. *Nat. Rev. Mol. Cell Biol.* **15,** 802–812 (2014).

63. Discher, D. E., Janmey, P. & Wang, Y.-L. Tissue cells feel and respond to the stiffness of their substrate. *Science* **310,** 1139–43 (2005).

64. Chrzanowska-Wodnicka, M. & Burridge, K. Rho-stimulated contractility drives the formation of stress fibers and focal adhesions. *J. Cell Biol.* **133,** 1403–15 (1996).

65. Gu, X. & Masters, K. S. Role of the Rho pathway in regulating valvular interstitial cell phenotype and nodule formation. *Am. J. Physiol. Heart Circ. Physiol.* **300,** H448–58 (2011).

66. Gu, X. & Masters, K. S. Role of the MAPK/ERK pathway in valvular interstitial cell calcification. *Am. J. Physiol. Heart Circ. Physiol.* **296,** H1748–H1757 (2009).

67. Dupont, S. *et al.* Role of YAP/TAZ in mechanotransduction. *Nature* **474,** 179–83 (2011).

68. Aragona, M. *et al.* A mechanical checkpoint controls multicellular growth through YAP/TAZ regulation by actin-processing factors. *Cell* **154,** 1047–59 (2013).

69. Liu, F. *et al.* Mechanosignaling through YAP and TAZ drives fibroblast activation and fibrosis. *Am. J. Physiol. - Lung Cell. Mol. Physiol.* **308,** L344–L357 (2015).

70. Benton, J. a, Kern, H. B. & Anseth, K. S. Substrate properties influence calcification in valvular interstitial cell culture. *J. Heart Valve Dis.* **17,** 689–99 (2008).

71. Gould, S. T., Darling, N. J. & Anseth, K. S. Small peptide functionalized thiol-ene hydrogels as culture substrates for understanding valvular interstitial cell activation and de novo tissue deposition. *Acta Biomater.* **8,** 3201–9 (2012).

72. Gould, S. & Anseth, K. Role of cell-matrix interactions on VIC phenotype and tissue depostion in 3D PEG hydrogels. *J. Tissue Eng. Regen. Med.* (2013). doi:10.1002/term.1836

73. Drolet, M., Arsenault, M., Couet, J. & Ms, C. Experimental Aortic Valve Stenosis in Rabbits. *J. Am. Coll. Cardiol.* **1097,** 1211–1217 (2003).

74. Sider, K. L. *et al.* Evaluation of a porcine model of early aortic valve sclerosis. *Cardiovasc. Pathol.* **23,** 289–97 (2014).

75. Witt, W., Büttner, P., Jannasch, A., Matschke, K. & Waldow, T. Reversal of myofibroblastic activation by polyunsaturated fatty acids in valvular interstitial cells from aortic valves. Role of RhoA/G-actin/MRTF signalling. *J. Mol. Cell. Cardiol.* **74,** 127–138 (2014).

76. Rodriguez, K. J., Piechura, L. M., Porras, A. M. & Masters, K. S. Manipulation of valve composition to elucidate the role of collagen in aortic valve calcification. *BMC Cardiovasc. Disord.* **14,** 29 (2014).

77. Hahn, M. S., McHale, M. K., Wang, E., Schmedlen, R. H. & West, J. L. Physiologic pulsatile flow bioreactor conditioning of poly(ethylene glycol)-based tissue engineered vascular grafts. *Ann. Biomed. Eng.* **35,** 190–200 (2007).

78. Wang, H., Tibbitt, M. W., Langer, S. J., Leinwand, L. A. & Anseth, K. S. Hydrogels preserve native phenotypes of valvular fibroblasts through an elasticity-regulated PI3K/AKT pathway. *Proc. Natl. Acad. Sci.* **110,** 19336–19341 (2013).

79. Peppas, N. A., Hilt, J. Z., Khademhosseini, A. & Langer, R. Hydrogels in Biology and Medicine: From Molecular Principles to Bionanotechnology. *Adv. Mater.* **18,** 1345–1360 (2006).

80. Tibbitt, M. W. & Anseth, K. S. Hydrogels as extracellular matrix mimics for 3D cell culture. *Biotechnol. Bioeng.* **103,** 655–63 (2009).

81. Parenteau-Bareil, R., Gauvin, R. & Berthod, F. Collagen-Based Biomaterials for Tissue Engineering Applications. *Materials (Basel).* **3,** 1863–1887 (2010).

82. Ye, Q. *et al.* Fibrin gel as a three dimensional matrix in cardiovascular tissue engineering. *Eur. J. Cardiothorac. Surg.* **17,** 587–91 (2000).

83. Masters, K. S., Shah, D. N., Leinwand, L. A. & Anseth, K. S. Crosslinked hyaluronan scaffolds as a biologically active carrier for valvular interstitial cells. *Biomaterials* **26,** 2517–25 (2005).

84. DeForest, C. A. & Anseth, K. S. Advances in Bioactive Hydrogels to Probe and Direct Cell Fate. *Annu. Rev. Chem. Biomol. Eng.* **3,** 421–444 (2012).

85. Hoyle, C. E. & Bowman, C. N. Thiol-ene click chemistry. *Angew. Chemie - Int. Ed.* **49,** 1540–1573 (2010).

86. Malkoch, M. *et al.* Synthesis of well-defined hydrogel networks using click chemistry. *Chem. Commun. (Camb).* 2774–2776 (2006). doi:10.1039/b603438a

87. Hern, D. L. & Hubbell, J. A. Incorporation of adhesion peptides into nonadhesive hydrogels useful for tissue resurfacing. *J. Biomed. Mater. Res.* **39,** 266–76 (1998).

88. West, J. L. & Hubbell, J. A. Polymeric Biomaterials with Degradation Sites for Proteases Involved in Cell Migration. *Macromolecules* **32,** 241–244 (1999).

89. Fairbanks, B. D. *et al.* A Versatile Synthetic Extracellular Matrix Mimic via Thiol-Norbornene Photopolymerization. *Adv. Mater.* **21,** 5005–5010 (2009).

90. Quinlan, A. M. T. & Billiar, K. L. Investigating the role of substrate stiffness in the persistence of valvular interstitial cell activation. *J. Biomed. Mater. Res. Part A* **087257,** 2474–82 (2012).

91. Wang, H., Haeger, S. M., Kloxin, A. M., Leinwand, L. A. & Anseth, K. S. Redirecting Valvular Myofibroblasts into Dormant Fibroblasts through Light-mediated Reduction in Substrate Modulus. *PLoS One* **7,** e39969 (2012).

92. Yip, C. Y. Y., Chen, J.-H., Zhao, R. & Simmons, C. A. Calcification by valve interstitial cells is regulated by the stiffness of the extracellular matrix. *Arterioscler. Thromb. Vasc. Biol.* **29,** 936–42 (2009).

93. Baker, B. M. & Chen, C. S. Deconstructing the third dimension: how 3D culture microenvironments alter cellular cues. *J. Cell Sci.* **125,** 3015–24 (2012).

94. Grinnell, F., Ho, C., Tamariz, E., Lee, D. J. & Skuta, G. Dendritic Fibroblasts in Three-dimensional Collagen Matrices. **14,** 384–395 (2003).

95. Ochsner, M., Textor, M., Vogel, V. & Smith, M. L. Dimensionality controls cytoskeleton assembly and metabolism of fibroblast cells in response to rigidity and shape. *PLoS One* **5,** e9445 (2010).

96. Pontes Soares, C. *et al.* 2D and 3D-organized cardiac cells shows differences in cellular morphology, adhesion junctions, presence of myofibrils and protein expression. *PLoS One* **7,** e38147 (2012).

97. Harunaga, J. S. & Yamada, K. M. Cell-matrix adhesions in 3D. *Matrix Biol.* **30,** 363–8 (2011).

98. Adelöw, C., Segura, T., Hubbell, J. A. & Frey, P. The effect of enzymatically degradable poly(ethylene glycol) hydrogels on smooth muscle cell phenotype. *Biomaterials* **29,** 314–26 (2008).

99. Green, J. A. & Yamada, K. M. Three-dimensional microenvironments modulate fibroblast signaling responses. *Adv. Drug Deliv. Rev.* **59,** 1293–8 (2007).

100. Benton, J. A., Fairbanks, B. D. & Anseth, K. S. Characterization of valvular interstitial cell function in three dimensional matrix metalloproteinase degradable PEG hydrogels. *Biomaterials* **30,** 6593–603 (2009).

101. Kloxin, A. M., Kasko, A. M., Salinas, C. N. & Anseth, K. S. Photodegradable hydrogels for dynamic tuning of physical and chemical properties. *Science* **324,** 59–63 (2009).

102. Rosales, A. M., Mabry, K. M., Nehls, E. M. & Anseth, K. S. Photoresponsive Elastic Properties of Azobenzene-Containing Poly(ethylene-glycol)-Based Hydrogels. *Biomacromolecules* **16,** 798–806 (2015).

103. Benton, J. A. Soluble and microenvironmental factors that modulate myofibroblast and calcific differentiation of valvular interstitial cells. (2009).

104. Rajamannan, N. M., Gersh, B. & Bonow, R. O. Calcific aortic stenosis: from bench to the bedside--emerging clinical and cellular concepts. *Heart* **89,** 801–5 (2003).

Chapter 2

Thesis Objectives

Valvular interstitial cells (VICs) are active regulators of valve homeostasis, responsible for secretion and remodeling of the valve extracellular matrix; however, misregulation of VIC activity has also been implicated in valve disease[1]. As a result of VIC activity, the modulus of the valve leaflets can substantially change during development, injury and repair, and disease progression, eventually influencing the ability of the valve to functional properly. For example, in disease, persistent activation of VICs to the myofibroblast phenotype results in deposition of large quantities of collagen and proteoglycans, causing a thickening and stiffening of the valve[2]. In contrast, during development and typical tissue repair, VICs activation is transient and reduced before excessive remodeling leads to a reduction in valve function[3].

Beyond changes in matrix deposition and stiffening, many characteristics of the local microenvironment influence VIC activity, including matrix density, adhesion ligands, growth factor sequestration and matrix modulus. These factors not only affect cell phenotype directly but also influence variables such as cell shape. Generally speaking, cells sense the extracellular matrix (ECM) through focal adhesions that can involve different integrins and proteins, further complicating the understanding of this outside-in signaling[4–6]. Understanding the molecular level details as to how extracellular signals are translated to the nucleus to influence cell fate

remains a challenge for the field. This paucity of information has led to many pioneering studies of cell-matrix interactions in culture. For example, many of these matrix interactions can be isolated and studied on 2D surfaces, and these experiments have helped define our current understanding of the role of extracellular adhesive ligands, stiffness, and composition in directing and maintaining VIC function. However, large gaps remain and our understanding of VIC responses *in vivo* would benefit from more advanced culture systems and measurements in 3D systems. For example, 2D biomaterial substrates have been used to study mechanosensing and its influence on VIC phenotype[7–9], but much less is known about how VICs respond to matrix elasticity in a 3D environment, where many aspects of matrix signaling are highly coupled (e.g., MMP activity, cell shape, and local material properties). Thus, this thesis research aims to understand how mechanical signaling from the extracellular matrix influences VIC function in 3D, using synthetic extracellular matrix mimic that provide a more physiologically relevant context.

To understand how matrix mechanics and dimensionality coordinate together to direct VIC phenotype, we hypothesize that VIC phenotype can be assessed by the temporal presentation of mechanical and biochemical matrix cues to elucidate mechanisms regulating the fibroblast-to-myofibroblast transition. To test this hypothesis, we propose to develop hydrogel platforms for VIC culture that allows control of the presentation of microenvironmental cues in 3D and over time, and to further study the impact of these cues on the VIC phenotype, especially the transition between the fibroblast and myofibroblast phenotype. Ultimately, this insight into the modulation of VIC phenotype may guide efforts to prevent or treat valve disease by better understanding how matrix signaling influences VICs and then using this knowledge in tissue engineering applications or to identify small molecule inhibitors that might direct VICs towards

a desired phenotype *in vivo*. To achieve these goals, the specific aims of this research are to:

Aim 1. Investigate the role of dimensionality in directing VIC phenotype using peptide-functionalized poly(ethylene glycol) (PEG) hydrogels. VICs will be seeded on or encapsulated in hydrogel materials that are engineered to serve as simplified, synthetic mimics of the extracellular valve environment. Cells will be characterized by immunostaining for traditional myofibroblast markers, such as α-smooth muscle actin (αSMA) stress fibers, and quantifying mRNA levels of αSMA, S100A4, and other genes. As a control, we will compare molecular markers of VICs cultured on or in these 2D and 3D hydrogels to those directly isolated from aortic valves or cultured on traditional tissue culture polystyrene (TCPS). Transcriptional analysis will be performed to obtain a global comparison of the VIC phenotypes and to identify specific cellular functions that are most influenced by the culture platform. Additionally, this analysis will be used to identify representative markers of the VIC myofibroblast phenotype. We hypothesize that encapsulation of VICs in 3D hydrogels will most closely recapitulate the native phenotype.

Aim 2. Probe changes in VIC activation in response to matrix elasticity in 3D environments. VICs will first be encapsulated in hydrogels of varying moduli and characterized by measuring cell elongation, immunostaining for αSMA, and performing qPCR to measure αSMA mRNA levels. We will then develop a platform to dynamically increase the modulus of these VIC-laden hydrogels *in situ* and at any selected time point during the culture (e.g., after the cells have elongated). The effects of this step change in modulus on VIC phenotype will be quantified by immunostaining for αSMA and measuring mRNA levels of myofibroblast- and fibroblast-related genes.

Aim 3. Develop a high-throughput cell encapsulation platform to screen the effects of temporal presentation of multiple microenvironmental cues on the VIC fibroblast-to-myofibroblast transition. Both matricellular and biochemical signaling can influence VIC activation, with synergistic or antagonistic effects. To screen through the many conditions that may be important in the regulation of VIC phenotype, we will develop a high-throughput system to encapsulate VICs within 3D hydrogels and measure the percentage of activated VICs, cell morphology, and αSMA expression as a function of matrix properties. To recapitulate the changing environment present in fibrotic diseases, dynamic alterations in the hydrogel matrix will be induced by photoinitiated thiol-ene reactions. A fibronectin-derived adhesive ligand will be introduced to elucidate the effects of shifts in matrix composition on VIC phenotype, while *in situ* stiffening will recreate the increases in valve modulus that occur throughout the progression of valve development and/or disease. Ultimately, these matrix cues will be studied in combination with pro-inflammatory cytokines that are implicated in aortic stenosis and VIC activation.

Upon completion of these aims, we will have an improved understanding of phenotypic differences between VIC fibroblasts and myofibroblasts. Further, we will identify culture platforms that enable the study of the fibroblast-to-myofibroblast transition *in vitro*. Using these culture platforms, we will determine which mechanical cues lead to VIC activation. Since valve disease progression involves a complex interplay between many mechanical and biochemical cues, the high-throughput screening platform will enable us to investigate a wide range of potentially activating or deactivating signals, both individually and in combination. Additionally, the dynamic nature of this platform will recapitulate the dramatic changes in the

diseased valve, and will facilitate the characterization of VIC phenotype in response to sequential stimuli. This understanding of how VIC response to biochemical treatments varies in response to the changing ECM could contribute to the identification of ranges of disease severity at which treatments may be effective.

2.1. References

1. Durbin, A. D. & Gotlieb, A. I. Advances towards understanding heart valve response to injury. *Cardiovasc. Pathol.* **11,** 69–77 (2002).

2. Chen, J. H. & Simmons, C. A. Cell-matrix interactions in the pathobiology of calcific aortic valve disease: critical roles for matricellular, matricrine, and matrix mechanics cues. *Circ. Res.* **108,** 1510–24 (2011).

3. Rabkin-Aikawa, E., Farber, M., Aikawa, M. & Schoen, F. J. Dynamic and reversible changes of interstitial cell phenotype during remodeling of cardiac valves. *J. Heart Valve Dis.* **13,** 841–7 (2004).

4. Choquet, D., Felsenfeld, D. P. & Sheetz, M. P. Extracellular matrix rigidity causes strengthening of integrin-cytoskeleton linkages. *Cell* **88,** 39–48 (1997).

5. Gieni, R. S. & Hendzel, M. J. Mechanotransduction from the ECM to the genome: are the pieces now in place? *J. Cell. Biochem.* **104,** 1964–87 (2008).

6. Moore, S. W., Roca-Cusachs, P. & Sheetz, M. P. Stretchy proteins on stretchy substrates: the important elements of integrin-mediated rigidity sensing. *Dev. Cell* **19,** 194–206 (2010).

7. Kloxin, A. M., Benton, J. A. & Anseth, K. S. In situ elasticity modulation with dynamic substrates to direct cell phenotype. *Biomaterials* **31,** 1–8 (2010).

8. Wang, H., Haeger, S. M., Kloxin, A. M., Leinwand, L. A. & Anseth, K. S. Redirecting Valvular Myofibroblasts into Dormant Fibroblasts through Light-mediated Reduction in Substrate Modulus. *PLoS One* **7,** e39969 (2012).

9. Quinlan, A. M. T. & Billiar, K. L. Investigating the role of substrate stiffness in the persistence of valvular interstitial cell activation. *J. Biomed. Mater. Res. Part A* **087257,** 2474–82 (2012).

Chapter 3

Microarray analyses to quantify advantages of 2D and 3D hydrogel culture systems in maintaining the native valvular interstitial cell phenotype

---

Abstract

Valvular interstitial cells (VICs) actively maintain and repair heart valve tissue; however, persistent activation of VICs to a myofibroblast phenotype can lead to aortic stenosis. To better understand and quantify how microenvironmental cues influence VIC phenotype and myofibroblast activation, we compared expression profiles of VICs cultured on poly(ethylene glycol) (PEG) gels to those cultured on tissue culture polystyrene (TCPS), as well as fresh isolates. In general, VICs cultured in or on hydrogel matrices had lower levels of activation (<10%), similar to levels seen in healthy valve tissue, while VICs cultured on TCPS were ~75% activated myofibroblasts. VICs cultured on TCPS also exhibited a higher magnitude of perturbations in gene expression than soft hydrogel cultures when compared to the native phenotype. Using peptide-modified PEG gels, VICs were seeded on (2D), as well as encapsulated in (3D), matrices of the same composition and modulus. Despite similar levels of activation, VICs cultured in 2D had distinct variations in transcriptional profiles compared to those in 3D hydrogels. Genes related to cell structure and motility were particularly affected by the dimensionality of the culture platform, with higher expression levels in 2D than in 3D. These

results indicate that dimensionality may play a significant role in dictating cell phenotype (e.g., through differences in polarity, diffusion of soluble signals), and emphasize the importance of using multiple metrics when characterizing cell phenotype.

3.1. Introduction

VICs are the primary cell type found within heart valves. In patients with aortic stenosis, VICs remodel their surrounding extracellular matrix (ECM) in a manner that causes pathological stiffening of the valve[1,2]; this fibrotic stiffening can then lead to regurgitation or obstruction of blood flow[3]. Currently, there are no pharmaceutical therapeutics that have proven to be effective for the reversal of aortic stenosis, and the main treatment option is surgical replacement of the valve[4]. While advances have occurred in minimally invasive valve replacement therapies, a better understanding of VIC biology may provide alternative solutions to valve replacement by focusing on reversal or slowing of disease progression. To address this need, *in vivo* models are highly relevant, but their complex nature makes it difficult to elucidate specific mechanisms of VIC activation and disease progression. In contrast, *in vitro* systems provide a high level of control, but these systems are limited by physiological relevance and must be evaluated for their ability to recapitulate mechanism of interest. For these reasons, *in vivo* and *in vitro* experiments are complementary and both approaches are needed.

In healthy cardiac valves, the majority of VICs exhibit a quiescent fibroblast phenotype[5]; however, in patients with valve disease, many VICs become activated to a myofibroblast phenotype. The VIC myofibroblast phenotype is characterized by the presence of prominent α-smooth muscle actin (αSMA) stress fibers and associated with increased proliferation, ECM remodeling, and cytokine secretion[2,6]. *In vitro* culture systems afford an opportunity to study this

transition, especially as a function of VIC-matrix interactions and in the absence of the complex signaling milieu that occurs *in vivo*. However, dramatic changes occur in the VIC phenotype when they are isolated from valve tissue and cultured using traditional methods, and this aphysiological response can complicate the identification of new approaches to regulate the pathological VIC myofibroblast phenotype.

Culturing VICs on supra-physiologically stiff, 2D tissue culture polystyrene (TCPS) (i.e., > 5 orders of magnitude stiffer than compliant valves[7]) alters many of the signals that the cells receive[8]. Unfortunately, with VICs, some of the functions most highly correlated to valve disease progression are also the ones that are most dramatically affected by culture on TCPS, making it difficult to study this transition and/or its reversal. Specifically, plating VICs on TCPS leads to high levels of myofibroblast activation and renders it nearly impossible to study the quiescent fibroblast phenotype[8].

Wang *et al.* provided one of the first reports quantifying the effect of TCPS culture on porcine VICs by performing a microarray experiment to measure mRNA levels in freshly isolated VICs compared to VICs cultured on TCPS. Results showed that over 4000 genes were differentially regulated, which was two orders of magnitude higher than that observed with transforming growth factor-β (TGF-β) treatment[8]. This is significant, as TGF-β is a potent cytokine that is known to cause activation of myofibroblasts in many tissues, and mis-regulation of TGF-β signaling has been implicated in heart valve problems related to the use of the anti-obesity drug, FEN-PHEN[9]. Thus, microenvironment is hypothesized to play an important role in regulating the VIC phenotype, and Wang *et al.* further demonstrated that culturing VICs on soft hydrogel substrates restored expression levels of many critical genes to levels measured in freshly isolated cells.

While seeding VICs on softer, more biomechanically relevant substrates instead of TCPS helps recapitulate some aspects of the native VIC phenotype, there are many differences between TCPS and hydrogel matrices, as well as many differences between the cellular microenvironment *in vivo* and hydrogel substrates *in vitro*. To begin to deconvolute some of these differences, this work aims to elucidate the effects of dimensionality of the matrix on VIC interactions and phenotype. Clearly, removing cells from their three-dimensional native environment and seeding them on two-dimensional surfaces can significantly affect their phenotype. As one specific example, previous reports have shown that increasing substrate modulus in 2D leads to higher levels of VIC myofibroblast activation[10], while the opposite effect was observed in 3D[11].

To evaluate the impact of microenvironment on VIC phenotype, additional metrics are necessary. αSMA stress fibers are a hallmark of the myofibroblast phenotype, but a more complete description is warranted, especially at the molecular level to better define the differences between VIC fibroblasts and myofibroblast. Such a global characterization would provide metrics to distinguish between populations that have similar levels of VIC activation, but potentially different functional characteristics. For example, nearly 100% of VICs cultured on TCPS either with or without TGF-β exhibit αSMA stress fibers; however, the addition of TGF-β does result in an increase in contractility and inhibition of proliferation and apoptosis[12]. These functional differences in VIC populations with equivalent activation levels demonstrate the importance of performing a more in-depth, systematic characterization of VIC phenotype rather than relying on a single metric. We hypothesize that populations of VICs cultured in different environments that have the same percentage of activated myofibroblasts can exhibit very distinct transcriptional profiles.

Here, we examine the phenotypes of VICs cultured on hydrogel surfaces (2D) and then compare this to VICs encapsulated within the same hydrogel formulation (3D) using traditional metrics alongside microarray experiments to measure global gene expression. As a control, VIC expression in hydrogel matrices is directly contrasted to freshly isolated VICs, as well as VICs cultured on TCPS. This quantitative approach provides insight into many cell functions through the measurement of gene expression levels to demonstrate how *in vitro* culture platforms influence VIC phenotype. Aortic VICs were used for this study as aortic stenosis is the most common valve disease in developed countries[13]. Ultimately, these results should improve the field's understanding of the impact of the design of *in vitro* culture platforms on primary cell phenotype, especially fibroblast and myofibroblast characteristics. Changes in dimensionality can impact a wide range of cell functions, and this knowledge should prove useful in the development of matrices for expanding and culturing cells *ex vivo*, as well as the engineering of cell delivery vehicles for *in vivo* tissue regeneration.

3.2. Materials and Methods

3.2.1. VIC isolation and culture

VICs were isolated from aortic valve leaflets of fresh porcine hearts (Hormel) using a previously described protocol[14]. Leaflets were excised and rinsed in Earle's Balanced Salt Solution (Life Technologies) supplemented with 1% penicillin-streptomycin (Life Technologies) and 0.5 ug/mL fungizone (Life Technologies). Leaflets were then incubated in 250 units/mL collagenase type II (Worthington) for 30 min at 37°C and vortexed for 30 s to remove endothelial cells. Next, a second incubation in collagenase was performed for 1 hour at 37°C. Digested leaflets were then vortexed for 2 min and cells were separated from valve debris by

filtration through a 100 μm cell strainer. The cell solution was centrifuged and the cell pellet was re-suspended in growth media composed of Media 199 (Life Technologies) supplemented with 15% fetal bovine serum (FBS, Life Technologies), 1% penicillin-streptomycin and 0.5 ug/mL fungizone. Freshly isolated VICs were then used for RNA isolation or plated on tissue culture polystyrene (TCPS, Fisher Scientific) and grown to ~80% confluency before use in experiments. VICs were then seeded on 2D hydrogels at 25,000 cells/cm^2, on TCPS at 12,500 cells/cm^2, or encapsulated in 3D hydrogels at 10 million cells/mL. Hydrogel formulations are described in the next section. Experiments were performed in low-serum (1% FBS) media supplemented with 1% penicillin-streptomycin (Life Technologies) and 0.5 ug/mL fungizone (Life Technologies) in a 37°C incubator with 5% CO_2.

3.2.2. Synthesis of poly(ethylene glycol)-norbornene (PEG-nb)

8-arm PEG-nb was synthesized as described previously[15,16]. Briefly, stoichiometric amounts of 8-arm PEG (40 kDa, JenKem) and 4-dimethylaminopyridine (Sigma-Aldrich) were dissolved in anhydrous dichloromethane (Sigma-Aldrich). A two-fold excess of each 5-norbornene-2-carboxylic acid (Sigma-Aldrich) and N-N'-diisopropylcarbodiimide (Sigma-Aldrich) were added and reaction vessel was purged with argon. After reacting overnight on ice while stirring, product was precipitated in 4°C ethyl ether (Fisher Scientific). The product was then filtered and dried by vacuum. Next, the PEG-nb was dissolved in water and purified by dialysis. The final product was lyophilized, and the overall end group functionality was characterized by proton nuclear magnetic resonance imaging to confirm >90% functionalization.

3.2.3. Hydrogel formation and characterization

5 wt% 8-arm PEG-nb was crosslinked with a dithiol-containing, matrix metalloprotease (MMP)-degradable peptide KCGPQG↓IWGQCK (American Peptide Company, Inc.) and with 2 mM CRGDS adhesive peptide (American Peptide Company, Inc.) at a ratio of 0.55 thiols per norbornene. The photoinitiator lithium phenyl-2,4,6-trimethylbenzoylphosphinate (LAP) was added at a concentration of 1.7 mM. All components were dissolved in phosphate buffered saline (PBS, Life Technologies). Non-stoichiometric ratios of the thiol and –ene functionalities were used to control the final crosslinking density, and ultimately, the gel connectivity and shear modulus to permit cell spreading in cell-laden hydrogels within 48 hours.

2D hydrogels were fabricated on glass coverslips that had been thiolated by vapor deposition of 3-(mercaptopropyl) trimethoxysilane in an 80°C oven to facilitate covalent anchoring of the gels to the coverslips. First, the monomer solution was pipetted onto a SigmaCote (Sigma-Aldrich) treated glass slide and covered with a thiolated coverslip such that the final gel thickness was ~100 μm. For 3D hydrogels, 10 million cells/mL were suspended in the monomer solution, and 29 μL of the cell-monomer solution were added to a mold (5 mm diameter) placed on a SigmaCote treated glass slide. Hydrogels for rheological characterization were formed in the same manner as the 3D hydrogels but without embedded cells. All hydrogels were polymerized by exposure to UV light (~2 mW/cm^2 at 365 nm) for 3 min, as determined by monitoring the evolution of the elastic modulus and its plateau. Gels were then placed in wells containing low-serum media (1% FBS). 2D gels were allowed to swell overnight before seeding with cells. To characterize the materials properties of the hydrogels, the shear elastic moduli (G') of the swollen hydrogels were measured using a DHR3 rheometer (TA Instruments) and a parallel plate geometry. Frequency and strain sweeps were performed to ensure that

measurements were taken within the linear regime. Young's modulus was calculated from G' assuming a Poisson's ratio of 0.5[17].

3.2.4. Immunostaining for αSMA and f-actin

VICs were fixed overnight in 10% formalin (Sigma-Aldrich) 48 h after seeding or encapsulation. Next, samples were washed with PBS, permeabilized with 0.05% TritonX100 (Fisher Scientific) in PBS, and then treated with 1% bovine serum albumin (BSA, Sigma-Aldrich) in PBS with Tween20 (Sigma-Aldrich) to prevent non-specific staining. Samples were treated overnight at 4°C with the primary antibody, mouse anti-αSMA (Abcam) diluted 1:200 in the 1% BSA solution. Next, the samples were washed with PBS before incubation with the secondary antibody, goat-anti-mouse AlexaFluor 488 (1:300, Life Technologies) and TRITC-phalloidin (1:300, Sigma-Aldrich) overnight. Finally, cell nuclei were stained with 4'-6-diamidino-2-phenylindole (DAPI, Life Technologies). Samples were imaged on a 710 LSM NLO confocal microscope (Zeiss) at 20x magnification with at least 3 fields of view per sample. For 3D samples, slices were taken at 10 μm intervals and images show a maximum intensity projection of 11 slices. The percentage of myofibroblasts in each sample was determined by manually counting the number of cells with and without organized αSMA stress fibers. Three biological replicates were performed per condition.

3.2.5. RNA isolation and quantitative real-time polymerase chain reaction (qRT-PCR)

RNA was isolated from VICs 48 h after seeding or encapsulating using TriReagent (Sigma-Aldrich) with two 1-bromo-3-chloropropane (Sigma-Aldrich) extractions and precipitation by 2-propanol (Sigma-Aldrich) according to the manufacturer's instructions. RNA

pellets were washed twice with 75% ethanol (Sigma-Aldrich) and re-suspended in water. RNA concentration and quality were assessed with a ND-1000 Nanodrop Spectrophotometer.

For qRT-PCR, cDNA was synthesized using the iScript cDNA Synthesis kit (Bio-Rad) and an Eppendorf Mastercycler. 0.05 ng/μL cDNA, 300 nM custom primers (Illumina), and 10 μL SYBR Green Supermix (Bio-Rad) were combined with water using an EpMotion 5370 (Eppendorf) for a final volume of 20 μL in each well. Expression of αSMA (F: 5'-GCAAACAGGAATACGATGAAGCC-3', R: 5'-AACACATAGGTAACGAGTCAGAGC-3') was normalized to a reference gene, ribosomal protein L30 (RPL30, F: 5'-GCTGGGGTACAAGCAGACTC-3', R: 5'-AGATTTCCTCAAGGCTGGGC-3'). mRNA levels were determined by running samples on an iCycler (Bio-Rad) and comparing the C_T values for each sample to a standard curve. Three technical replicates were performed for each biological replicate.

3.2.6. Porcine genome microarrays and analysis

RNA was isolated as described above. Only samples with a concentration greater than 100 ng/μL, 260/280 ≥ 1.8, and 260/230 ≥ 1.8 were used in the microarray experiments. Each condition included 3 biological replicates. RNA quality assessment and microarrays were performed by the Genomics and Microarray Core and University of Colorado at Denver. Samples were hybridized to Affymetrix Porcine Gene 1.0 ST arrays. Data were analyzed using Expression Console (Affymetrix), Transcriptome Analysis Console (Affymetrix), Spotfire (TIBCO), the Database for Annotation, Visualization and Integrated Discovery (DAVID, National Institute of Allergy and Infectious Diseases & National Institute of Health)[18,19], the Panther Classification System (Gene Ontology Consortium)[20,21], and PathwayLinker[22].

Differences were considered significant if there was a fold change greater than 2 or less than -2 and a p-value less than 0.05 unless otherwise specified.

3.2.7. Statistics

At least 3 biological replicates using cells from separate pools of porcine hearts were performed for each experiment. For analysis of VIC activation by immunostaining, over 100 cells were analyzed per sample. Conditions were compared using one-way ANOVAs in Prism (GraphPad) or the Transcriptome Analysis Console. In figures, error bars represent the standard error of the mean.

3.3. Results

3.3.1. VIC αSMA expression changes with culture platform

VICs were cultured on surfaces of hydrogels (2D) or encapsulated within hydrogels (3D) with the same composition and a Young's modulus of 390 Pa. Cells cultured in the gel formulations were then compared to cells cultured on traditional plates (TCPS) (Figure 3.1). The fibronectin-derived adhesive peptide CRGDS was incorporated to facilitate cell attachment to the matrix. Additionally, an enzymatically-degradable peptide was incorporated within the network to allow cells to locally degrade the matrix to permit cell spreading. The hydrogels were formed with an excess of –ene functionalities to reduce the crosslinking density, and therefore reduce the modulus. This formulation was chosen because the low crosslinking density permits cell spreading in 3D matrices within the timeframe of the experiments (48 hr). This modulus is also similar to the modulus of the aortic valve (E_{valve} ~ 1.1 -1.6 kPa; E_{gel} = 0.39 kPa; E_{TCPS} ~ 10^6 kPa).

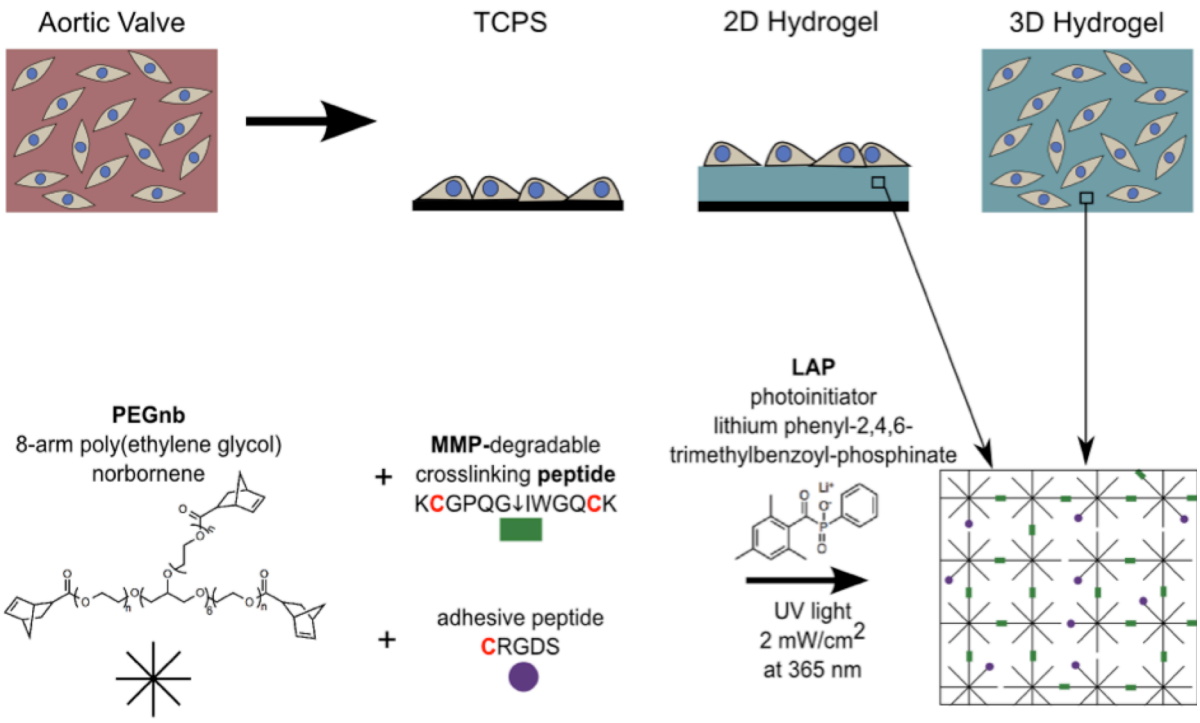

Figure 3.1. VIC culture platforms. VICs were isolated from porcine aortic valves and either saved for RNA isolation or plated and expanded to ~80% confluency. Then, cells were seeded on TCPS or 2D hydrogels or encapsulated within 3D hydrogels of the same formulation. Hydrogel matrices were formed by a photointiated thio-ene polymerization of 8-arm PEGnb (40 kDa) and an MMP-degradable peptide. The cleavage site is indicated by an arrow. A fibronectin-derived peptide, CRGDS, was incorporated to facilitate cell adhesion to the hydrogels. The cysteines indicated in red react with the norbornene groups on the PEG through a. thiol-ene, photoclick reaction.

VICs were stained for αSMA and f-actin after 48 hr of culture to give the cells time to attach to the matrix and spread out. VICs cultured on both TCPS and 2D hydrogel surfaces had elongated morphologies and prominent f-actin stress fibers (Figure 3.2A-C). In contrast, cells encapsulated within 3D hydrogels were smaller and had a more rounded morphology with protrusions extending into the matrix. VICs are likely less elongated in 3D because they must first degrade the local matrix before they can elongate. On TCPS, most VICs exhibited organized αSMA stress fibers, a hallmark of the myofibroblast phenotype. In contrast, VICs cultured on 2D

hydrogels or within 3D hydrogels expressed very little αSMA. Quantification of these images shows that hydrogel culture resulted in less than 5% activation, consistent with levels found in healthy aortic valves[5], in contrast to over 75% activation on TCPS (Figure 3.2D).

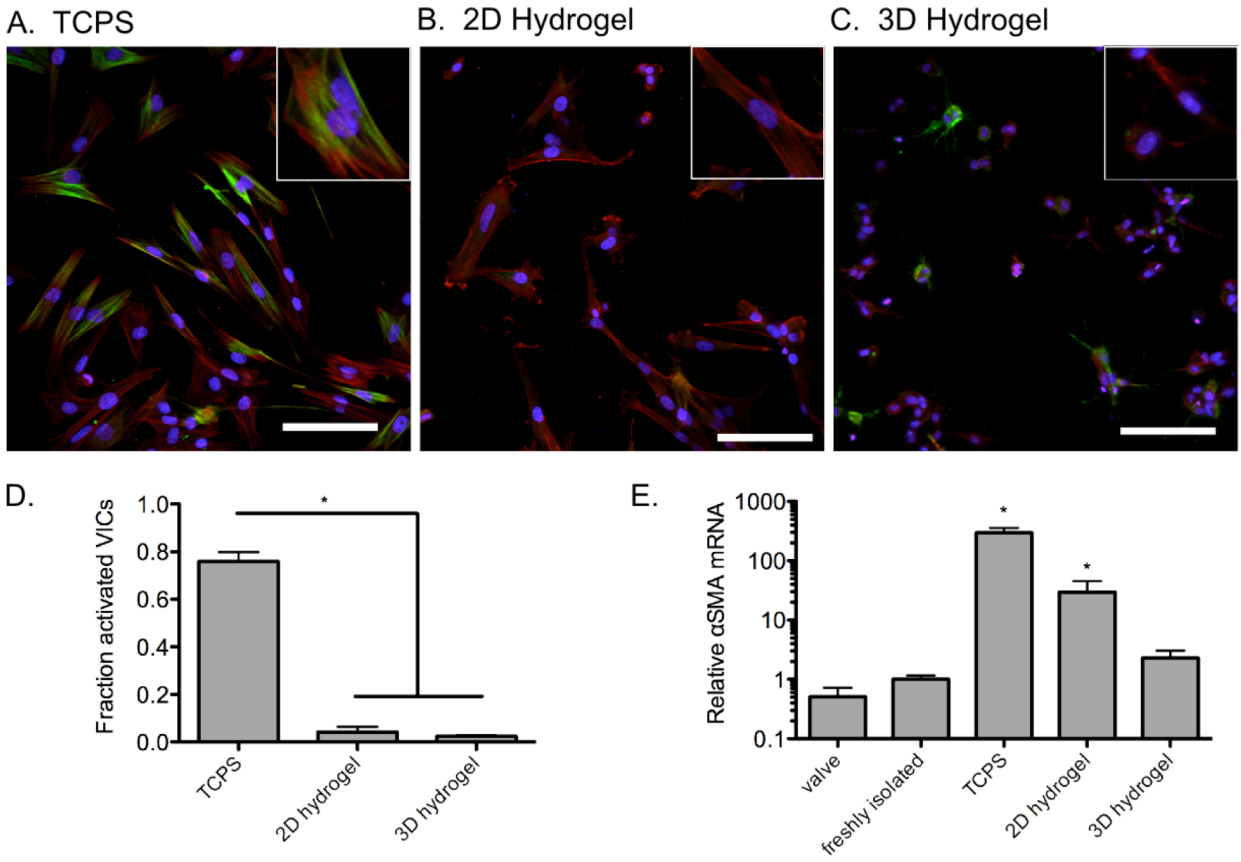

Figure 3.2. Characterization of VIC activation and αSMA expression. VICs A) on TCPS, B) on 2D hydrogels, and C) within 3D hydrogels were immunstained for αSMA (green), f-actin (red), and nuclei (blue). Scale bar = 100 μm. D) Images were quantified by counting the fraction of cells exhibiting αSMA stress fibers, a hallmark of the activated myofibroblast phenotype. On TCPS, most VICs were activated. With either the 2D or 3D hydrogel culture platforms, very low levels of activation were observed. * indicates $p<0.05$. E) qRT-PCR demonstrated that αSMA mRNA was greatly increased when VICs were cultured on TCPS compared to cells within the valve or to freshly isolated cells. When VICs were instead cultured on 2D hydrogels, there was an order of magnitude reduction in αSMA mRNA. In 3D hydrogels, the αSMA mRNA level was further reduced and was not significantly higher the freshly isolated VICs. * indicates $p<0.05$ compared to freshly isolated VICs.

αSMA expression was also examined at the mRNA level using qRT-PCR (Figure 3.2E). Freshly isolated VICs contained a similar level of αSMA mRNA as VICs still residing within the valve, indicating that the isolation procedure did not significantly perturb the VIC fibroblast phenotype towards a myofibroblast. In contrast, culturing VICs on TCPS resulted in an approximately 300-fold increase in αSMA expression. By simply culturing VICs on a softer 2D hydrogel, the αSMA mRNA was reduced by an order of magnitude compared to TCPS, and this was further reduced when the VICs were cultured within a 3D hydrogel where the αSMA level was only ~2-fold higher than the freshly isolated cells. While 2D and 3D hydrogel culture resulted in similar levels of VIC activation as measured by immunostaining for αSMA stress fibers, there was a large difference in αSMA mRNA expression. As one might expect differences at the gene and protein level, this result motivated our interest in better characterizing and quantifying the VIC phenotype through multiple measures.

3.3.2. VIC expression levels are highly dependent on the culture microenvironment

mRNA expression levels in VICs cultured on TCPS, 2D hydrogels, or within 3D hydrogels were compared to freshly isolated VICs using a porcine DNA microarray. VICs cultured on TCPS had differential expression compared to freshly isolated cells for 3304 probesets (out of 25470), where a difference was defined as a fold change greater than 2 or less than -2 and a p-value less than 0.05 to achieve statistical and biological significance (Figure 3.3A). The mRNA levels of many genes perturbed by TCPS culture returned to levels consistent with freshly isolated cells when VICs were instead cultured on top of or within soft hydrogels (E~390 Pa). However, one should note that each *in vitro* culture platform resulted in differential expression for many genes compared to freshly isolated VICs. For example, 2076 probe sets had

different levels of expression in all 3 *in vitro* conditions, which implies that stimuli present *in vivo* that were not incorporated into these *in vitro* cultures, such as signaling from other cell types and the mechanical deformation of the valve, also have an influence on the transcriptional profile. Here, we focus on the differences that arise from different culture substrates and the dimensionality of the microenvironment.

To assess the overall impact of the culture platform on the transcriptome, the data were translated into a complementary cumulative distribution to account for both the number of differentially regulated genes, as well as the magnitude of the changes (Figure 3.3B). In this representation, the number of genes that had a minimum fold change was plotted against the fold change. While TCPS culture did not result in more differentially expressed genes than hydrogel culture conditions, fold changes of greater magnitude were observed. In fact, the distribution is very similar for all of the culture conditions for low fold changes, but there is a divergence at a fold change of ~32. In the region of large fold changes, there are many more genes that are highly perturbed in VICs cultured on TCPS compared to either hydrogel condition. Additionally, 3D hydrogel cultures resulted in a somewhat lower incidence of the highly-differential genes than 2D hydrogels.

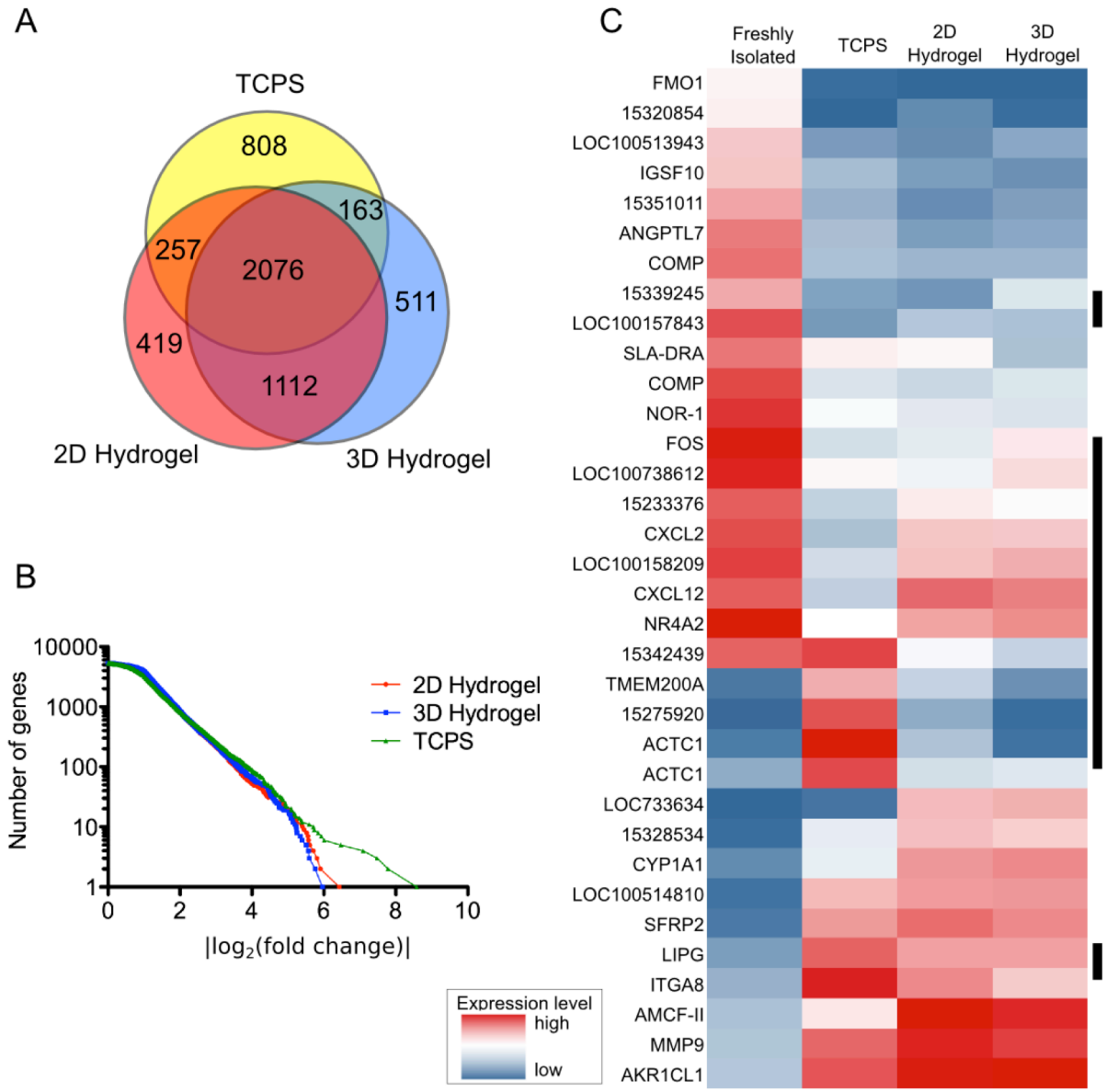

Figure 3.3. Culture platform directs VIC transcriptional profile. A) Venn diagram showing the number of genes in each culture condition with expression levels different than those seen in freshly isolated VICs. The center region of 2076 genes were differentially regulated in all *in vitro* conditions. B) Complementary cumulative distribution showing the number of genes with up to the given difference in RMA-normalized bi-weight averages. The tail on the TCPS distribution indicates that for a number of genes, expression levels are extremely affected by culture on TCPS. C) Heat map showing the expression levels of all genes with a $\log_2$(fold change) greater than 5 or less than -5 in any culture condition compared to freshly isolated cells and ordered by hierarchical clustering. Red represents high expression, blue represents low expression, and white represents an average level of expression. Genes with expression levels that were drastically altered by TCPS culture but recovered with culture on/in 2D or 3D hydrogels are marked on the side by the black lines.

The tails of this distribution were further examined by extracting out those genes with a fold change greater than 32 or less than -32 and representing the expression levels of these genes in a heat map (Figure 3.3C). Here, red represents high expression, blue represents low expression, and white represents average expression. This group includes genes related to cytoskeletal organization [α-cardiac muscle actin 1 (ACTC1)], cell-matrix interactions [integrin α8 (ITGA8)], matrix remodeling [MMP9, cartilage oligomeric matrix protein (COMP), keratocan-like protein (LOC100157843)], and chemokine activity (CXCL2, CXCL12). The subset of genes that are highlighted with black lines to the right of the figure were greatly perturbed by TCPS culture, but their expression levels were largely recovered in one or both of the hydrogel platforms.

3.3.3. Functions and pathways influenced by the culture platform

There are a number of functions and pathways that have been closely tied to VIC-matrix interactions that are important in regulation of VIC phenotype[8,23–28]. Here, we focused on some key functional categories to better understand the major differences between VICs cultured on TCPS, 2D or 3D hydrogels, and fresh isolates. Specifically, heat maps were generated to compare differentially expressed genes involved in cell-matrix interactions, cytoskeletal organization and contractility, TGF-β signaling, and matrix remodeling (Figure 3.4). The fold change compared to freshly isolated VICs is represented by the color, where warmer colors (red) indicate higher expression, and cooler colors (blue) indicate lower expression. Lighter colors represent expression levels similar to freshly isolated cells, and white indicates an expression level identical to the freshly isolated cells. In this analysis, many genes related to the cell

cytoskeleton and contractility are upregulated by plating VICs on TCPS; in contrast, expression levels of many of these upregulated genes are reduced to levels more similar to freshly isolated cells by culture on 2D hydrogels. Interestingly, a number of genes, including ACTA2 (αSMA), ACTC1, tropomyosin 1 (TPM1), and TPM2 remain at elevated levels regardless of the culture environment.

When comparing 2D versus 3D hydrogel cultures, the 3D environment results in expression patterns that are much more similar to freshly isolated VICs. This result suggests that dimensionality may play an important role in VIC cytoskeletal organization. The unnatural polarity and spread morphology observed in 2D cultures may drive changes in protein organization into cytoskeletal structures, as well as changes in the expression of these proteins at the mRNA level. While most of these genes were elevated in 2D, a few [ACTC1, calponin 1 (CNN1), and myosin (MYO, LOC100049650)] had lower expression in 3D hydrogels than in freshly isolated VICs. Perhaps over time, as encapsulated VICs remodel their microenvironment and are able to spread and develop more mature matrix interactions, these levels would become closer to those seen in the fresh isolate.

Focal adhesions are key transducers of the outside-in signaling that enables cells to sense cues from the extracellular matrix and generate forces. In our analysis, focal adhesion genes followed a similar pattern, with TCPS cultures exhibiting large differences in genes related to focal adhesions while the hydrogel platforms led to expression levels that were similar to freshly isolated VICs. For all of these genes, except ITGB1 and talin 1 (TLN1), 3D hydrogel culture more closely recapitulated the expression levels of freshly isolated VICs than the 2D hydrogel surfaces. Filamin B (FLNB), ITGA8, and vinculin (VCL) were the most upregulated by culture on TCPS. ITGA8 is an integrin that can bind ECM proteins, and FLNB and VCL are both

involved in anchoring focal adhesions to the actin cytoskeleton. ITGA2, another integrin, was dramatically downregulated on TCPS. Intuitively, overall upregulation of focal adhesion genes on TCPS might contribute to the ability of VICs to generate additional force and form αSMA stress fibers on this stiff substrate, leading to pathological activation.

Beyond cell-matrix interactions, TGF-β signaling is one of the key signaling pathways that has been implicated in VIC activation and in progression of valve disease. While it may not be intuitive that cytokine signaling would be influenced by the extracellular environment, expression levels of genes in this pathway were dependent on the culture platform. Genes related to TGF-β signaling were both up- and downregulated by culture on TCPS, while both hydrogel culture systems resulted in mostly reduced expression of these genes. The magnitudes of the differences in TGF-β signaling genes were smaller than those reported for the other categories. More of these genes were upregulated on TCPS than in 3D hydrogels, consistent with the higher activation levels and αSMA expression on TCPS; however, TGFB1 does not fit this trend. Interestingly, ITGA8 encodes a subunit of an integrin pair that binds the latent TGF- β1 protein, a step required for the protein to become active[29]. This indicates a mechanism by which a somewhat lower TGFB1 expression level could still lead to greater activation of the TGF-β signaling cascade. Bone morphogenetic proteins are also involved in the TGF-β signaling pathway and are important in the formation of calcific nodules frequently seen in patients with valve disease[30,31]. BMP3 was highly upregulated only by culture on TCPS, indicating a possible shift to a more osteoblast-like phenotype.

Matrix remodeling is a complex series of events that involve cell secretory properties (e.g., deposition of collagen), as well as secretion of proteases and inhibitors of those proteases (e.g., MMPs and TIMPs). When examining several genes related to matrix remodeling, a

number of genes, including various collagens, fibrillin 1 (FBN1), heparanase (HPSE), and ADAM metallopeptidase 19 (ADAM19) were elevated in VICs on TCPS, and the expression levels were more consistent with freshly isolated VICs in hydrogel matrices. Interestingly, on TCPS, some of the proteases (HPSE and ADAM19) were even more upregulated than the ECM proteins.

Matrix metalloproteases (MMPs) did not follow a consistent trend, with relatively constant expression of MMP2, upregulation of MMP14 only in hydrogel culture, and upregulation of MMP9 in all *in vitro* conditions. Genes encoding laminin α subunits, LAMA2 and LAMA4, had opposite trends, with lower LAMA2 expression and higher LAMA4 expression *in vitro*. This is interesting because it shows that VICs may alter the type of laminin expressed based on their microenvironment, with *in vitro* culture resulting in more of the laminin with a truncated α subunit. Among the *in vitro* conditions, VICs produce more LAMA4 in the 2D conditions (TCPS and 2D hydrogel) than in 3D hydrogels, perhaps indicating a response to the unnatural 2D environment.

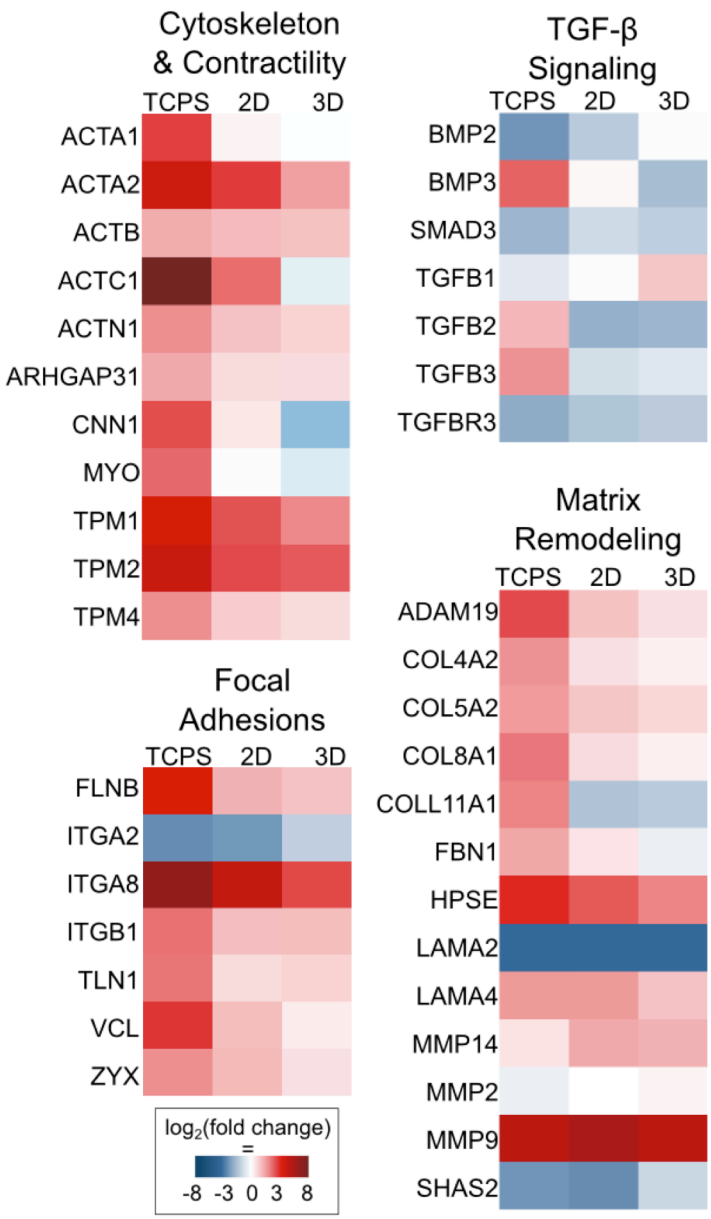

Figure 3.4. Culture platform influences functions critical to valve disease. Heat maps showing gene expression of differentially expressed genes for selected cell functions: cytoskeletal organization and contractility, TGF-β signaling, focal adhesions, and matrix remodeling. Fold change is represented by color on a log scale. Boxes closer to white represent expression levels similar to the freshly isolated VICs. White = same expression levels as freshly isolated VICs, blue = downregulated, red = upregulated.

3.3.4. The influence of dimensionality on VIC phenotype

In addition to better defining the VIC phenotype and studying the effect of culture microenvironment on alteration of this phenotype, we also sought to differentiate the effects of a 2D versus 3D culture environment in maintaining VIC phenotype. In particular, since 3D culture environments render many biological assays more difficult, we sought to quantify critical differences that might arise in VICs that are cultured in an identical matrix, but with a difference in dimensionality.

Using the Affymetrix Transcriptome Analysis Console, we directly compared mRNA levels in VICs seeded on soft hydrogel surfaces (2D) versus those encapsulated within the same hydrogel formulation (3D); 159 differentially expressed probe sets were identified using a cutoff of p-value less than 0.05 and fold change greater than 2 or less than -2. The functional importance of these genes was assessed using DAVID and the Panther gene ontology terms. At a macroscopic level, genes related to cell structure and motility, developmental processes, and proliferation and differentiation were enriched in the population of genes with higher expression in 2D, while transport-related genes were overrepresented in the genes with higher expression in 3D (Figure 3.5). Changes in cell structure and motility-related gene expression in response to the dimensionality show that observed differences in morphology and migration are not simply a result of physically confining the cells, but are also influenced by the underlying transcriptional profile. Developmental processes were also enriched on 2D hydrogels, indicating that the response to dimensionality may result in activation of similar cell functions as the changing extracellular environment in development. Cell proliferation and differentiation genes were also influenced by hydrogel dimensionality; however, this group includes both genes that promote [ephrin type A receptor 4 (EPHA4), KIT] and inhibit [inhibin beta A (INHBA)] proliferation.

Collectively, this assessment shows that while there are differences in the regulation of proliferation, it is difficult to elucidate the overall influence of dimensionality on proliferation based on these results alone. Genes with higher expression in encapsulated VICs were associated with transport of various molecules, including ions and lipids, in and out of the cell. The differences in these membrane channels are likely a result of the unnatural polarity induced in the VICs when they are seeded on a 2D surface.

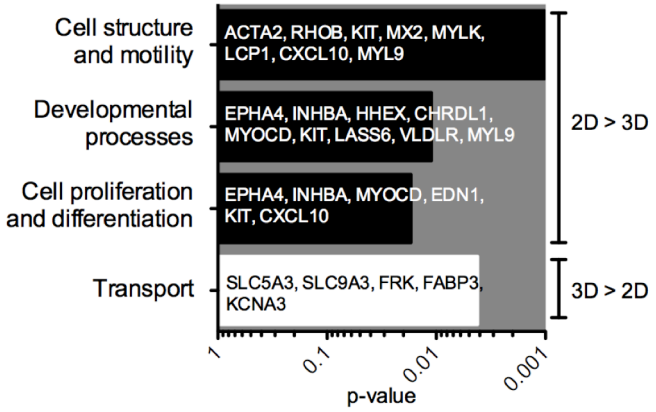

Figure 3.5. Biological processes influenced by dimensionality. Analysis with DAVID of biological processes (Panther database) that are enriched with genes that are differentially expressed in 2D vs. 3D hydrogels. Genes involved in cell structure and motility, developmental processes, and cell proliferation and differentiation had increased expression on 2D hydrogels, while genes associated with transport had higher expression in 3D hydrogels.

As not all phenotypic changes can be observed at the mRNA level, PathwayLinker was used to map differentially expressed genes (2D vs. 3D hydrogels), as well as the proteins that directly interact with the translated transcripts (Figure 3.6, Supplementary Information). While pathways of interest can be analyzed individually, this approach can obscure many complex ways in which signaling pathways interact. For example, tissue plasminogen activator (PLAT) is

a protein that regulates tissue remodeling[32], but Figure 3.6 shows that PLAT interacts with proteins involved in cell adhesion signaling, actin cytoskeleton organization, and TGF-β signaling. These interactions demonstrate the difficulty of independently studying any one of these pathways in isolation. Another gene of particular interest is KIT, a kinase involved in activation of several signaling pathways, including AKT, RAS, and MAPK[33]. The high level of connectivity to other genes of interest suggests that this kinase could be a key regulator of the VIC response to dimensionality.

3.4. Discussion

VICs are important regulators of valve ECM, but pathological VIC activation leads to excessive collagen deposition, a disorganized matrix, and valve fibrosis[6]. Mechanisms contributing to this disease state are still being elucidated, and there are no clinical treatments to slow or reverse valve fibrosis[4]. While there are no large animal models of valve disease that extend beyond the stage of early valve sclerosis, several research groups have developed mouse models of valve disease that often involve a combination of genetic and diet modifications[34,35]. While much is learned from these animal models, *in vitro* models of valve cells would provide complementary information and allow for more detailed hypothesis testing to support or help refine ideas related to targets for reversing fibrosis. However, traditional culture of VICs primarily leads to a myofibroblast phenotype[8], and it is difficult, at best, to characterize the quiescent VIC fibroblasts or study conditions that would lead to reversal of the pathogenic VIC myofibroblast population. Part of the complexity is that VICs receive cues from the extracellular matrix that cannot be recapitulated by culture on TCPS, which has a stiffness that is greater than six orders of magnitude higher than valve tissue.

In this study, soft (E = 390 Pa) hydrogels were used as a culture platform to study VICs under conditions in which they are not always activated to the myofibroblast phenotype, as seen when using traditional cell culture methods[8]. Specifically, we used PEG-based hydrogels with an MMP-degradable crosslinking peptide and the fibronectin-derived CRGDS peptide to mimic aspects of the extracellular matrix by allowing local cell remodeling, spreading, and adhesion. The gels were formed via a cytocompatible photoinitiated thiol-ene polymerization[16]. This platform allows for the use of the exact same material in both 2D and 3D hydrogel culture conditions, and this synthetic polymer system also enables precise control over the mechanical and biochemical matrix cues presented to VICs. While the local modulus around the VICs may vary over time due to cellular remodeling of the matrix, these PEG-based hydrogels maintain consistent bulk mechanical properties throughout the 48 hr culture time, while VICs encapsulated within collagen or Matrigel can contract the matrix and dramatically alter the material properties [36]. In this study, only one adhesive ligand (CRGDS) was tested, but others have shown that adhesive peptides derived from different ECM proteins can influence VIC secretory properties and ECM deposition[25]. Investigating the influence of various adhesive ligand sequences on VIC gene expression would likely lead to identification of different integrin signaling cascades and aid in the design of matrices for valve regeneration. Here, we chose to focus on the influence of dimensionality of VIC function, as previous work has demonstrated that dimensionality has a greater impact on embryonic stem cell gene expression than specific ECM proteins (e.g., collagen vs. gelatin)[37].

Many efforts to elucidate the effects of dimensionality compare cells in native tissue or aggregates to those cultured on TCPS[38–41]. These experiments are certainly pioneering and relevant, but many variables change from native ECM to TCPS, in addition to the dimensionality

(e.g., modulus, chemical composition). Because of this, one must use caution when drawing conclusions about the importance of dimensionality, and this motivated our experimental design to use a highly controlled hydrogel matrix in this study. Consistent with previous studies[8], we have shown that VICs cultured on TCPS have a dramatically altered phenotype compared to freshly isolated cells. In addition to an increased proportion of cells expressing the myofibroblast phenotype (Figure 3.2), culturing VICs on TCPS results in significant changes in expression levels for 3304 probe sets.

In this study, we found that each of the *in vitro* culture conditions resulted in some differences in gene expression levels compared to the freshly isolated cells (Figure 3A). It is not surprising that a number of genes would always be different in an *in vitro* culture system, as there are a number of complex stimuli that influence VICs *in vivo*. For example, none of the culture platforms include any cell types other than the VICs. Specifically, valvular endothelial cells have been shown to play a role in regulating VIC phenotype[42–45]. Cells involved in the inflammatory response, such as macrophages and T lymphocytes, have also been excluded from this study. This is not necessarily a disadvantage though, because excluding other cell types allows one to focus on the effects of matrix mechanics and eliminate confounding interactions that could occur in a model with added complexity. Another simplification in these *in vitro* studies is the mechanically static nature of all of the culture platforms. *In vivo*, the valve is exposed to bending, stretching, and blood flow. These stresses on the cells can also influence their phenotype and these dynamics warrant future study, but we expect that using static culture platforms introduces some of the differences in gene expression that are common to each culture method.

While both 2D and 3D hydrogel conditions had a greater number of differentially expressed genes than TCPS culture, using the standard criteria of fold change greater than 2 and p-value less than 0.05, the distribution of the fold changes shows that TCPS leads to a population of genes that have very high fold changes not seen in hydrogel culture (Figure 3B). Additionally, this distribution reveals that culture in 3D hydrogels results in slightly fewer genes with extreme fold changes than 2D hydrogel substrates. Many of the highly perturbed genes, including ACTC1, NR4A2, ITGA8, and FOS, returned to levels more consistent with freshly isolated VICs in one or both of the hydrogel culture platforms.

Culture on TCPS dramatically changes VIC phenotype. Conventional VIC characterization methods may suggest that TCPS represents a fibrotic microenvironment, but our results show that it represents something more extreme than typical disease. When the cells are characterized simply by the most common methods of αSMA quantification or staining for αSMA stress fibers, these cells appear to be acting similarly to diseased VICs, with higher levels of αSMA and a large fraction of cells exhibiting the myofibroblast phenotype. However, upon a more global examination of gene expression levels, we have seen that culturing VICs on TCPS results in more changes in gene expression than exist when comparing healthy and stenotic aortic valves in a similar experiment. Bosse *et al.* found that 1002 of 54675 probe sets showed significant differences between expression in healthy and stenotic valves[30]. When the same criteria are applied to this study, 6316 out of 25470 probe sets showed differences between freshly isolated VICs and VICs cultured on TCPS. While results obtained from different array chips are not directly comparable, this significant difference supports the idea that even though VICs cultured on TCPS resemble diseased VICs more than healthy VICs, TCPS may still be a poor model for valve disease because so many additional genes are also perturbed. For example,

if one were to screen for inhibitors of pathogenic VIC myofibroblasts on TCPS, certain candidates may be missed as the VIC context is important and can influence receptor signaling, concentration profiles, and mechanotransduction.

This study demonstrates that the choice of culture platform (TCPS, 2D hydrogel, or 3D hydrogel) can influence many genes and cellular functions associated with VIC activation and valve disease, such as cytoskeletal organization and contractility, focal adhesions, TGF-β signaling, and matrix remodeling. Overall, these findings demonstrate the importance of choosing a culture platform relevant to the pathway or function of interest to ensure that critical genes are not vastly up- or downregulated. Genes related to cytoskeletal organization were expressed at different levels in each of the culture conditions. 3D hydrogels resulted in an expression profile most similar to freshly isolated VICs, and 2D hydrogels did not perturb expression levels as much as TCPS. This indicates that both the dimensionality and the substrate modulus are influencing cytoskeletal organization. This same finding held true for focal adhesion genes, where 3D hydrogel culture best recapitulated the expression levels in freshly isolated VICs. As focal adhesions are the key structures that mediate the interaction between cells and the ECM, it is interesting to note that VICs in different culture conditions are not only interacting with different environments, but are also changing the way in which they mediate their interactions with their environment. In contrast, TGF-β signaling genes had similar levels of expression in both 2D and 3D hydrogels, indicating that dimensionality has less of an influence on this pathway. The modulus of the matrix has been implicated in the ability of fibroblasts to activate TGF-β1 from its latent form[46], so the matrix modulus may play a larger role in TGF-β signaling.

The up- or downregulation of many matrix remodeling genes was unpredictable, with TCPS increasing the level of some ECM genes (LAMA4, many collagens) and decreasing the expression of others (LAMA2, SHAS2). Similarly, proteases were both upregulated (MMP9, HPSE) and downregulated (MMP2). It is perhaps counterintuitive that the proteases HPSE and ADAM19 were more highly expressed in cells on a 2D surface than they are in cells entrapped within a 3D matrix. The matrix stiffness may play a role, but does not entirely account for this difference. It is possible that this result is a function of the relatively short (48 hr) time point at which these samples were collected, and further investigation as a function of time, when more extensive matrix remodeling has occurred, should provide added insight. From this data, it is difficult to conclude whether this would result in overall increases in ECM deposition, yet it seems clear that this transcriptional profile of matrix remodeling genes would result in different tissue architecture. For the most part, expression levels in hydrogel cultures were more similar to those seen in freshly isolated VICs; however, LAMA2 and MMP9 remained highly perturbed in all conditions.

While 3D hydrogel culture resulted in expression levels that were slightly more similar to freshly isolated VICs than the 2D hydrogel culture, there were not dramatic differences in expression patterns of these matrix remodeling genes. The physical remodeling of the matrix must be highly dependent on dimensionality as 3D environments necessitate cell degradation of the matrix to spread or migrate, and the dimensionality of the environment would almost certainly influence the ability of the cells to incorporate secreted ECM proteins into the surrounding matrix. These changes may be more apparent at a later time point than the 48 hour culture studied here, as most studies of tissue engineering of a valve look at time points weeks or months after seeding[47,48]. With respect to this, microarray data presenting expression levels of

ECM-related genes could be complemented by studies focused on histological staining of gels or thorough quantitative assays to measure ECM proteins.

The global view comparing RNA levels in different culture platforms to freshly isolated cells also provides valuable insight into the choice of reference or "housekeeping" genes. Traditionally, internal standards have been chosen because they did not appear to vary after treatment with various drugs or other molecules. A number of genes have become commonly accepted internal standards, including GAPDH, ACTB (β-actin), and genes encoding ribosomal proteins. While the expression levels of these genes may not vary significantly among experiments on TCPS, these microarray results show that some of these genes may be a poor choice when comparing *in vitro* to *in vivo* experiments (Figure 3.7, Supplementary Information). Specifically, both GAPDH and ACTB are expressed at significantly different levels on TCPS compared to freshly isolated VICs. Many ribosomal genes were much more consistently expressed, with RPS18, RPL30, and RPL32 not exhibiting any significant differences between any conditions. These findings are generally consistent with a previous study comparing thousands of human and mouse arrays, which found high variability in ACTB, GAPDH, HPRT1, and B2M and instead recommended mostly genes encoding ribosomal proteins[49].

Collectively, this study provides quantitative measures of the importance of the culture platform on VIC behavior *in vitro*. Building on these findings, future studies to identify pathways that might be leveraged to prevent or reverse valve disease could be enabled by exploiting soft, 3D hydrogel environments that better recapitulate native gene expression levels. Such studies are difficult to perform on TCPS, as it significantly perturbs baseline expression levels of key myofibroblast markers and might lead to false negatives when screening for useful therapeutics. Additionally, signaling cascades initiated by therapeutics may have important interactions with

mechanotransduction pathways[50]. While 3D hydrogel culture led to transcriptional profiles more similar to freshly isolated VICs, there are still many differences. In order to study a pathway of interest that involves many of these differentially regulated genes, it may be worthwhile to develop new culture platforms that better recapitulate the desired pathway by modifying matrix characteristics, such as the modulus or the functionalization with peptides, or by focusing on other elements present *in vivo*, such as valvular endothelial cells or cyclic strain. Many of these questions could be addressed by modifying the materials presented here to incorporate additional complexity, as PEG hydrogels are amenable to co-culture with valvular endothelial cells[45], integration into microfluidic devices[51], and culture with bioreactors[52].

3.5. Conclusions

Microarray analysis of VIC transcriptional profiles reveals and quantifies how cell phenotype *in vitro* is highly dependent on the culture platform. This global transcriptome analysis shows that TCPS culture results in higher-magnitude changes to gene expression levels than either 2D or 3D culture. Culture on TCPS greatly perturbed many genes related to cytoskeletal organization and contractility, focal adhesions, TGF-β signaling, and matrix remodeling, demonstrating the importance of considering which culture platforms are appropriate for studying specific cell functions or pathways. While characterizing the percentage of VICs expressing the myofibroblast or fibroblast phenotype is a useful metric, we have demonstrated that populations of VICs with the same activation levels can have dramatically different phenotypes, which emphasizes the importance of using multiple measures to characterize cell response to microenvironmental cues.

3.6. Acknowledgements

The authors would like to thank Dr. William Wan for helpful discussions and An Doan and Wen Hua Ren at the Genomics and Microarray Core and University of Colorado at Denver for microarray experiments. The authors would also like to acknowledge support to KMM from an NIH Pharmaceutical Biotechnology Training Grant and funding from Howard Hughes Medical Institute (HHMI).

3.7. References

1. Durbin, A. D. & Gotlieb, A. I. Advances towards understanding heart valve response to injury. *Cardiovasc. Pathol.* **11,** 69–77 (2002).

2. Liu, A. C., Joag, V. R. & Gotlieb, A. I. The emerging role of valve interstitial cell phenotypes in regulating heart valve pathobiology. *Am. J. Pathol.* **171,** 1407–18 (2007).

3. Merryman, W. D. & Schoen, F. J. Mechanisms of calcification in aortic valve disease: role of mechanokinetics and mechanodynamics. *Curr. Cardiol. Rep.* **15,** 355 (2013).

4. Lindman, B. R., Bonow, R. O. & Otto, C. M. Current management of calcific aortic stenosis. *Circ. Res.* **113,** 223–37 (2013).

5. Rabkin-Aikawa, E., Farber, M., Aikawa, M. & Schoen, F. J. Dynamic and reversible changes of interstitial cell phenotype during remodeling of cardiac valves. *J. Heart Valve Dis.* **13,** 841–7 (2004).

6. Bowler, M. A. & Merryman, W. D. In vitro models of aortic valve calcification: solidifying a system. *Cardiovasc. Pathol.* **24,** 1–10 (2015).

7. Miyake, K., Satomi, N. & Sasaki, S. Elastic modulus of polystyrene film from near surface to bulk measured by nanoindentation using atomic force microscopy. *Appl. Phys. Lett.* **89,** 18–21 (2006).

8. Wang, H., Tibbitt, M. W., Langer, S. J., Leinwand, L. A. & Anseth, K. S. Hydrogels preserve native phenotypes of valvular fibroblasts through an elasticity-regulated PI3K/AKT pathway. *Proc. Natl. Acad. Sci.* **110,** 19336–19341 (2013).

9. Hutcheson, J. D., Setola, V., Roth, B. L. & Merryman, W. D. Serotonin receptors and heart valve disease-It was meant 2B. *Pharmacol. Ther.* **132,** 146–157 (2011).

10. Kloxin, A. M., Benton, J. A. & Anseth, K. S. In situ elasticity modulation with dynamic substrates to direct cell phenotype. *Biomaterials* **31,** 1–8 (2010).

11. Mabry, K. M., Lawrence, R. L. & Anseth, K. S. Dynamic stiffening of poly(ethylene glycol)-based hydrogels to direct valvular interstitial cell phenotype in a three-dimensional environment. *Biomaterials* **49,** 47–56 (2015).

12. Walker, G. A., Masters, K. S., Shah, D. N., Anseth, K. S. & Leinwand, L. A. Valvular myofibroblast activation by transforming growth factor-beta: implications for pathological extracellular matrix remodeling in heart valve disease. *Circ. Res.* **95,** 253–60 (2004).

13. Carabello, B. A. Introduction to aortic stenosis. *Circ. Res.* **113,** 179–85 (2013).

14. Johnson, C. M., Hanson, M. N. & Helgeson, S. C. Porcine cardiac valvular subendothelial cells in culture: cell isolation and growth characteristics. *J. Mol. Cell. Cardiol.* **19,** 1185–93 (1987).

15. Fairbanks, B. D. *et al.* A Versatile Synthetic Extracellular Matrix Mimic via Thiol-Norbornene Photopolymerization. *Adv. Mater.* **21,** 5005–5010 (2009).

16. Benton, J. A., Fairbanks, B. D. & Anseth, K. S. Characterization of valvular interstitial cell function in three dimensional matrix metalloproteinase degradable PEG hydrogels. *Biomaterials* **30,** 6593–603 (2009).

17. Bryant, S. J. & Anseth, K. S. Hydrogel Scaffolds.

18. Huang, D. W., Sherman, B. T. & Lempicki, R. A. Systematic and integrative analysis of large gene lists using DAVID bioinformatics resources. *Nat. Protoc.* **4,** 44–57 (2009).

19. Huang, D. W., Sherman, B. T. & Lempicki, R. A. Bioinformatics enrichment tools: Paths toward the comprehensive functional analysis of large gene lists. *Nucleic Acids Res.* **37,** 1–13 (2009).

20. Mi, H., Muruganujan, A. & Thomas, P. D. PANTHER in 2013: Modeling the evolution of gene function, and other gene attributes, in the context of phylogenetic trees. *Nucleic Acids Res.* **41,** 377–386 (2013).

21. Mi, H. & Thomas, P. Protein Networks and Pathway Analysis. *Methods Mol. Biol.* **563,** 123–140 (2009).

22. Farkas, I. J., Szántó-Várnagy, Á. & Korcsmáros, T. Linking proteins to signaling pathways for experiment design and evaluation. *PLoS One* **7,** 1–5 (2012).

23. Yip, C. Y. Y., Chen, J.-H., Zhao, R. & Simmons, C. A. Calcification by valve interstitial cells is regulated by the stiffness of the extracellular matrix. *Arterioscler. Thromb. Vasc. Biol.* **29,** 936–42 (2009).

24. Gu, X. & Masters, K. S. Regulation of valvular interstitial cell calcification by adhesive peptide sequences. *J. Biomed. Mater. Res. A* **93,** 1620–30 (2010).

25. Gould, S. & Anseth, K. Role of cell-matrix interactions on VIC phenotype and tissue depostion in 3D PEG hydrogels. *J. Tissue Eng. Regen. Med.* (2013). doi:10.1002/term.1836

26. Fayet, C., Bendeck, M. P. & Gotlieb, A. I. Cardiac valve interstitial cells secrete fibronectin and form fibrillar adhesions in response to injury. *Cardiovasc. Pathol.* **16,** 203–11 (2007).

27. Duan, B., Hockaday, L. A., Kapetanovic, E., Kang, K. H. & Butcher, J. T. Stiffness and adhesivity control aortic valve interstitial cell behavior within hyaluronic acid based hydrogels. *Acta Biomater.* **9,** 7640–50 (2013).

28. Cushing, M. C., Liao, J.-T. & Anseth, K. S. Activation of valvular interstitial cells is mediated by transforming growth factor-beta1 interactions with matrix molecules. *Matrix Biol.* **24,** 428–37 (2005).

29. Lu, M. *et al.* Integrin alpha8beta1 mediates adhesion to LAP-TGFbeta1. *J. Cell Sci.* **115,** 4641–4648 (2002).

30. Bossé, Y. *et al.* Refining molecular pathways leading to calcific aortic valve stenosis by studying gene expression profile of normal and calcified stenotic human aortic valves. *Circ. Cardiovasc. Genet.* **2,** 489–98 (2009).

31. O'Brien, K. D. Pathogenesis of calcific aortic valve disease: a disease process comes of age (and a good deal more). *Arterioscler. Thromb. Vasc. Biol.* **26,** 1721–8 (2006).

32. Eitzman, D. T. *et al.* Bleomycin-induced pulmonary fibrosis in transgenic mice that either lack or overexpress the murine plasminogen activator inhibitor-1 gene. *J. Clin. Invest.* **97,** 232–237 (1996).

33. Edling, C. E. & Hallberg, B. c-Kit-A hematopoietic cell essential receptor tyrosine kinase. *Int. J. Biochem. Cell Biol.* **39,** 1995–1998 (2007).

34. Miller, J. D., Weiss, R. M. & Heistad, D. D. Calcific aortic valve stenosis: methods, models, and mechanisms. *Circ. Res.* **108,** 1392–412 (2011).

35. Miller, J. D. *et al.* Lowering plasma cholesterol levels halts progression of aortic valve disease in mice. *Circulation* **119,** 2693–2701 (2009).

36. Butcher, J. T. & Nerem, R. M. Porcine aortic valve interstitial cells in three-dimensional culture: comparison of phenotype with aortic smooth muscle cells. *J. Heart Valve Dis.* **13,** 478–85; discussion 485–6 (2004).

37. Wei, J. *et al.* The importance of three-dimensional scaffold structure on stemness maintenance of mouse embryonic stem cells. *Biomaterials* **35,** 7724–7733 (2014).

38. Chambers, K. F., Mosaad, E. M. O., Russell, P. J., Clements, J. A. & Doran, M. R. 3D Cultures of Prostate Cancer Cells Cultured in a Novel High-Throughput Culture Platform Are More Resistant to Chemotherapeutics Compared to Cells Cultured in Monolayer. *PLoS One* **9,** e111029 (2014).

39. DiMarco, R. L. *et al.* Engineering of three-dimensional microenvironments to promote contractile behavior in primary intestinal organoids. *Integr. Biol. (Camb).* **6,** 127–42 (2014).

40. Huang, Y. & Hsu, S. Acquisition of epithelial-mesenchymal transition and cancer stem-like phenotypes within chitosan-hyaluronan membrane-derived 3D tumor spheroids. *Biomaterials* **35,** 10070–10079 (2014).

41. Rodriguez, K. J., Piechura, L. M. & Masters, K. S. Regulation of valvular interstitial cell phenotype and function by hyaluronic acid in 2-D and 3-D culture environments. *Matrix Biol.* **30,** 70–82 (2011).

42. Butcher, J. T. & Nerem, R. M. Valvular endothelial cells and the mechanoregulation of valvular pathology. *Philos. Trans. R. Soc. Lond. B. Biol. Sci.* **362,** 1445–57 (2007).

43. Butcher, J. T. & Nerem, R. M. Valvular endothelial cells regulate the phenotype of interstitial cells in co-culture: effects of steady shear stress. *Tissue Eng.* **12,** 905–15 (2006).

44. Bernardini, C. *et al.* Differential expression of nitric oxide synthases in porcine aortic endothelial cells during LPS-induced apoptosis. *J. Inflamm. (Lond).* **9,** 47 (2012).

45. Gould, S. T., Matherly, E. E., Smith, J. N., Heistad, D. D. & Anseth, K. S. The role of valvular endothelial cell paracrine signaling and matrix elasticity on valvular interstitial cell activation. *Biomaterials* **35,** 3596–3606 (2014).

46. Wipff, P.-J., Rifkin, D. B., Meister, J.-J. & Hinz, B. Myofibroblast contraction activates latent TGF-beta1 from the extracellular matrix. *J. Cell Biol.* **179,** 1311–23 (2007).

47. Nakayama, Y. *et al.* In-body tissue-engineered aortic valve (Biovalve type VII) architecture based on 3D printer molding. *J. Biomed. Mater. Res. B. Appl. Biomater.* 10–12 (2014). doi:10.1002/jbm.b.33186

48. Schmidt, D. *et al.* Minimally-invasive implantation of living tissue engineered heart valves: a comprehensive approach from autologous vascular cells to stem cells. *J. Am. Coll. Cardiol.* **56,** 510–20 (2010).

49. De Jonge, H. J. M. *et al.* Evidence based selection of housekeeping genes. *PLoS One* **2,** 1–5 (2007).

50. Park, C. Y. *et al.* High-throughput screening for modulators of cellular contractile force. *Integr. Biol.* (2015). doi:10.1039/C5IB00054H

51. Burdick, J. A. & Anseth, K. S. Photoencapsulation of osteoblasts in injectable RGD-modified PEG hydrogels for bone tissue engineering. *Biomaterials* **23,** 4315–23 (2002).

52. Hahn, M. S., McHale, M. K., Wang, E., Schmedlen, R. H. & West, J. L. Physiologic pulsatile flow bioreactor conditioning of poly(ethylene glycol)-based tissue engineered vascular grafts. *Ann. Biomed. Eng.* **35,** 190–200 (2007).

3.8. Supplementary Information

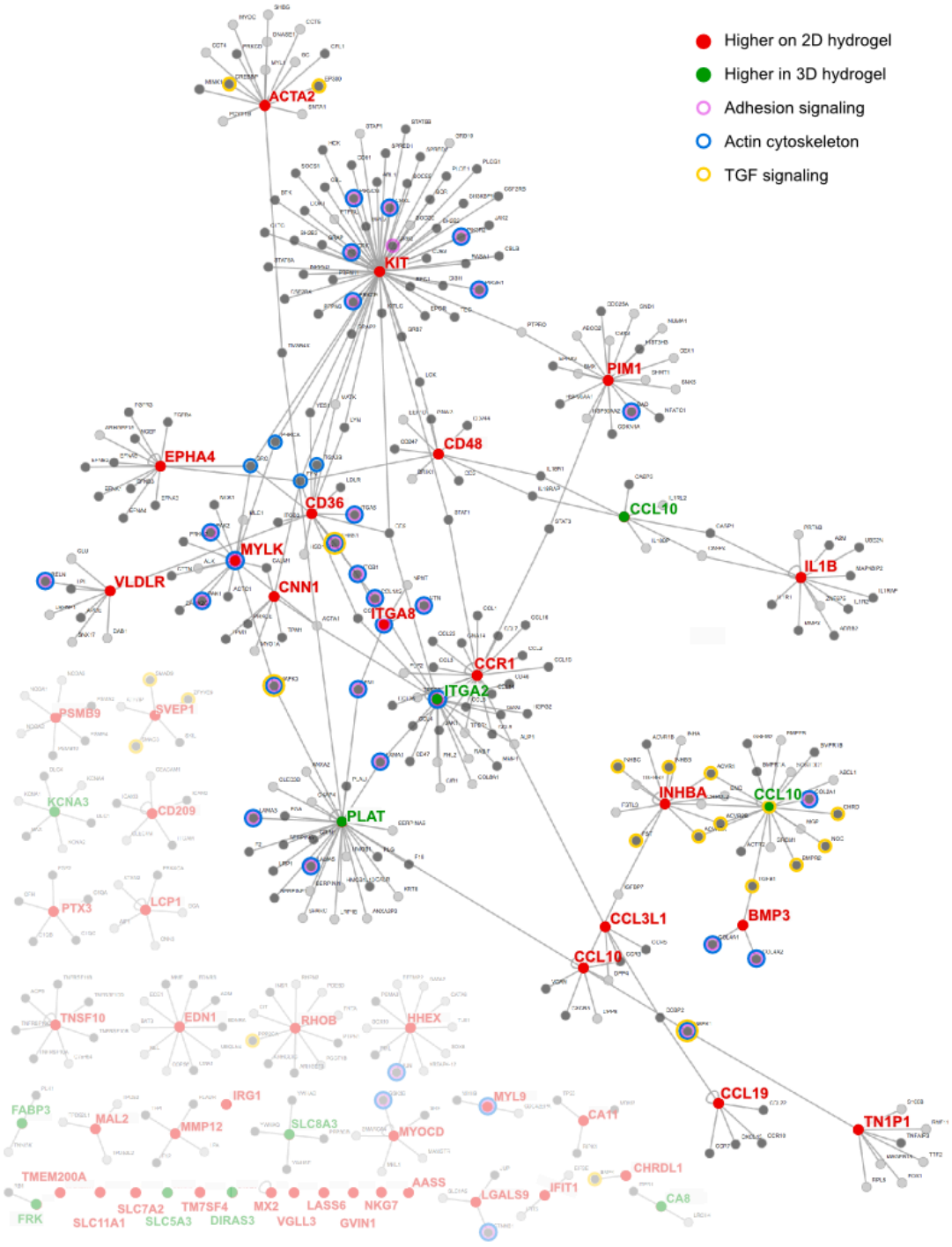

Figure 3.6. Map of genes that are differentially expressed in 2D or 3D hydrogel cultures. Genes upregulated on 2D hydrogels (red) or in 3D hydrogels (green) are connected to proteins with which they have first-order interactions. Genes involved in pathways related to adhesion signaling (pink), actin cytoskeleton (blue), and TGF-β signaling (yellow) are highlighted.

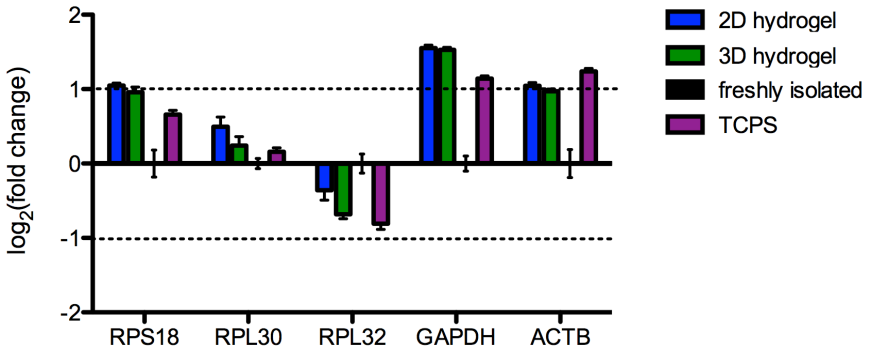

Figure 3.7. Expression levels of some traditional housekeeping genes from porcine microarray study. GAPDH, which has a greater than 2-fold change in expression in all of the culture platforms, is not a good choice for comparing *in vitro* and *in vivo* data. RPL30 has fairly consistent expression levels across all of the culture platforms.

Chapter 4

Dynamic stiffening of poly(ethylene glycol)-based hydrogels to direct valvular interstitial cell phenotype in a three-dimensional environment

---

Abstract

Valvular interstitial cells (VICs) are active regulators of valve homeostasis and disease, responsible for secreting and remodeling the valve tissue matrix. As a result of VIC activity, the valve modulus can substantially change during development, injury and repair, and disease progression. While two-dimensional biomaterial substrates have been used to study mechanosensing and its influence on VIC phenotype, less is known about how these cells respond to matrix modulus in a three-dimensional environment. Here, we synthesized MMP-degradable poly(ethylene glycol) (PEG) hydrogels with elastic moduli ranging from 0.24 kPa to 12 kPa and observed that cell morphology was constrained in stiffer gels. To vary gel stiffness without substantially changing cell morphology, cell-laden hydrogels were cultured in the 0.24 kPa gels for 3 days to allow VIC spreading, and then stiffened *in situ* via a second, photoinitiated thiol-ene polymerization such that the gel modulus increased from 0.24 kPa to 1.2 kPa or 13 kPa. VICs encapsulated within soft gels exhibited αSMA stress fibers (~40%), a hallmark of the myofibroblast phenotype. Interestingly, in stiffened gels, VICs became deactivated to a quiescent fibroblast phenotype, suggesting that matrix stiffness directs VIC phenotype

independent of morphology, but in a manner that depends on the dimensionality of the culture platform. Collectively, these studies present a versatile method for dynamic stiffening of hydrogels and demonstrate the significant effects of matrix modulus on VIC myofibroblast properties in three-dimensional environments.

4.1. Introduction

Valvular interstitial cells (VICs) are the most prevalent cell type in heart valves and actively regulate the progression of valve disease[1]. In a healthy valve, the majority of VICs are quiescent fibroblasts[2]. These cells can be activated to myofibroblasts, which exhibit increased proliferation, cytokine secretion, and matrix remodeling, and are associated with disease progression[1,3–5]. The fraction of the population of VICs exhibiting the myofibroblast phenotype changes throughout a person's development and lifetime. Early in development, the majority of VICs are positive for αSMA. In healthy adults, almost all of the VICs are quiescent, but activation levels are increased once again in diseased valves[6].

VIC phenotype has been characterized using various metrics. Alpha smooth muscle actin (αSMA) is a commonly used marker for myofibroblast-like cells[7,8]. The presence of organized αSMA stress fibers as determined by immunostaining is often used to classify VICs as quiescent fibroblasts (no stress fibers) or activated myofibroblasts (stress fibers present)[3,9,10]. In contrast, the mesenchymal marker S100A4 (also known as fibroblast-specific protein 1) has been shown to increase when VICs are quiescent[11]. These measures provide useful readouts for a general screen to determine how VIC phenotype responds to various treatments or culture conditions.

With respect to the VIC microenvironment, the matrix mechanics can be an important regulator of VIC phenotype, where elastic modulus has been shown to influence VIC

myofibroblast activation. While variations exist in the values reported for the threshold for activation, 2D experiments generally show that lower substrate elasticities (< ~5 kPa) lead to mostly quiescent VICs and higher substrate elasticities (> ~25 kPa) activate most VICs to myofibroblasts, with a range of activation levels observed at intermediate elasticities[9,10]. These trends recapitulate aspects of valve disease, with the stiffer, disease-like substrates leading to the myofibroblast phenotype that is more prevalent in diseased valves. Additionally, this activation is reversible and responsive to changes in the local environmental mechanics, where *in situ* softening of hydrogels has been used to study VIC deactivation[12]. Substrate modulus has also been shown to influence VIC morphology and calcification, with stiffer substrates leading to a more spread, elongated morphology and higher levels of calcium deposition[10,13]. While there has been much progress in understanding how VICs respond to mechanical and biochemical cues in two dimensions, less is known about how these factors may influence phenotype in a three-dimensional environment.

The dimensionality of a cell's microenvironment can profoundly impact function (e.g., proliferation, morphology, polarity, motility), and changes in dimensionality can limit cell-cell interactions, availability of soluble factors[14], and even influence gene expression[15]. Butcher *et al.* encapsulated VICs in collagen gels and found that encapsulated VICs (3D) expressed less αSMA compared to VICs seeded on top of collagen gels (2D)[16]. As a complement to collagen and other naturally-derived protein matrices, Benton *et al.* encapsulated VICs within proteinase-degradable, PEG-based hydrogels and found that when the adhesive peptide, RGDS, was incorporated, the cells attached to the matrix via $\alpha_v\beta_3$ integrins and were able to spread and elongate within the hydrogel[17]. Furthermore, αSMA expression was found to increase with culture time over 14 days and was dependent on TGF-β1 treatment. These studies have improved

our understanding of how VICs behave in response to 3D culture, and have motivated the study of the influence of matrix mechanics on VIC phenotype in 3D.

To elucidate cellular response to mechanical cues in 3D, VICs have been co-encapsulated with PEG microrods of varying moduli within Matrigel; VICs exposed to stiff microrods exhibited reduced αSMA production and decreased proliferation[18]. This study showed a relationship between the presence of stiff microrods and myofibroblast deactivation, but provided mechanical differences by the use of discrete regions of higher modulus rather than changing the modulus in the entire volume to which the cells were exposed. To more directly measure forces exerted by encapsulated cells, VICs have been encapsulated in fibrin gels attached to posts providing a range of boundary stiffnesses, where it was observed that the combination of stiff boundary posts and addition of TGF-β1 resulted in increased cell force generation[19]. Duan *et al.* encapsulated VICs within hyaluronic acid-based hydrogels to study their response to modulus in a 3D environment. Hydrogel modulus was varied by changing the hyaluronic acid molecular weight and degree of methacrylation and by incorporating methacrylated gelatin into the hydrogels. By immunostaining, they demonstrated an increased number of αSMA-positive VICs in softer hydrogels[8]. Although VICs were found to be more myofibroblast-like in the lower-modulus environment, interpretation of these results is somewhat confounded by the coupling of cell morphology with the density of the surrounding matrix.

In general, a significant obstacle to studying cellular responses to matrix mechanical properties in 3D is separating highly coupled variables. For example, when cells are encapsulated in a matrix metalloproteinase (MMP)-degradable synthetic hydrogel or natural gel (e.g., collagen, Matrigel, hyaluronan), the cells are able to spread and elongate because they locally remodel their environment. This remodeling often means softening of the local gel, and

a complex coupling of cell shape and local material properties. In other words, it can be difficult, at best, to independently control local gel chemistry, mechanics, and cellular interactions/morphologies, and while advances in light microscopy allow detailed characterization of real time changes in cell functions, it can be more difficult to similarly characterize real time changes in gel properties.

To address some of this complexity, materials with dynamic control of the cell microenvironment can help de-convolute some of these variables. For example, Burdick and co-workers used a hydrogel platform with staged crosslinking to create interpenetrating networks of hydrogels with varying degradability and the ability to increase modulus (i.e., stiffen) after initial gel formation[20]. They demonstrated the temporal effects of a modulus increase on mesenchymal stem cells in 2D where cells on stiffened substrates had larger cell area and exerted greater traction forces[21]. This system was also adapted for 3D experiments to show that the formation of a secondary, non-degradable network around encapsulated mesenchymal stem cells directed the cells towards adipogenesis, while cells encapsulated in gels that did not undergo secondary crosslinking favored osteogenesis[22].

Building on this concept, we use PEG-based hydrogels formed via a photochemical thiol-ene polymerization to study the influence of matrix modulus on VIC activation in 3D environments. VICs were encapsulated within MMP-degradable, PEG-based hydrogels of varying moduli. VIC phenotype was assessed by quantitative real-time polymerase chain reaction (qRT-PCR) and by immunostaining for αSMA. To control for differences in cell morphology that typically arise when encapsulating cells in hydrogels with varying crosslinking density, we developed a cytocompatible *in situ* stiffening system. VICs encapsulated in low-modulus gels were allowed to spread and elongate, and then stoichiometric amounts of an 8-arm

PEG-norbornene and an 8-arm PEG-thiol along with a photoinitiator were diffused into the gel. Photopolymerization of the cell-laden gel containing the stiffening solution increased the modulus of the gel without compromising cell viability. These dynamically stiffening gels give the experimenter control of the local environment surrounding the cells in three dimensions without altering cell morphology.

4.2. Materials and Methods

4.2.1. Synthesis of poly(ethylene glycol)-norbornene (PEGnb)

PEG-norbornene was synthesized using a previously described protocol[23]. Briefly, equimolar amounts of 8-arm PEG (JenKem) with a molecular weight of either 10 kDa or 40 kDa and 4-dimethylaminopyridine (Sigma-Aldrich) were dissolved in a minimal amount of anhydrous dichloromethane (Sigma-Aldrich), under argon in a round bottom flask. 16 equivalents each of 5-norbornene-2-carboxylic acid (Sigma-Aldrich) and N-N'-diisopropylcarbodiimide (Sigma-Aldrich) were added and reacted overnight on ice. Product was precipitated in 4°C ethyl ether (Fisher Scientific), filtered, and then dried by vacuum. PEG-norbornene was purified by dialysis and lyophilized. Greater than 90% functionalization was achieved as determined by proton nuclear magnetic resonance imaging and rheological characterization of the crosslinked product.

4.2.2. VIC isolation and culture

VICs were isolated from fresh porcine hearts (Hormel) as previously described[24]. Aortic valve leaflets were removed and rinsed in a wash solution containing Earle's Balanced Salt Solution (Life Technologies) with 1% penicillin-streptomycin (Life Technologies) and 0.5

μg/mL fungizone (Life Technologies). Then, the leaflets were incubated in 250 units/mL collagenase (Worthington) solution for 30 min. at 37°C and vortexed to remove endothelial cells. Cells were then incubated with collagenase solution for 60 min. at 37°C and vortexed. This solution was filtered with a 100 μm cell strainer and centrifuged. The cell pellet was resuspended in growth media consisting of Media 199 with 15% fetal bovine serum (FBS, Life Technologies), 2% penicillin-streptomycin (Life Technologies), and 0.5 μg/mL fungizone (Life Technologies). Cells were cultured at 37°C and 5% CO_2 on tissue culture polystyrene (TCPS) for expansion before experiments. Cells were passaged using trypsin (Life Technologies) digestion. For experiments, media serum level was reduced to 10% FBS to reduce proliferation.

4.2.3. Hydrogel formation and characterization

VICs were encapsulated within MMP-degradable, PEG-based hydrogels using a photoinitiated thiol-ene reaction[25]. Eight-arm PEG-norbornene was reacted with the peptide crosslinker KCGPQG↓IWGQCK (American Peptide Company, Inc.) and 2 mM CRGDS adhesive peptide (American Peptide Company, Inc.) in serum-free, phenol red-free media (Life Technologies) using the photoinitiator lithium phenyl-2,4,6-trimethylbenzoylphosphinate (LAP, 1.7 mM) (Figure 4.1). Cells in suspension were added to the gel precursor solution for a final concentration of 10 million cells/mL. 29 μL of gel solution was added to a 6 mm rubber mold on top of a glass slide treated with SigmaCote (Sigma-Aldrich) to prevent attachment of the gel to the slide. The solution was polymerized under UV light centered around 365 nm at 2 mW/cm^2 for 3 minutes. The shear modulus of the swollen hydrogels was measured using an Ares 4400 rheometer (TA Instruments) with a parallel plate geometry. Both frequency sweeps and strain sweeps were performed to ensure that measurements were representative of the linear

viscoelastic regime. The shear modulus (G') was measured and converted to Young's modulus (elastic modulus, E) using the formula $E = 2G(1+\nu)$ with $\nu = 0.5$[26]. The loss modulus is much lower than the storage modulus (G" << G') for all gel conditions, indicating that these gels primarily exhibit elastic behavior (data not shown).

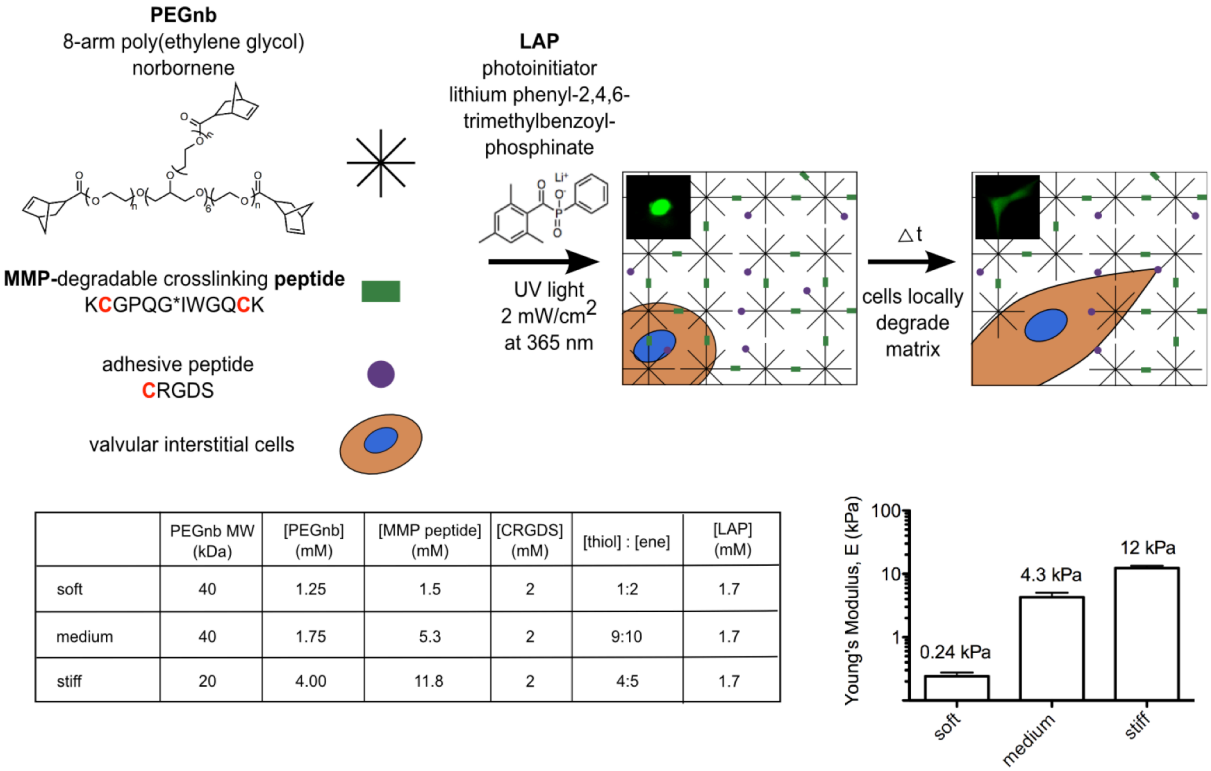

	PEGnb MW (kDa)	[PEGnb] (mM)	[MMP peptide] (mM)	[CRGDS] (mM)	[thiol] : [ene]	[LAP] (mM)
soft	40	1.25	1.5	2	1:2	1.7
medium	40	1.75	5.3	2	9:10	1.7
stiff	20	4.00	11.8	2	4:5	1.7

Figure 4.1. Schematic of VIC encapsulation within PEG-based hydrogels. PEGnb average molecular weight and concentration of PEGnb and MMP-degradable crosslinking peptide were varied as shown in the table to achieve a range of moduli. VICs were encapsulated at a density of 10 million cells per mL of gel. Insets (50 μm) show Live/Dead staining at day 0 and day 2.

4.2.4. Hydrogel stiffening and characterization

Stiffening solutions were comprised of 8-arm 10 kDa PEG-norbornene (2 or 10 mM), 8-arm 10 kDa PEG-thiol (2 or 10 mM), and LAP (2.5 mM). For control gels, the PEG-thiol was

replaced with cysteine (Sigma-Aldrich) to create a reacting formulation that did not form a gel. Gels were soaked in the stiffening solution for 12 minutes. Gels were then removed from solution and the excess swelling solution was blotted from the surface before polymerization with UV light (2 mW/cm^2 at 365 nm) for 3 minutes. The shear modulus after stiffening was measured as described for the initial gel formation.

4.2.5 Cell viability and morphology analysis

Cell viability was measured using a Live/Dead cytotoxicity kit (Life Technologies), which is a membrane integrity assay. Cell-laden hydrogels were incubated in PBS containing 1 μM calcein and 4 μM ethidium homodimer for 30 minutes. Cells were imaged on a 710 LSM NLO confocal microscope (Zeiss) and maximum intensity projections were created from 11 images each 10 μm apart for a total height of 100 μm. Fraction of live cells was quantified by manual counting. Morphology measurements were made using ImageJ to measure the length and width of cells based on calcein (live) staining.

4.2.6. RNA isolation and quantitative real-time polymerase chain reaction (qRT-PCR)

Messenger RNA (mRNA) was isolated from VICs using TriReagent (Sigma-Aldrich) with isopropanol (Sigma-Aldrich) extraction and ethanol (Sigma-Aldrich) washes according to the manufacturer's instructions. Reverse transcription was performed using the iScript cDNA Synthesis kit (Bio-Rad) and the Eppendorf Mastercycler. qRT-PCR was performed using an iCycler machine and iQ SYBR Green Supermix (Bio-Rad) with custom primers (Table 4.1, Illumina) at 300 nM. Each well also contained 0.05 ng/μL of the cDNA. Values were calculated

by comparing each sample to a standard curve, and data was normalized to an internal standard, L30. αSMA, S100A4, CTGF, COL1A1, MMP1, and L30 expression levels were measured.

Table 4.1. Primer sequences for qRT-PCR.

Gene	Forward Primer (5' – 3')	Reverse Primer (5' – 3')
L30	GCTGGGGTACAAGCAGACTC	AGATTTCCTCAAGGCTGGGC
αSMA	GCAAACAGGAATACGATGAAGCC	AACACATAGGTAACGAGTCAGAGC
S100A4	GAGCTAAAGGAGTTGCTGACC	CTGTCCAGGTTGCTCATCAG
CTGF	CTGGTCCAGACCACAGAGTGG	GCAGAAAGCGTTGTCATTGG
MMP1	GGCATCCAGGCCATCTATG	CACTTGTGGGGTTTGTGGG
COL1A1	GGGCAAGACAGTGATTGAATACA	GGATGGAGGGAGTTTACAGGAA

4.2.7. Immunostaining for αSMA and f-actin

Cells were fixed with 10% formalin (Sigma-Aldrich). Samples were then washed with PBS and permeablized with 0.05% TritonX100 (Fisher Scientific) in PBS. Non-specific staining was blocked with 1% bovine serum albumin (BSA, Sigma-Aldrich) in PBS with Tween20 (Sigma-Aldrich) and then incubated with mouse anti-αSMA (Abcam) overnight at 4°C. Samples were then washed and incubated with the secondary antibody, goat-anti-mouse AlexaFluor 488 (Life Technologies) and TRITC-phalloidin (Sigma-Aldrich). Next, cells were treated with 4',6-diamidino-2-phenylindole (DAPI, Life Technologies) to stain the cell nuclei. Cells were imaged on a 710 LSM NLO confocal microscope (Zeiss). Myofibroblast percentages were quantified by manually counting cells expressing organized αSMA stress fibers.

4.2.8. Statistical Analysis

For each experiment, at least 3 biological replicates were included. Each biological replicate consisted of cells pooled from separate groups of porcine hearts. For qRT-PCR, each biological replicate is an average of at least 3 technical replicates. For morphology analysis, at least 25 cells were analyzed per condition per replicate. At least 100 cells per condition per replicate were analyzed for cell viability and immunostaining experiments. Data were compared using one-way ANOVAs and Tukey post-tests in Prism 5 (GraphPad Software, Inc). Data is presented as mean ± standard error unless otherwise noted.

4.3. Results

4.3.1. VIC response to matrix mechanics in 3D

To study VIC response to stiffness in 3D, cells were first encapsulated in peptide-functionalized PEG hydrogels of varying moduli (Figure 4.1). A range of moduli from 0.24 kPa to 12 kPa was achieved by varying the molecular weight and concentration of 8-arm PEGnb while controlling the ratio of –ene groups on the PEGnb to thiol groups on the peptides. The softest modulus, 0.24 kPa, is somewhat softer than the 0.39 kPa gels in Chapter 3. This modulus was chosen to promote VIC spreading in less than 3 days of culture. These gels were crosslinked using a peptide (KCGPQG↓IWGQCK) that can be cleaved by MMPs secreted by VICs [17]. The fibronectin-derived adhesive peptide CRGDS was incorporated at 2 mM to facilitate cell adhesion to the gel. There was a dependence on overall cell viability on hydrogel modulus, from ~90% viability in 0.24 kPa gels to ~60% viability in 12 kPa gels after 2 days (Figure 4.2B). This decrease in viability with matrix stiffness may be due to factors related to cell-matrix interactions and overall morphology and their influence on apoptosis. Here, only VICs in the 0.24 kPa gel were able to spread and elongate after 2 days, while VICs encapsulated in the 4 kPa or 12 kPa

gels remained smaller and rounded (Figure 4.2A). mRNA levels were measured using qRT-PCR to characterize phenotypic differences over the range of gel moduli. There was an inverse relationship between gel modulus and αSMA mRNA expression in this system, with the cells in the 12 kPa gel containing only ~20% as much αSMA mRNA as the 0.24 kPa gels (Figure 4.2C). Immunostaining showed activated myofibroblasts with αSMA stress fibers only in the 0.24 kPa gels, while the 4 kPa and 12 kPa did not exhibit organized αSMA or f-actin fibers (Figure 4.7, Supplementary Information). Based on these data alone, it was unclear whether this observation was due to a direct response to gel modulus or a result of differences in cell viability or morphology.

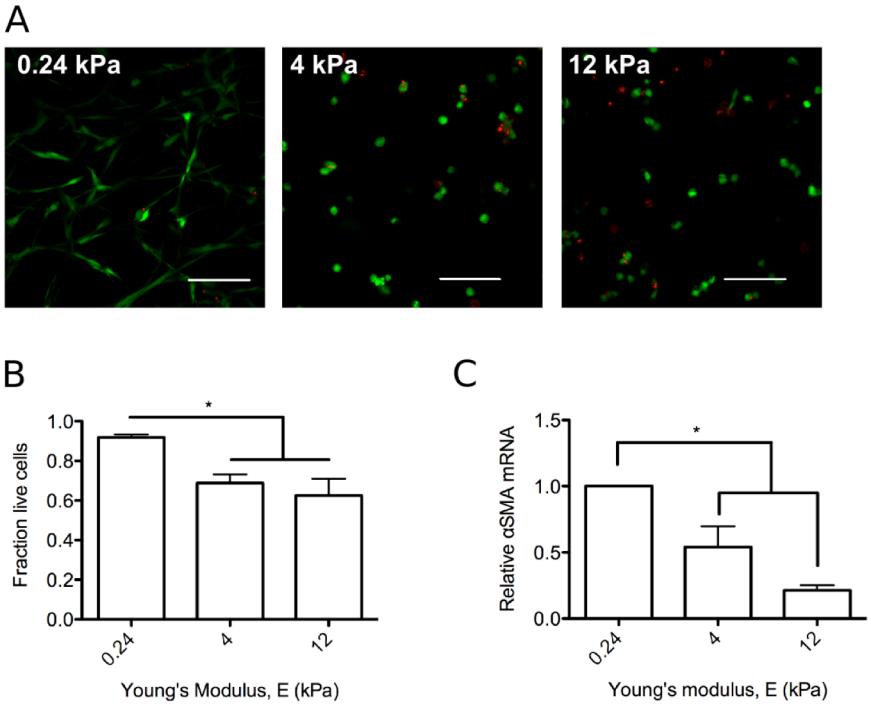

Figure 4.2. A. Live/Dead staining of VICs 48 hours after encapsulation within hydrogels. VICs within 0.24 kPa hydrogels exhibit an elongated morphology and high cell viability, while VICs within 4 kPa and 12 kPa retained a rounded morphology and experienced greater cell death. Scale bar = 100 μm. B. Quantification of Live/Dead staining shows decreased cell viability with increasing modulus. C. Increasing modulus correlates with decreasing αSMA mRNA relative to the L30 internal standard as determined by qRT-PCR. * = $p<0.05$.

4.3.2. Dynamic stiffening of cell-laden hydrogels

To decouple the effects of morphology versus matrix mechanics on VIC activation, an approach to stiffen the hydrogel modulus *in situ* was pursued. VICs were first encapsulated within the low-modulus (0.24 kPa) hydrogel, where the low crosslinking density facilitated timely cell spreading. Encapsulated cells were allowed 3 days to locally remodel the gels and spread and elongate within the gels post-encapsulation. Then, the gels were stiffened by swelling in solutions containing equal amounts of 8-arm PEGnb and 8-arm PEG-thiol, as well as the photoinitiator, LAP, that were subsequently photopolymerized *in situ*. For the soft "to medium" condition, PEGnb (2 mM) and PEG-thiol (2 mM) were added. For the soft "to stiff" condition, the concentrations of PEGnb and PEG-thiol were both increased to 10 mM. Using this approach, a greater than 50-fold increase in modulus was achieved (Figure 4.3). The final gel modulus was dependent on the concentration of PEG in the stiffening solution, with the "to medium" solution increasing the modulus from 0.24 kPa to 1.2 kPa and the "to stiff" solution increasing the modulus to 13 kPa. By stiffening, the cell-defined matrix is transformed to a more user-defined, non-degradable environment in which the cells are unable to elicit significant changes in the local modulus.

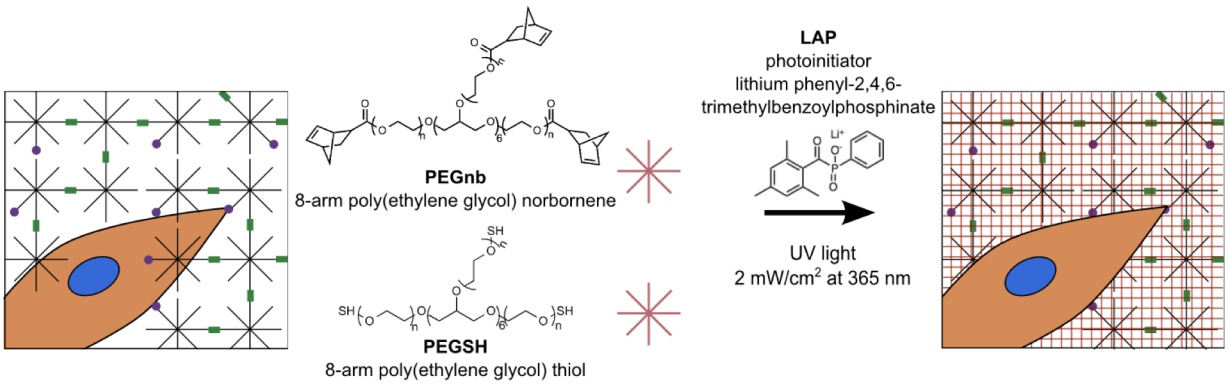

	PEGnb MW (kDa)	[PEGnb] (mM)	PEGSH MW (kDa)	[PEGSH] (mM)	[thiol] : [ene]	[LAP] (mM)
to medium	10	2	10	2	1:1	2.5
to stiff	10	10	10	10	1:1	2.5

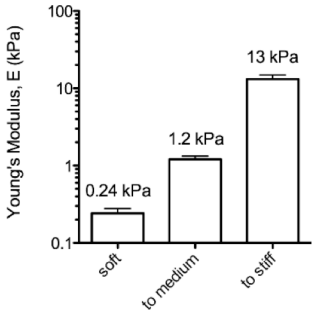

Figure 4.3. Schematic of stiffening the cell-laden hydrogels. 8-arm PEG-thiol, 8-arm PEGnb, and LAP were swollen into the cell-laden gels for 12 minutes. Gels were then re-polymerized using UV light to increase the gel modulus. Final stiffened modulus was varied by changing the concentration of PEG-thiol and PEGnb while maintaining a stoichiometric reaction.

Cell viability was measured 2 days post-stiffening by live/dead staining (Figure 4.4B). Here, we note high levels of survival, indicating a stronger effect of VIC spreading and morphology on viability compared to matrix modulus. Furthermore, VIC morphology was characterized 2 days after stiffening by quantifying the average cell aspect ratio (cell length/cell width) in each of the conditions (Figure 4.4C). Note that VICs maintained a similar morphology across the entire range of moduli studied, with the average cell aspect ratio in stiffened gels only ~30% lower than in soft gels. For comparison, the differences in the aspect ratio of cell directly encapsulated in the 0.24 kPa, 4 kPa, and 12 kPa hydrogels (Figure 4.3) varied by as much as

70%. Thus, the similar morphology in the stiffening system across the range of moduli studied aided in decoupling gel modulus and cell morphology, two frequently paired variables.

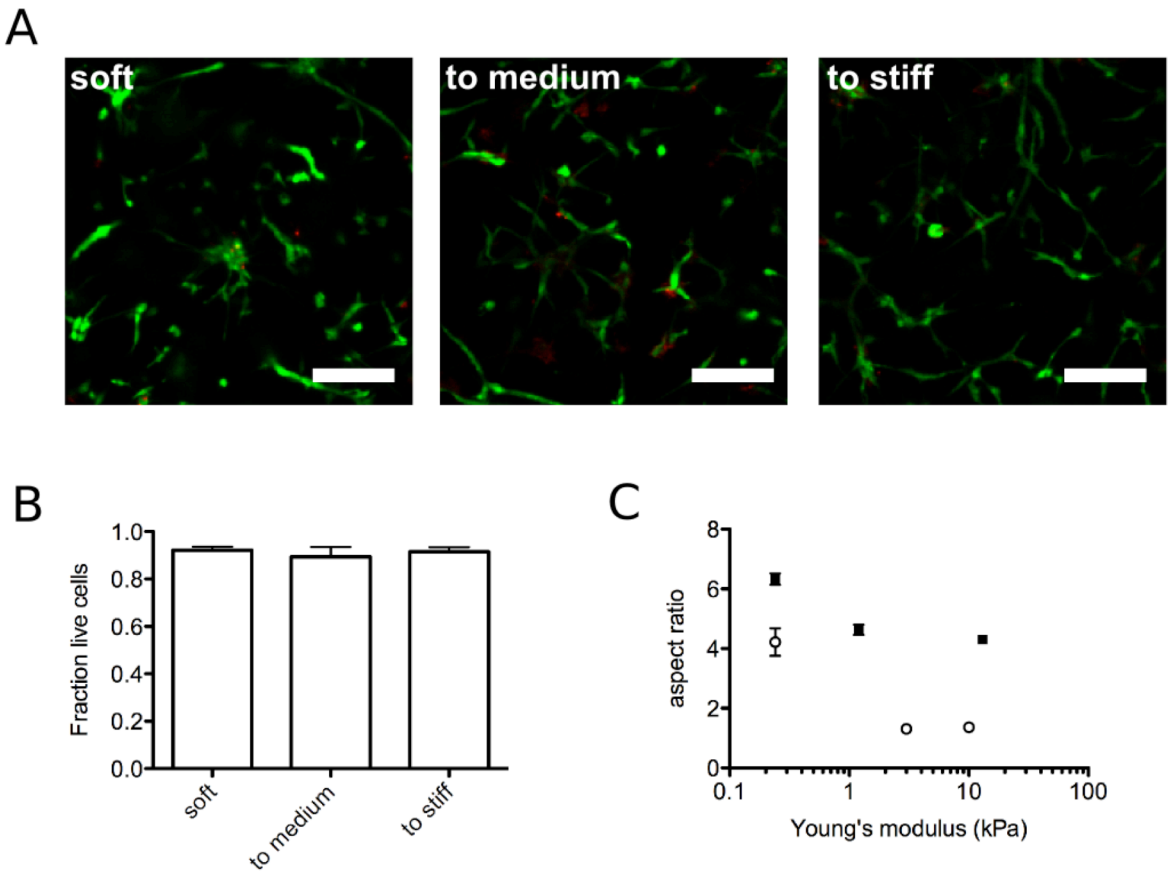

Figure 4.4. A. Live/Dead staining of VICs encapsulated within soft and stiffened hydrogels 48 hours after stiffening. VICs in all conditions exhibited an elongated morphology and high cell viability. Scale bar = 100 μm. B. Quantification of Live/Dead staining shows high cell viability across the range of moduli. C. Quantification of cell aspect ratio. High modulus standard encapsulations result in greatly reduced cell aspect ratio, while aspect ratio in stiffened gels remains approximately the same as in the softest condition. * = $p<0.05$.

4.3.3. Hydrogel modulus directs VIC phenotype in 3D

Using this *in situ* stiffening approach, we found that αSMA mRNA levels decreased with stiffening. VICs in gels stiffened to 13 kPa exhibited only 23 ± 2% as much αSMA mRNA as

VICs in the 0.24 kPa gels (Figure 4.5). This trend was confirmed by immunostaining for αSMA stress fibers (Figure 4.5A). In the soft gels, 42 ± 6% of VICs exhibited organized stress fibers containing αSMA, a hallmark of the myofibroblast phenotype. Only 13 ± 3% of VICs in gels stiffened to 1.2 kPa exhibited αSMA stress fibers; however, some diffuse αSMA staining was also visible. VICs in gels stiffened to 13 kPa displayed very little αSMA in either form (2.5 ± 0.1% activation) (Figure 4.5B). To ensure that these phenotypic changes were not due to exposure to the swelling solution, radical intermediates, or UV light, the stiffening process was performed on VICs encapsulated in soft gels, but the 8-arm PEG-thiol was replaced with cysteine to make a reacting stiffening solution that would not form a gel. We found that the stiffening process did not lead to any statistically significant differences in activation levels (Figure 4.5C).

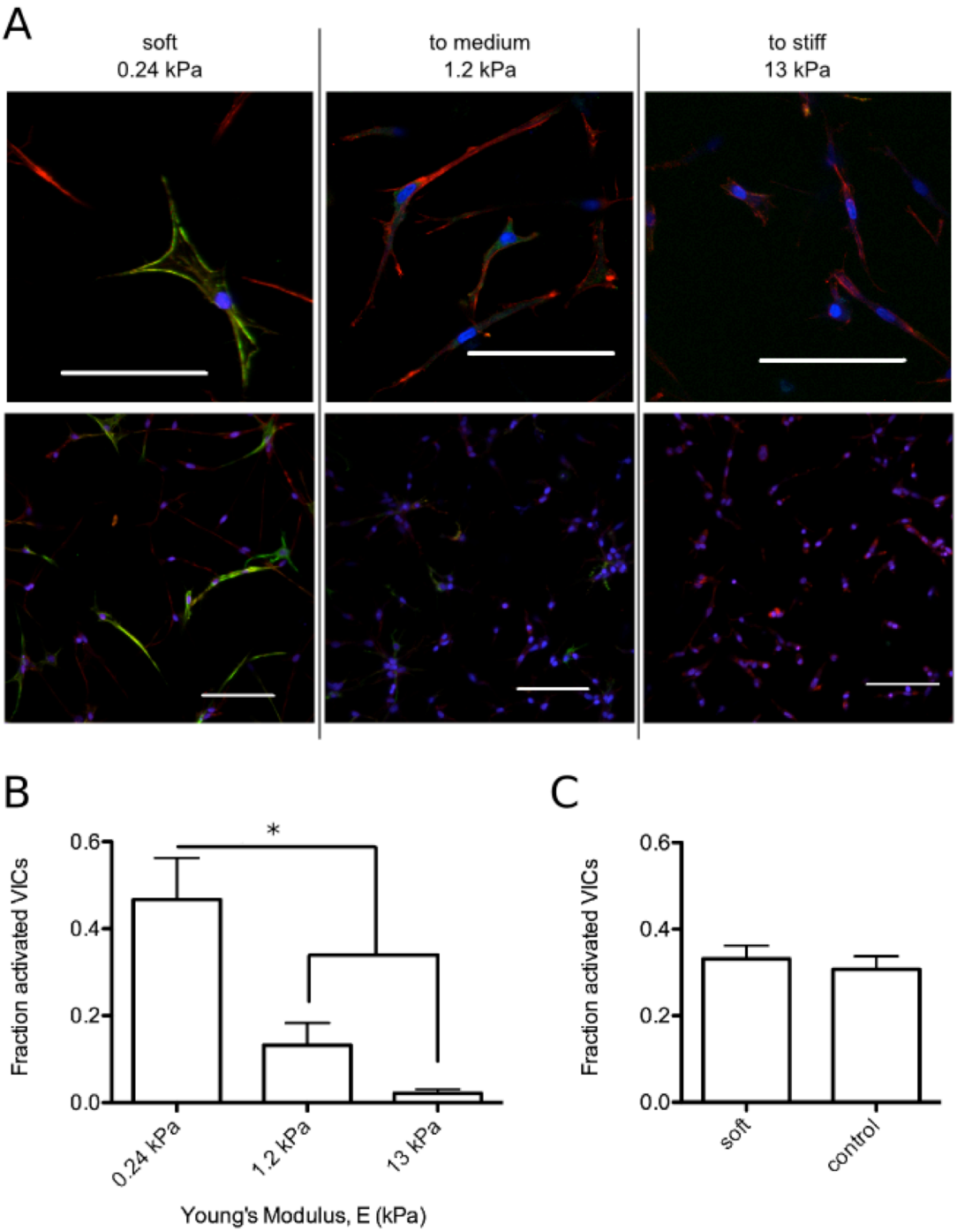

Figure 4.5. A. Immunostaining for αSMA (green), f-actin (red) and nuclei (blue) with two representative images per condition. In soft gels, many cells exhibit αSMA stress fibers. In "to medium" gels, there are fewer cells positive for stress fibers, but diffuse αSMA is common. In "to stiff" gels, very little αSMA is present in either form. Scale bars = 100 μm. B. Fraction of activated VICs as defined by the presence of αSMA stress fibers was quantified. Activation decreased with increasing final modulus. C. A non-gelling formulation of the stiffening solution was used as a control to show that the UV light, radical intermediates, and other possible strains of the stiffening process were not responsible for the reduction in activation. * = $p<0.05$.

Further evidence for the deactivation of VICs upon matrix stiffening was collected by analyzing gene expression. Here, αSMA mRNA levels decreased with increasing stiffness. The myofibroblast marker CTGF also showed a downward trend with stiffening (Figure 4.6). In contrast, increasing stiffness led to an increase in mRNA levels of S100A4, which has been correlated to decreases in activation and αSMA expression in VICs and in other cells types [11,27,28]. Genes associated with matrix remodeling were also investigated. While a greater than 3-fold increase in MMP1 mRNA expression was seen in each of the stiffened conditions compared to the VICs in the soft gels, expression of the collagen type I precursor Col1A1 remained relatively unchanged by stiffening at the time point examined in this experiment (Figure 4.6). Together, these data indicate that VICs cultured in 0.24 kPa hydrogels tend towards a myofibroblast-like phenotype, with a spread morphology and strong matrix interactions. In contrast, if the surrounding gel environment is stiffened *in situ*, VICs appeared to revert to a more quiescent fibroblast phenotype. We hypothesize that this phenotypic change is due to changes in the modulus of the extracellular environment and is not caused by differences in morphology. While an elongated morphology is likely required for activation to the myofibroblast phenotype, this morphology alone does not appear to direct cells to the activated state.

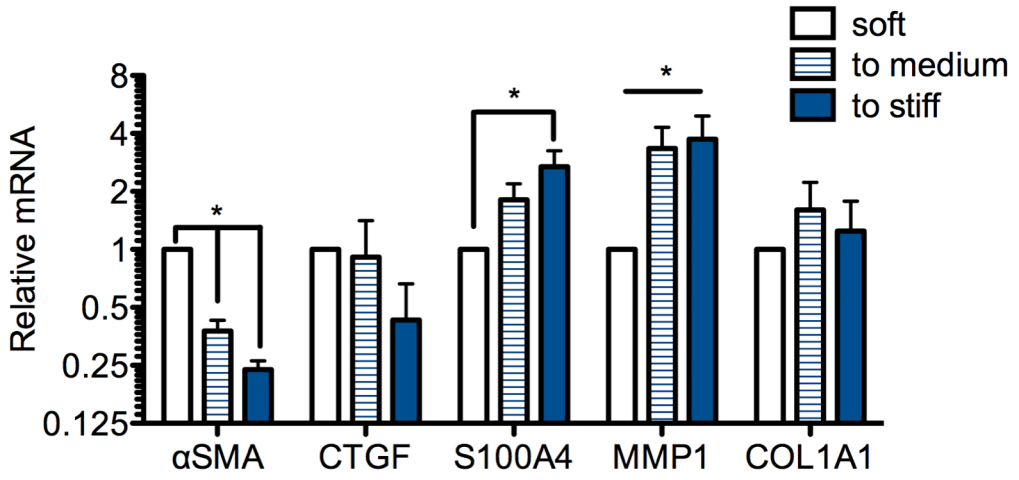

Figure 4.6. qRT-PCR comparing genes of interest in soft (white), to medium (striped), and to stiff (solid) conditions. All genes were normalized to the L30 housekeeping gene. Myofibroblast markers αSMA and CTGF decreased with increasing modulus. The fibroblast marker S100A4 increased with increasing modulus. MMP was higher in the stiffened gels than in the soft gel. Col1A1 was unchanged in the examined conditions. * = $p < 0.05$. Flat line indicates $p < 0.05$ for ANOVA but no significant differences in post-tests.

4.4. Discussion

Many factors influence how cells respond to cues from their local microenvironment. Matrix density, adhesivity, and elastic modulus can all affect cell phenotype directly, but also influence variables such as cell shape. Generally speaking, cells sense the ECM through focal adhesions that can involve different integrins and proteins, further complicating the understanding of this outside-in signaling. Many of these matrix interactions can be isolated and studied on 2D surfaces, and these experiments have helped define our understanding of the role of the extracellular space in directing and maintaining cell function. However, in other cases, understanding of cellular responses *in vivo* may benefit from more advanced culture systems and measurements in 3D systems. In this work, we were interested in better understanding how mechanical signaling from the extracellular matrix can contribute to VIC function.

VICs are key regulators in valve repair and disease, which involve dynamic changes in the extracellular environment with time. Here, we sought to exploit some unique material chemistry to show how VICs and their myofibroblast properties might respond to dynamic changes in stiffness in a 3D environment. Specifically, these experiments employed a peptide-functionalized hydrogel synthesized with thiol-ene chemistry to create proteolytically degradable hydrogels (Figure 4.1). These gels were then subsequently stiffened on demand using a secondary, non-degradable network (Figure 4.3). One significant advantage of this system is the ability to study the impact of matrix stiffness on cells while keeping a similar morphology across a large range of elastic moduli that are relevant to valve tissue properties. Additionally, the use of a non-degradable stiffening network provides more control over the local modulus experienced by the cells throughout the course of the experiment compared to a proteolytically degradable network.

In most hydrogel culture systems, stiffer gels arise from networks with a higher density of crosslinks or polymer content, so this necessitates that cells cleave more crosslinks to achieve a spread morphology similar to those observed in softer gels with lower crosslinking density. This coupling of morphology to network density makes it difficult to deconvolute the effects of cell morphology from matrix stiffness, where cell shape can correlate to underlying matrix adhesion and density. The ability to independently study morphology and stiffness is of significant interest because of the many ways in which cell morphology can direct cell phenotype[29,30]. Here, we follow an approach by Khetan *et al.* to attribute phenotypic changes in VICs directly to changes in modulus by eliminating morphology as a variable through *in situ* stiffening of soft gels[20].

Specific to the VICs, an advantage of the stiffening platform was the high cell viability achieved across the entire range of moduli studied, compared to decreasing viability observed when VICs are directly encapsulated in stiff gels and restricted to a rounded morphology for extended culture times (Figures 2, 4). Differences in cell viability are important not only because of changes in cell density, but also because there is a possibility that one might inadvertently select for a specific population of VICs. The latter can be especially problematic for primary VICs, which represent a heterogeneous population of cells isolated from valve tissue[31].

The specific hydrogel moduli evaluated as part of this study correspond to moduli of relevance to aortic valves. The 0.24 kPa gels are softer than adult valves and might be viewed as corresponding more closely to a developing valve. The 1.2 kPa gels approach the moduli measured in healthy adult valves, which has been reported to range from 1.1 kPa to 1.6 kPa for the ventricularis and fibrosa valve layers, respectively[32]. Finally, the 12 kPa gels were chosen to provide a higher modulus condition, as matrix stiffening occurs in diseased valves. While 12 kPa is not an upper limit or dividing threshold for myofibroblast activation or the onset of valve fibrosis, it is stiffer than what might be expected in a healthy valve.

Early efforts to study VIC-matrix interactions and mechanotransduction have observed that seeding VICs on softer (~7 kPa) hydrogel substrates better preserves their native phenotype compared to culture on tissue culture polystyrene (TCPS)[33]. This study identified thousands of genes that were differentially regulated on TCPS compared to freshly isolated cells and found that three of the genes upregulated on TCPS (αSMA, CTGF, and Col1A1) were expressed at levels closer to freshly isolated cells when the VICs were instead cultured on the soft hydrogel. Additionally, the percentage of VICs seeded on soft gels exhibiting αSMA stress fibers was similar to the percentage found in the valve, while much higher levels of activation were

observed on TCPS. To better understand the role of substrate mechanics in regulating these profound differences that were observed with culture conditions, VIC response to dynamic changes in substrate modulus was also studied; specifically, VICs were seeded on a hydrogel with photodegradable moieties to allow *in situ* softening. These experiments revealed that VIC activation on stiff substrates is reversible, and the myofibroblast phenotype can be deactivated by a reduction in the substrate modulus[12]. While softening systems have been exploited to study the response of VICs to a dynamic softening of the matrix environment, there are few examples of studying how *increases* in the matrix modulus influence cell phenotype *in situ*. Studying cellular responses to increases in modulus is important because many *in vivo* processes involve increases in tissue stiffness. For example, increases in tissue stiffness are frequently associated with fetal development, the progression of fibrotic diseases, and cancerous tumors[34–36]. As a result, there is a growing interest in biomaterials scaffolds for 3D cell culture that enable one to stiffen the matrix mechanics on demand. In this regard, one system that allows *in situ* modulation of gel mechanics was developed by the Burdick group to study mesenchymal stem cell fate[37]. The initial hydrogels were formed using via a Michael addition of acrylated hyaluronic acid with cysteine-containing MMP-degradable peptides where the acrylate functionality was in excess. Later, gels were stiffened using a photoinitiated radical polymerization of the remaining acrylate groups. By using a photoinitiated reaction for the secondary crosslinking, they were able to avoid stimuli that are known to elicit cellular responses, such as pH or temperature. Here, we develop a complementary approach using a peptide functionalized PEG-based system that allows the formation of highly defined step-growth networks with tailored presentation of peptide signaling moieties, along with highly defined control of biomechanics and biodegradation. These material characteristics are important to control for VIC cultures, and PEG can provide an

alternative to hyaluronic acid, which can influence VIC phenotype upon degradation into lower molecular weight fragments[38]. Finally, the thiol-ene reaction mechanism has been shown to be more cytocompatible for some highly sensitive primary cell types, and also allows tethering of many growth factors without a loss in activity[39–41].

Perhaps most unexpectedly, trends in VIC phenotype (e.g., myofibroblast activation) with stiffness in 3D environment were quite different from those observed in 2D cultures. Specifically, VIC activation typically correlates with stiffness of the culture substrate in 2D experiments[9,12], and this observation is consistent with clinical reports of higher levels of persistent myofibroblasts during fibrotic valve disease progression. However, less is known about how myofibroblast properties correlate with VIC cultures in 3D, and this can be important for tissue engineers seeking to regenerate functional valve leaflets or for biochemists seeking to identify small molecule inhibitors that might reverse valve disease. When encapsulated in hydrogel environments, VICs respond to the stiffness of their environment in a manner that one might expected for a well-functioning valve: in an initially soft matrix in early stages of development or in valve tissue that has been damaged after injury, VICs become activated myofibroblasts and deposit additional extracellular matrix proteins. When the matrix surrounding the cells has reached an appropriate density and stiffness, VICs return to a quiescent phenotype, preventing the pathological state of continued activation and tissue deposition. In the dynamic gel conditions examined here, where VICs were encapsulated in soft gels, allowed to spread, and then *in situ* stiffened, VICs residing in the stiffest gels were nearly all quiescent fibroblasts (Figure 4.5). These experiments supported the hypothesis that stiffness alone does not activate VICs to their myofibroblast phenotype and that additional stimuli may be necessary to promote their persistent activation, whether for healthy tissue remodeling or misregulation that

is related to disease progression. The observations of the dependence of VIC activation on matrix modulus are also consistent with aspects of fetal development, where the soft valve matrix leads to high percentages of activated myofibroblasts, but as the valve develops and stiffens, the percentage of myofibroblasts decreases[6,42]. Similar levels of deactivation are seen after stiffening VIC-laden hydrogels with either degradable or non-degradable networks, providing additional evidence to support the role of modulus in deactivation (Figure 4.8, Supplementary Information). It would be interesting to expand the range of bioscaffold elasticities and the timing of the stiffening to see if certain culture conditions are more reminiscent of valve development versus disease progression.

Beyond examining αSMA protein expression and organization, the VIC phenotype was further characterized in these 3D gel environments using qRT-PCR to examine mRNA levels of myofibroblast markers, fibroblast markers, and matrix remodeling genes (Figure 4.6). Consistent with the immunostaining results, αSMA mRNA levels were highest for VICs encapsulated in the softest gels, and increasing gel stiffness correlated with decreasing αSMA expression. CTGF, another myofibroblast marker, was also examined. While there was greater variation seen in the CTGF mRNA levels, a general trend of decreasing CTGF was observed. The lower expression of both of these myofibroblast markers in the stiffened gels is consistent with the lower activation levels seen by immunostaining. S100A4, an indicator of the quiescent fibroblast phenotype, was also examined. S100A4 increased with increasing stiffness, suggesting that VICs were deactivated to the fibroblast phenotype upon stiffening. Collectively, the changes in expression of these three markers are consistent with the immunostaining data (Figure 4.5), which showed more myofibroblasts in the soft gels than in the stiffened gels.

One of the major differences between 2D and 3D hydrogel cultures is that encapsulated cells must degrade and remodel their surrounding environment to spread. As a result, one might expect variations in MMP activity as a function of dimensionality, and increased matrix deposition and MMP activity are typically associated with VIC myofibroblasts. For example, MMP1 was found to be about 17 times as prevalent in stenotic human aortic valves compared to healthy valves, while a 23 fold increase was reported in COL1A1 mRNA, a precursor of type I collagen[43]. Interestingly, we observed that MMP1 mRNA expression was higher in the stiffer gels, where almost all VICs are quiescent (Figure 4.6). This increased expression with stiffening may be a result of the degradability of the gels. With the stiffening approach, the cells become constrained by the non-degradable network and may express more MMPs in an attempt to modify their local environment. In contrast, the VICs remaining in degradable, soft gels may be able to cleave crosslinks even with lower MMP expression. This explanation is consistent with the nearly equal levels of MMP1 mRNA in both of the stiffened conditions ("to medium" and "to stiff"), but it would be interesting to adjust the stiffening formulation to also study a proteolytically degradable system. However, interpretation of such experiments would be confounded by local changes that would occur in matrix mechanics with different degradation rates of the loosely and densely crosslinked formulations. Finally, no statistically significant differences in COL1A1 were observed in this study across the conditions (Figure 4.6), but it is possible that changes in COL1A1 would be observed on a longer timescale than the other markers that were examined here. Even if no differences are measurable at the mRNA level, long-term studies of the deposition of collagen within the gels should provide more insight as to how modulus and MMP activity may direct matrix remodeling in 3D. Here, we intentionally selected earlier time points to test hypotheses related to VIC response to changes in the synthetic

ECM matrix, before they significantly alter their microenvironment through significant ECM deposition.

In summary, peptide-functionalized hydrogels formed through thiol-ene photopolymerizations provide a versatile platform for 3D culture of VICs. Through sequential reaction steps, this platform enabled us to transition from simple, cellularly-remodeled materials to a user-defined system with *in situ* tunable mechanical properties. While we only showed the effect of a single stiffening event on VIC phenotype, it would be possible to repeat the stiffening procedure multiple times to simulate the more gradual stiffening that would occur *in vivo*. It might be particularly interesting to repeatedly stiffen with degradable gel formulations and couple these experiments with real time measurements of VIC functions and matrix remodeling (e.g., traction force microscopy).

4.5. Conclusions

In summary, we developed an approach for *in situ* stiffening of cell-laden hydrogels using thiol-ene chemistry, and the synthetic methods were implemented to study VIC phenotype in 3D environments. VICs encapsulated within soft (E = 0.24 kPa) gels had an elongated morphology and high levels of expression of the αSMA myofibroblast marker, while VICs encapsulated within higher modulus (E = 4-12 kPa) gels were mostly rounded and had low levels of αSMA expression. To delineate morphological effects from modulus effects, an *in situ* gel stiffening approach was pursued. In 0.24 kPa gels, ~40% of VICs were activated to the myofibroblast phenotype, but when stiffened to 13 kPa, only ~2% of VICs remained activated 2 days after the stiffening. This response was also evaluated at the mRNA level, where more than a 70% reduction in αSMA levels was observed. This trend of reduced activation with increasing

microenvironmental stiffness is counter to observations when VICs are cultured on 2D hydrogel surfaces, and implies that factors associated with dimensionality may play an important role in better understanding VIC phenotypic changes, especially the myofibroblast-to-fibroblast transition.

4.6. Acknowledgements

The authors would like to thank Samuel Payne for help with VIC cultures and Dr. Huan Wang for PCR primers. The authors would also like to acknowledge support to KMM from an NIH Pharmaceutical Biotechnology Training Grant, funding from an NIH grant (R01 HL089260) and HHMI.

4.7. References

1. Durbin, A. D. & Gotlieb, A. I. Advances towards understanding heart valve response to injury. *Cardiovasc. Pathol.* **11,** 69–77 (2002).

2. Rajamannan, N. M. *et al.* Calcific Aortic Valve Disease: Not Simply a Degenerative Process: A Review and Agenda for Research From the National Heart and Lung and Blood Institute Aortic Stenosis Working Group * Executive Summary: Calcific Aortic Valve Disease - 2011 Update. *Circulation* **124,** 1783–1791 (2011).

3. Liu, A. C., Joag, V. R. & Gotlieb, A. I. The emerging role of valve interstitial cell phenotypes in regulating heart valve pathobiology. *Am. J. Pathol.* **171,** 1407–18 (2007).

4. Fayet, C., Bendeck, M. P. & Gotlieb, A. I. Cardiac valve interstitial cells secrete fibronectin and form fibrillar adhesions in response to injury. *Cardiovasc. Pathol.* **16,** 203–11 (2007).

5. Liu, A. C. & Gotlieb, A. I. Characterization of cell motility in single heart valve interstitial cells in vitro. *Histol. Histopathol.* **22,** 873–82 (2007).

6. Rabkin-Aikawa, E., Farber, M., Aikawa, M. & Schoen, F. J. Dynamic and reversible changes of interstitial cell phenotype during remodeling of cardiac valves. *J. Heart Valve Dis.* **13,** 841–7 (2004).

7. Gould, S. T., Darling, N. J. & Anseth, K. S. Small peptide functionalized thiol-ene hydrogels as culture substrates for understanding valvular interstitial cell activation and de novo tissue deposition. *Acta Biomater.* **8,** 3201–9 (2012).

8. Duan, B., Hockaday, L. A., Kapetanovic, E., Kang, K. H. & Butcher, J. T. Stiffness and adhesivity control aortic valve interstitial cell behavior within hyaluronic acid based hydrogels. *Acta Biomater.* **9,** 7640–50 (2013).

9. Kloxin, A. M., Benton, J. A. & Anseth, K. S. In situ elasticity modulation with dynamic substrates to direct cell phenotype. *Biomaterials* **31,** 1–8 (2010).

10. Quinlan, A. M. T. & Billiar, K. L. Investigating the role of substrate stiffness in the persistence of valvular interstitial cell activation. *J. Biomed. Mater. Res. Part A* **087257,** 2474–82 (2012).

11. Witt, W., Büttner, P., Jannasch, A., Matschke, K. & Waldow, T. Reversal of myofibroblastic activation by polyunsaturated fatty acids in valvular interstitial cells from aortic valves. Role of RhoA/G-actin/MRTF signalling. *J. Mol. Cell. Cardiol.* **74,** 127–138 (2014).

12. Wang, H., Haeger, S. M., Kloxin, A. M., Leinwand, L. A. & Anseth, K. S. Redirecting Valvular Myofibroblasts into Dormant Fibroblasts through Light-mediated Reduction in Substrate Modulus. *PLoS One* **7,** e39969 (2012).

13. Yip, C. Y. Y., Chen, J.-H., Zhao, R. & Simmons, C. A. Calcification by valve interstitial cells is regulated by the stiffness of the extracellular matrix. *Arterioscler. Thromb. Vasc. Biol.* **29,** 936–42 (2009).

14. Baker, B. M. & Chen, C. S. Deconstructing the third dimension: how 3D culture microenvironments alter cellular cues. *J. Cell Sci.* **125,** 3015–24 (2012).

15. Birgersdotter, A., Sandberg, R. & Ernberg, I. Gene expression perturbation in vitro--a growing case for three-dimensional (3D) culture systems. *Semin. Cancer Biol.* **15,** 405–12 (2005).

16. Butcher, J. T. & Nerem, R. M. Porcine aortic valve interstitial cells in three-dimensional culture: comparison of phenotype with aortic smooth muscle cells. *J. Heart Valve Dis.* **13,** 478–85; discussion 485–6 (2004).

17. Benton, J. A., Fairbanks, B. D. & Anseth, K. S. Characterization of valvular interstitial cell function in three dimensional matrix metalloproteinase degradable PEG hydrogels. *Biomaterials* **30,** 6593–603 (2009).

18. Ayala, P., Lopez, J. I., Ph, D. & Desai, T. A. Microtopographical Cues in 3D Attenuate Fibrotic Phenotype and Extracellular Matrix Deposition : Implications for Tissue Regeneration. *J. Mol. Cell. Cardiol.* **16,** (2010).

19. Kural, M. H. & Billiar, K. L. Mechanoregulation of valvular interstitial cell phenotype in the third dimension. *Biomaterials* **35,** 1128–1137 (2013).

20. Khetan, S., Katz, J. S. & Burdick, J. A. Sequential crosslinking to control cellular spreading in 3-dimensional hydrogels. *Soft Matter* **5,** 1601 (2009).

21. Guvendiren, M. & Burdick, J. A. Stiffening hydrogels to probe short- and long-term cellular responses to dynamic mechanics. *Nat. Commun.* **3,** 792 (2012).

22. Khetan, S. *et al.* Degradation-mediated cellular traction directs stem cell fate in covalently crosslinked three-dimensional hydrogels. *Nat. Mater.* **12,** 458–65 (2013).

23. Fairbanks, B. D. *et al.* A Versatile Synthetic Extracellular Matrix Mimic via Thiol-Norbornene Photopolymerization. *Adv. Mater.* **21,** 5005–5010 (2009).

24. Johnson, C. M., Hanson, M. N. & Helgeson, S. C. Porcine cardiac valvular subendothelial cells in culture: cell isolation and growth characteristics. *J. Mol. Cell. Cardiol.* **19,** 1185–93 (1987).

25. Fairbanks, B. D., Schwartz, M. P., Bowman, C. N. & Anseth, K. S. Photoinitiated polymerization of PEG-diacrylate with lithium phenyl-2,4,6-trimethylbenzoylphosphinate: polymerization rate and cytocompatibility. *Biomaterials* **30,** 6702–7 (2009).

26. Bryant, S. J. & Anseth, K. S. Hydrogel Scaffolds.

27. Ryan, D. G. Involvement of S100A4 in Stromal Fibroblasts of the Regenerating Cornea. *Invest. Ophthalmol. Vis. Sci.* **44,** 4255–4262 (2003).

28. Calvo, F. *et al.* Mechanotransduction and YAP-dependent matrix remodelling is required for the generation and maintenance of cancer-associated fibroblasts. *Nat. Cell Biol.* **15,** 637–646 (2013).

29. Kilian, K. a, Bugarija, B., Lahn, B. T. & Mrksich, M. Geometric cues for directing the differentiation of mesenchymal stem cells. *Proc. Natl. Acad. Sci. U. S. A.* **107,** 4872–7 (2010).

30. Dupont, S. *et al.* Role of YAP/TAZ in mechanotransduction. *Nature* **474,** 179–83 (2011).

31. Wang, H., Sridhar, B., Leinwand, L. A. & Anseth, K. S. Characterization of cell subpopulations expressing progenitor cell markers in porcine cardiac valves. *PLoS One* **8,** e69667 (2013).

32. Chen, J.-H., Chen, W. L. K., Sider, K. L., Yip, C. Y. Y. & Simmons, C. A. B-Catenin Mediates Mechanically Regulated, Transforming Growth Factor-B1-Induced Myofibroblast Differentiation of Aortic Valve Interstitial Cells. *Arterioscler. Thromb. Vasc. Biol.* **31,** 590–7 (2011).

33. Wang, H., Tibbitt, M. W., Langer, S. J., Leinwand, L. A. & Anseth, K. S. Hydrogels preserve native phenotypes of valvular fibroblasts through an elasticity-regulated PI3K/AKT pathway. *Proc. Natl. Acad. Sci.* **110,** 19336–19341 (2013).

34. Butcher, J. T., Mcquinn, T. C., Sedmera, D., Turner, D. & Markwald, R. R. Transitions in Early Embryonic Atrioventricular Valvular Function Correspond With Changes in Cushion Biomechanics That Are Predictable by Tissue Composition. 1503–1511 (2007). doi:10.1161/CIRCRESAHA.107.148684

35. Wozniak, M. a & Chen, C. S. Mechanotransduction in development: a growing role for contractility. *Nat. Rev. Mol. Cell Biol.* **10,** 34–43 (2009).

36. Butcher, D. T., Alliston, T. & Weaver, V. M. A tense situation: forcing tumour progression. *Nat. Rev. Cancer* **9,** 108–22 (2009).

37. Khetan, S. & Burdick, J. A. Patterning network structure to spatially control cellular remodeling and stem cell fate within 3-dimensional hydrogels. *Biomaterials* **31,** 8228–34 (2010).

38. Rodriguez, K. J., Piechura, L. M. & Masters, K. S. Regulation of valvular interstitial cell phenotype and function by hyaluronic acid in 2-D and 3-D culture environments. *Matrix Biol.* **30,** 70–82 (2011).

39. Lin, C., Raza, A. & Shih, H. PEG hydrogels formed by thiol-ene photo-click chemistry and their effect on the formation and recovery of insulin-secreting cell spheroids. *Biomaterials* **32,** 9685–9695 (2011).

40. McCall, J. D. & Anseth, K. S. Thiol-ene photopolymerizations provide a facile method to encapsulate proteins and maintain their bioactivity. *Biomacromolecules* **13,** 2410–7 (2012).

41. McCall, J. D., Luoma, J. E. & Anseth, K. S. Covalently tethered transforming growth factor beta in PEG hydrogels promotes chondrogenic differentiation of encapsulated human mesenchymal stem cells. *Drug Deliv. Transl. Res.* **2,** 305–312 (2012).

42. Aikawa, E. *et al.* Human semilunar cardiac valve remodeling by activated cells from fetus to adult: implications for postnatal adaptation, pathology, and tissue engineering. *Circulation* **113,** 1344–52 (2006).

43. Bossé, Y. *et al.* Refining molecular pathways leading to calcific aortic valve stenosis by studying gene expression profile of normal and calcified stenotic human aortic valves. *Circ. Cardiovasc. Genet.* **2,** 489–98 (2009).

4.8. Supplementary Information

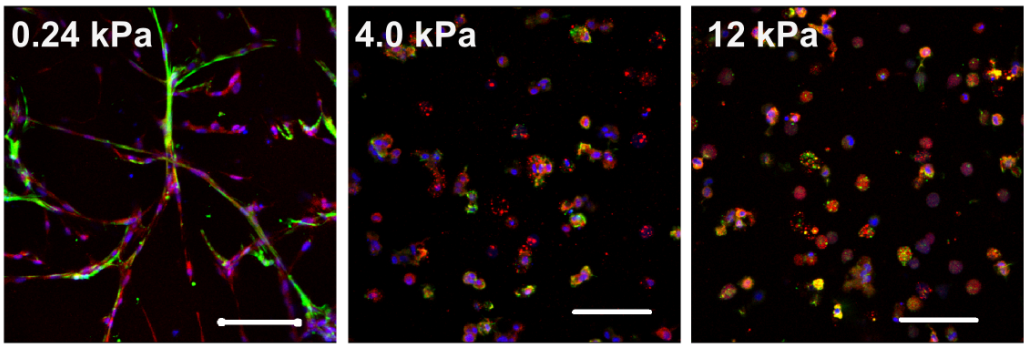

Figure 4.7. Immunostaining of standard encapsulation with varying modulus for αSMA (green), f-actin (red) and nuclei (blue). Scale bars = 100 μm.

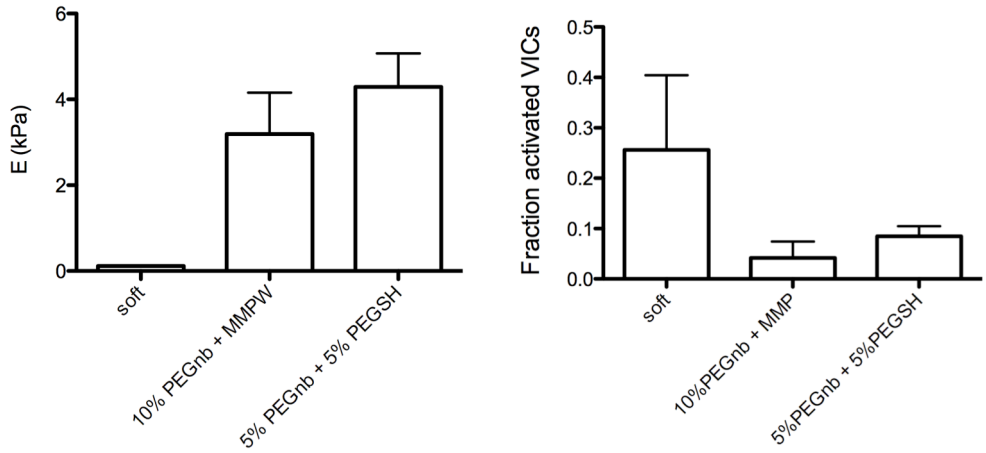

Supplementary Figure 4.8. VIC-laden hydrogels were stiffened with degradable (10wt%PEGnb + MMP-degradable peptide) or non-degradable (5wt%PEGnb + 5wt%PEGSH) networks with approximately equivalent moduli. Error bars indicate SEM. In both conditions, the increase in modulus resulted in a decrease in VIC activation. Error bars indicate SD, n=2.

Chapter 5

Three-dimensional high-throughput cell encapsulation platform to study dynamic changes to the extracellular matrix

---

Abstract

In their extracellular microenvironment, cells respond to a complex array of biochemical and mechanical cues that can vary in both time and space. Towards a better understanding as to how cell phenotype is influenced by these signals and their possible interactions, high-throughput methods that allow characterization of cell-laden matrices are valuable tools to screen through many combinations of variables, ultimately helping to evolve and test hypotheses related to cell-ECM signaling. Here, we developed a platform that allows high-throughput encapsulation of cells in peptide-functionalized poly(ethylene glycol) hydrogels, combined with imaging of these 3D microenvironments over time. This approach also allows the material environment to be dynamically modified by either 1. the introduction of soluble or tethered cytokines or 2. changes in the matrix properties (e.g., mechanics, adhesive ligands). To test and demonstrate the methods, aortic valvular interstitial cells (VICs), a population of cells responsible for the pathological fibrosis and matrix remodeling that leads to aortic stenosis, were encapsulated in PEG hydrogels. Arrays of gels were formed with a range of volumes (5-40 μL) and cell densities (0-10 million cells/mL gel). Cell viability remained high after encapsulation.

The fibronectin-derived adhesive peptide RGDS was tethered to the gels *in situ*. VIC response to the dynamic addition of RGDS was characterized by quantifying cell morphology and by measuring the expression of α-smooth muscle actin, a hallmark of the myofibroblast phenotype. VICs elongated in response to RGDS addition, and cell spreading occurred at a faster rate than in gels formed with RGDS in the initial polymerization. No spreading was observed without RGDS addition. Further, expression of αSMA was also dependent on matrix adhesion, with VICs exhibiting higher levels of αSMA in gels with RGDS.

5.1. Introduction

High-throughput screening platforms are a critical technology for the elucidation of complex biological mechanisms. The use of automated liquid handling systems has simplified screening in plates with 96 or more wells; however, the standard implementation of this technique involves culturing cells on tissue culture polystyrene (TCPS) or coated glass[1]. This method has proved useful in dramatically increasing the rate at which drug candidates can be tested, but cells on these supraphysiologically stiff 2D surfaces are likely to respond to stimuli much differently than cells *in vivo*. For example, prostate and breast cancer cells are both more susceptible to chemotherapeutics on TCPS than when encapsulated within extracellular matrix proteins[2,3]. Hepatocytes also showed elevated levels of drug metabolism on alginate substrates that facilitated cell-cell interactions compared to traditional TCPS culture[4].

The extracellular matrix can dramatically impact cell phenotype. To better understand these cues, microarrays have been developed to study cell-protein[5] and cell-polymer[6] interactions. Additionally, systems to test cellular response to 2D substrates of varying moduli have been developed[7,8]. To understand how ECM cues direct cell phenotype, it is not only the

matrix composition (e.g., protein content) that is important, but also the orientation in which the cells interact with the proteins. The dimensionality of the system in which cells are studied can influence a number of cell functions, including polarity, morphology, motility, and cell-cell interactions, as reviewed by Baker and Chen[9]. To explore cell response to drugs in a 3D environment, high-throughput platforms have been developed that encapsulate cells within alginate[10], Matrigel[11], agarose[12], poly(ethylene glycol) (PEG)[13], and arrays of other polymers[14]. With this wide range of materials, many options exist to give experimenters control over many matrix properties, such as chemical composition and matrix mechanics.

While great strides forward have been made in recapitulating specific cellular niches for high throughput experiments, the extracellular matrix properties can also change over time. For example, dramatic changes in ECM composition and mechanical properties are observed in fetal development[15], tumor growth[16], wound repair[17], and fibrotic disease progression[15,18]. In addition, the ECM is a reservoir of numerous growth factors that are often released during times of major matrix remodeling. Here, we focus on the aspects of dynamic matrix changes in the context of the aortic valve tissue, which undergoes fibrosis during the development of stenosis.

Changes in the ECM in aortic stenosis are actively mediated by the valvular interstitial cells (VICs), which are found throughout the aortic valve and exhibit mostly a fibroblast-like phenotype in healthy adult valves[19]. In disease, VICs can become activated to a myofibroblast phenotype, which is associated with increased ECM remodeling, contractility, and proliferation[20]. However, it is difficult to study this fibroblast-to-myofibroblast transition using traditional *in vitro* approaches, because culture of VICs on tissue culture polystyrene plates results in high levels of activated myofibroblasts and dramatically alters the phenotype of these cells[21]. Additionally, VICs both remodel their local matrix and receive cues from the ECM, and

these feedback loops make it difficult to ascertain the net effects of potential therapeutics *in vitro*. A wide range of changes in the ECM have been observed in aortic stenosis, including a shift in the type of collagen deposited[22], breakdown of the elastin fiber organization[23], increased secretion of proteoglycans[24], and increased expression of fibronectin[25]. Previous studies have shown that VIC αSMA expression and ECM deposition are dependent on the adhesive ligand sequence to which the cells are bound[26,27], indicating an important role of the biochemical composition of the ECM in determining VIC phenotype.

Here, we have developed a platform for the 3D encapsulation of cells in synthetic ECM mimics that can be modified at user-defined time points to recapitulate the dynamic nature of the cell niche *in vivo*. Cells were encapsulated in a PEG-based hydrogel using a photoinitiated thiol-ene reaction. This experimenter-initated polymerization permits the formation of cell-laden pre-polymer droplets in each well without premature gelation of the stock solutions. 8-arm PEG-norbornene is crosslinked by reaction with an MMP-degradable peptide flanked with thiol-containing cysteines on both ends, resulting in a matrix that cells can locally remodel to spread and move within the gel. PEG is relatively bioinert due to its hydrophilicity, so ECM-derived peptide sequences containing a single cysteine can be incorporated pendantly to facilitate cell-matrix interactions. Using this approach, adhesive site concentration can be tuned independently of other variables such as the matrix modulus. The fibronectin-derived peptide CRGDS was incorporated into the matrix either at initial gel formation or after 3 days of culture without an adhesive ligand, and the resulting VIC morphology and αSMA expression were quantified.

5.2. Materials and Methods

5.2.1. Cell culture

VICs were isolated from the aortic valves of fresh porcine hearts using a sequential collagenase (Worthington Biochemical) digestion, as described previously[28]. For expansion of cells before experiments, VICs were cultured at 37°C and 5% CO_2 on tissue culture polystyrene (TCPS, Corning) in growth media, which consisted of Media 199 (Life Technologies) supplemented with 15% fetal bovine serum (FBS, Life Technologies), 2% penicillin-streptomycin (Life Technologies), and 0.5 mg/mL fungizone (Life Technologies). Cells were passaged using trypsin (Life Technologies) digestion and used in experiments after 2-4 passages. For experiments, FBS in media was reduced to 1% to limit proliferation.

5.2.2. PEG-norbornene synthesis

8-arm PEG (40 kDa, JenKem) was functionalized with norbornene as described previously[28,29]. Briefly, stoichiometric amounts of PEG and 4-dimethylaminopyridine (Sigma-Aldrich) were dissolved in anhydrous dichloromethane (Sigma-Aldrich), and a two-fold excess of each 5- norbornene-2-carboxylic acid (Sigma-Aldrich) and N-N'-diisopropylcarbodiimide (Sigma-Aldrich) were added. The flask was purged with argon and then the reaction proceeded overnight on ice. The PEG-norbornene was then precipitated in 4°C ethyl ether (Fisher Scientific), filtered, and dried. The product was purified by dialysis and then lyophilized, and overall end group functionality was determined to be ~90% by proton nuclear magnetic resonance imaging.

5.2.3. High-throughput encapsulation

Encapsulations were performed on an automated liquid handler (EpMotion M5073, Eppendorf) to facilitate the high-throughput production of cell-laden hydrogels. To permit the covalent attachment of the hydrogels to the bottom of the 96 well glass bottom plate (PerkinElmer), the plate was treated with 95% ethanol (pH ~ 5.5) with 0.55vol% (3-mercaptopropyl) trimethoxysilane for 5 min, and was then rinsed with 95% ethanol.

A precursor solution of PEG-norbornene, MMP-degradable crosslinking peptide, and cells in phosphate-buffered saline (PBS, Life Technologies) was robotically mixed with either a solution containing the adhesive peptide CRGDS (American Peptide Company, Inc.) or PBS. After mixing, the polymer solutions contained 0.75 mM PEG-norbornene, 1.875 mM MMP-degradable peptide (KCGPQG↓IWGQCK, American Peptide Company, Inc.), and 1.7 mM lithium phenyl-2,4,6-trimethylbenzoylphosphinate (LAP) and 10 million cell/mL. This composition contains 2.25 mM excess –ene functionalities, which are available for tethering peptides or proteins at a later time point. Pipetting parameters were optimized for the precursor solution for accurate dispensation of reproducibly sized gels (15.5 mm/s aspiration, 33.0 mm/s dispense, delayed blow), with a volume of 10 μL per gel unless otherwise stated. These solutions were then pipetted into the wells of the thiolated plate. The polymerization of these gels was photoinitiated by a 2 min light exposure (2.5 mW/cm^2 @ 365 nm). After polymerization, 200 μL media was added to each well. For experiments to visualize the gel volume, an AlexaFluor maleimide 488 fluorescent label was covalently attached to the gel network.

5.2.4. Dynamic tethering of RGDS

Media was removed from the gels by inverting the plate. Then, gels were dosed with 30 μL of a solution containing either 1.25 or 5 mM CRGDS and 1.7 mM LAP in PBS. Alternatively, for gels with no RGDS tethering, 30 μL PBS was added to prevent drying. Plates were placed on a shaker for 30 min to facilitate the diffusion of RGDS and LAP throughout the gels. Next, RGDS was tethered by 2 min exposure to UV light. RGDS solutions were then removed from the gels, and 2x5 min washes were performed. To quantify the concentration of tethered RGDS, 5% of a TAMRA (Click Chemistry Tools) labeled peptide (TAMRA_Ahx_RGDSC) was added to the peptide swelling solution. The NH2-Ahx_RGDSC -H peptide was synthesized on resin before conjugating the fluorophore. Briefly, the TAMRA NHS ester was dissolved in DMF and added to the resin with a catalytic amount of DIEA and allowed to stir at room temperature for 3 hours. The labeled peptide was cleaved from the resin with a solution of TFA/triisopropyl silane/water/ phenol (90:2.5:2.5:5%), precipitated and washed in cold ether, before purification via reverse phase HPLC (Waters). Fluorescence was quantified on a BioTek H1 Synergy plate reader after an additional overnight wash, and tethered concentrations of RGDS were interpolated from the standard curve gels.

5.2.5. Cell viability and metabolic activity assays

VICs were treated with PBS containing 1 μM calcein (Life Technologies) and 4 μM ethidium homodimer (Life Technologies) for 25 min. 50 μm stacks of images were collected at 5 μm intervals using an Operetta high-content confocal microscope (PerkinElmer). Cell viability was quantified using Harmony software (PerkinElmer) to count the number of live and dead cells in each maximum intensity projection. To quantify metabolic activity, cells were treated with

PrestoBlue (Invitrogen) according to the manufacturer's instructions and fluorescence was measured on a BioTek H1 Synergy plate reader.

5.2.6. Measurement and quantification of cell morphology

VICs were treated with calcein for 30 min every 48 hrs and images were collected every 24 hrs on an Operetta high-content confocal microscope. For each field of view, 11 slices were imaged at 5 μm intervals, and a maximum intensity projection was used to produce 2D images of these 50 μm thick sections. Cell morphology was analyzed using Harmony software (PerkinElmer) to identify cells and calculate the aspect ratio. At least 150 cells were analyzed per replicate.

5.2.7. Immunostaining for αSMA

After 7 days of culture (4 days after RGDS addition), cells were fixed for 30 min in 10% formalin. Gels were washed with PBS and then VICs were permeabilized by treatment with PBS containing 0.05wt% Tween 20 (Sigma-Aldrich). Next, non-specific staining was blocked with 1% bovine serum albumin (BSA, Sigma-Aldrich). Then, mouse anti-αSMA (Abcam) diluted 1:200 in the BSA solution was added overnight at 4°C. Samples were washed 3 x 1 hr before addition of goat-anti-mouse AlexaFluor 488 (1:300, Life Technologies), rhodamine-phalloidin (1:300, Life Technologies), and DAPI (5 μg/mL, Life Technologies) overnight at 4°C. Samples were washed in PBS and then imaged on the PerkinElmer Operetta. 4 fields of view were imaged for each replicate, with 11 slices at 5 μm intervals. A maximum intensity projection was used to produce 2D images of these 50 μm sections. Harmony software was used to quantify the ratio of αSMA to DAPI (nuclei). Each cell was identified using the DAPI channel, and cell area

was identified using the f-actin channel. Then, the ratio of αSMA to DAPI was calculated for the cells. Each condition represents 4 replicates. Error bars represent the standard error, and a one-way ANOVA with a Newman-Keuls post-test was performed to analyze the statistical significance of the results.

5.3. Results

5.3.1. Development of high-throughput cell encapsulation platform

Arrays of hydrogels containing VICs were formed in 96-well plates using an automated liquid handler to form droplets of pre-gel solution containing suspended cells, which were then polymerized using a photoinitiated reaction (Figure 5.1). The gels were approximately 4 mm in diameter and with a height of 1 mm. Here, we have varied the presentation of the adhesive peptide, RGDS; however, this platform could also be used to vary other gel properties, such as gel modulus or susceptibility to cell cleavage, by changing the components in the precursor solution. 24 hours after encapsulation, approximately 75% of cells remained viable as determined by staining with calcein (live cells) and ethidium homodimer (dead cells).

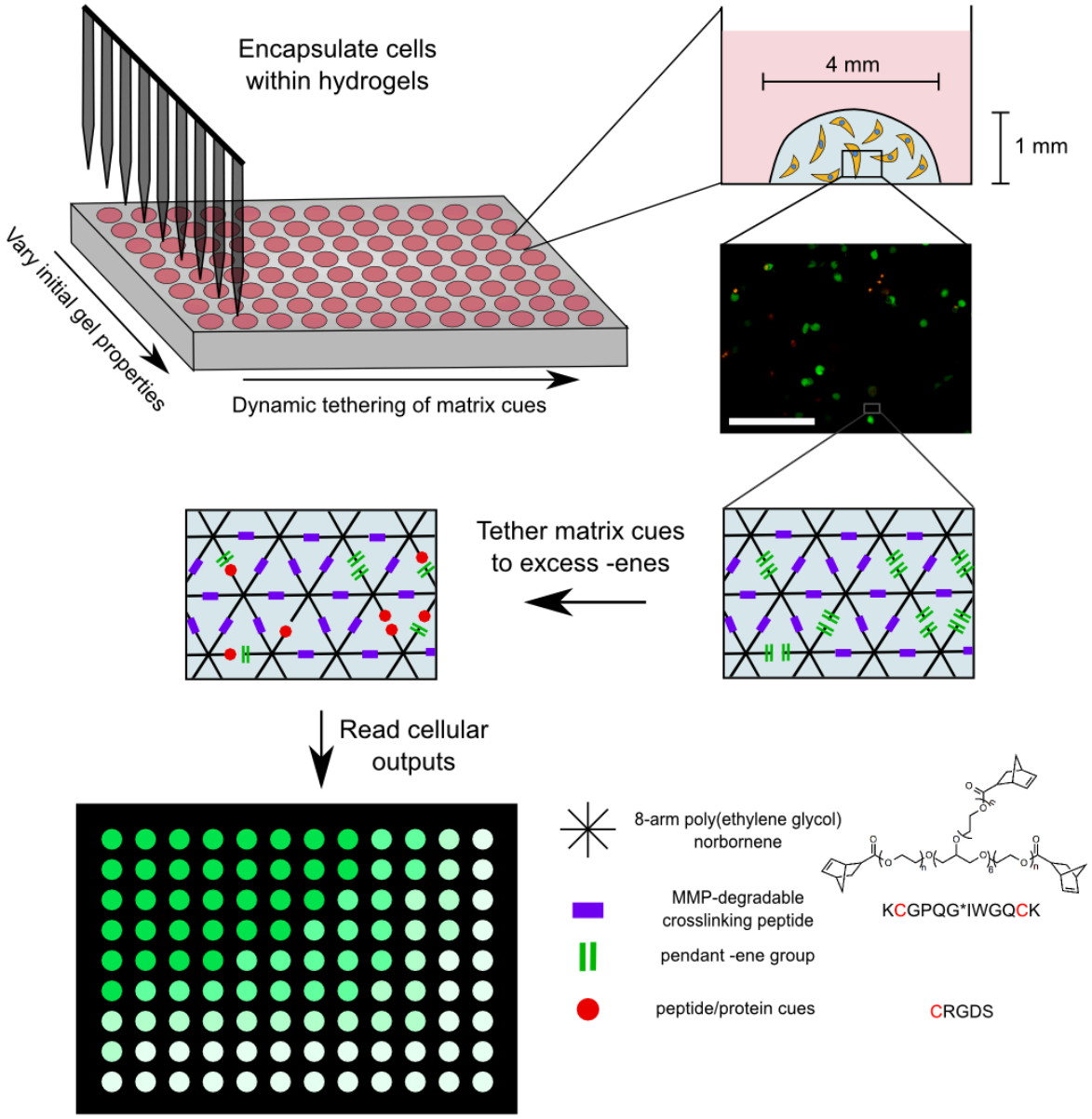

Figure 5.1. High-throughput, dynamic cell encapsulation platform. Cells suspended in a pre-polymer solution are added to a 96 well plate by an automated liquid handler. Initial gel properties, such as RGDS concentration, are varied by changing the concentration in the pre-polymer solution. Droplets are then polymerized by exposure to 365 nm light for 2 min via a thiol-ene reaction in which the norbornene groups on the PEG molecules react with the thiols on cysteine-containing peptides. High VIC viability was observed 24 hours after encapsulation (Scale bar = 100 μm, green = live, red = dead). Unreacted –enes can later by functionalized with peptide or protein cues using a second photoinitated reaction, allowing the measurement of cellular responses to dynamic changes in the ECM.

Arrays with hydrogels ranging from 5 – 40 µL were formed and relative size was determined through the incorporation of a fluorescent label (Figure 5.2A), demonstrating the ability to choose the scale of the encapsulation based on needs for downstream assays. 5 µL and 10 µL gels retained a rounded shape in the center of the wells, 20 µL frequently take on a more assymetric shape (Figure 5.2B). 40 µL gels coat the bottom of the well (not shown). The VICs are dispersed throughout the gel volume (Figure 5.2C), creating a 3D culture environment. Cell loading into the gels was also controlled over a range of 1 - 10 million cells per mL of gel as measured by a metabolic activity assay (Figure 5.2D).

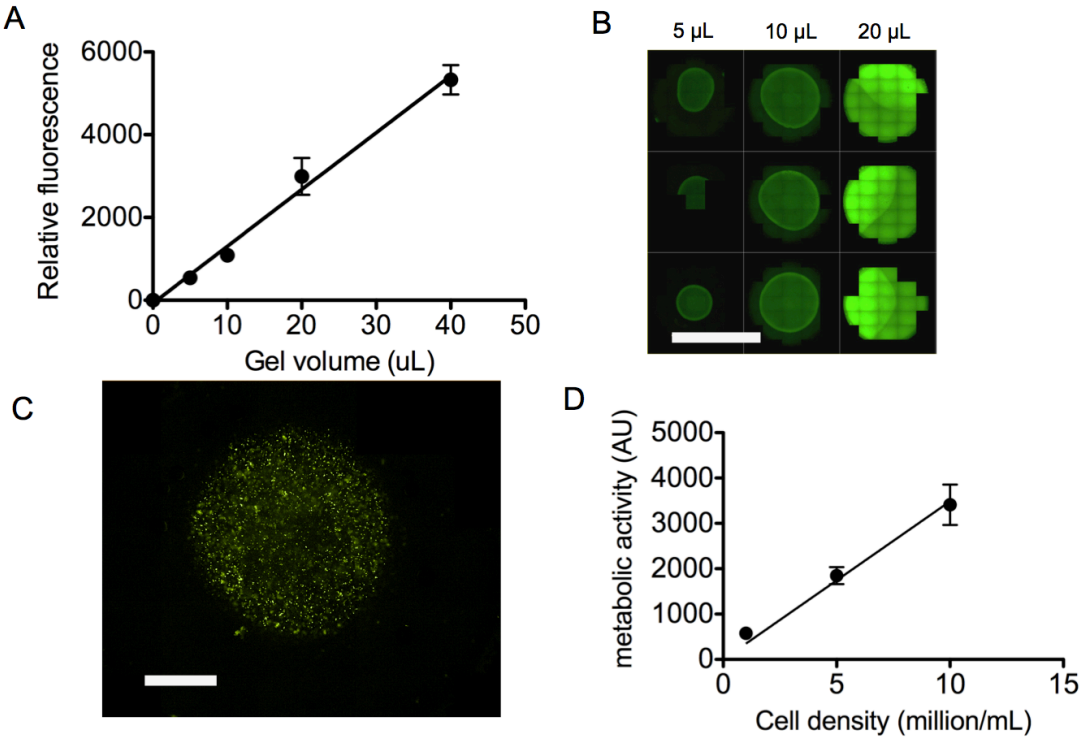

Figure 5.2. Characterization of hydrogel arrays. A) An array of gels of different sizes labeled with AlexaFluor 488 was formed. Quantification of fluorescent intensity showed that the fluorescent signal was directly proportional go gel size. B) Gels were visualized by stitching together images collected on the Operetta high-content confocal. Scale bar = 6 mm. C) VICs encapsulated within a gel and stained for calcein. Image represents a single slice 100 µm from the bottom of the gel. Scale bar = 1mm. D) Precise cell loading was achieved for cell densities between 1-10 million cells/mL of gel as quantified by a metabolic activity assay.

RGDS was tethered to the hydrogel matrices using a photoinitiated thiol-ene reaction. Concentration of incorporated RGDS was determined using a fluorescently labeled RGDS peptide and comparing fluorescent intensity in gels with dynamic tethering to gels initially formed to contain a range of RGDS concentrations (Figure 5.3A). Conditions leading to both high (1.5 mM) and low (0.4 mM) concentrations of RGDS were identified. Tethering RGDS did not influence cell viability (Figure 5.3B). Additionally, samples treated with the RGDS solution but not exposed to UV light were used as a control to determine that the 30 minute dosing with soluble RGDS did not harm cell viability by blocking integrins. No statistically significant differences in viability were observed in response to RGDS tethering or to the dosing with soluble RGDS.

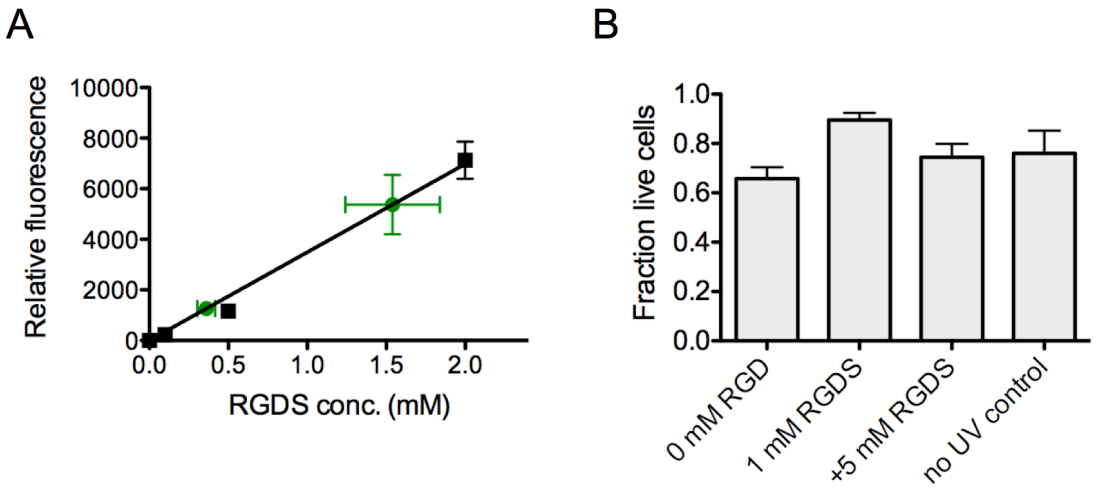

Figure 5.3. Characterization of RGDS addition. A) Fluorescently labeled RGDS was reacted into hydrogels during initial gel formation and fluorescent intensity was measured to form a standard curve (black squares). Then, gels with no RGDS were dosed with an RGDS/LAP solution and a photoinitated reaction was used to tether the peptide to the unreacted –ene functionalities within the gel. Fluorescence was measured to determine the concentration of tethered RGDS (green circles). B) Cell viability assay showed no loss in viability due to RGDS addition or to the 30 min treatment with soluble RGDS shown in the no UV control ($p > 0.05$ in one-way ANOVA). Error bars show +/- SEM.

5.3.2. RGDS addition promotes VIC spreading within gels

VICs were encapsulated within hydrogels containing either 0 or 1 mM RGDS and morphology was quantified by measuring the length/width ratios of the cells. After 3 days, VICs began to spread within gels containing RGDS, but remained rounded in gels with no adhesive ligand (Figure 5.4). At this point, either 1.5 mM or 0.4 mM RGDS was dynamically tethered into the gel. By day 4, only 24 hours after tethering, VICs had responded to the RGDS addition by spreading, and had already managed to reach nearly the same aspect ratio as the VICs that had been encapsulated within RGDS-containing gels for all 4 days. In 0 mM RGDS gels with no addition of adhesive ligand, the cells remained rounded throughout the experiment. Changes in cell morphology in response to dynamic tethering of RGDS were independent of the concentration of RGDS over the range tested (0.4 – 1.5 mM). Similar trends were observed in a stiffer gel (0.875 mM PEG), but longer times were required for spreading (Figure 5.6, Supplementary Information).

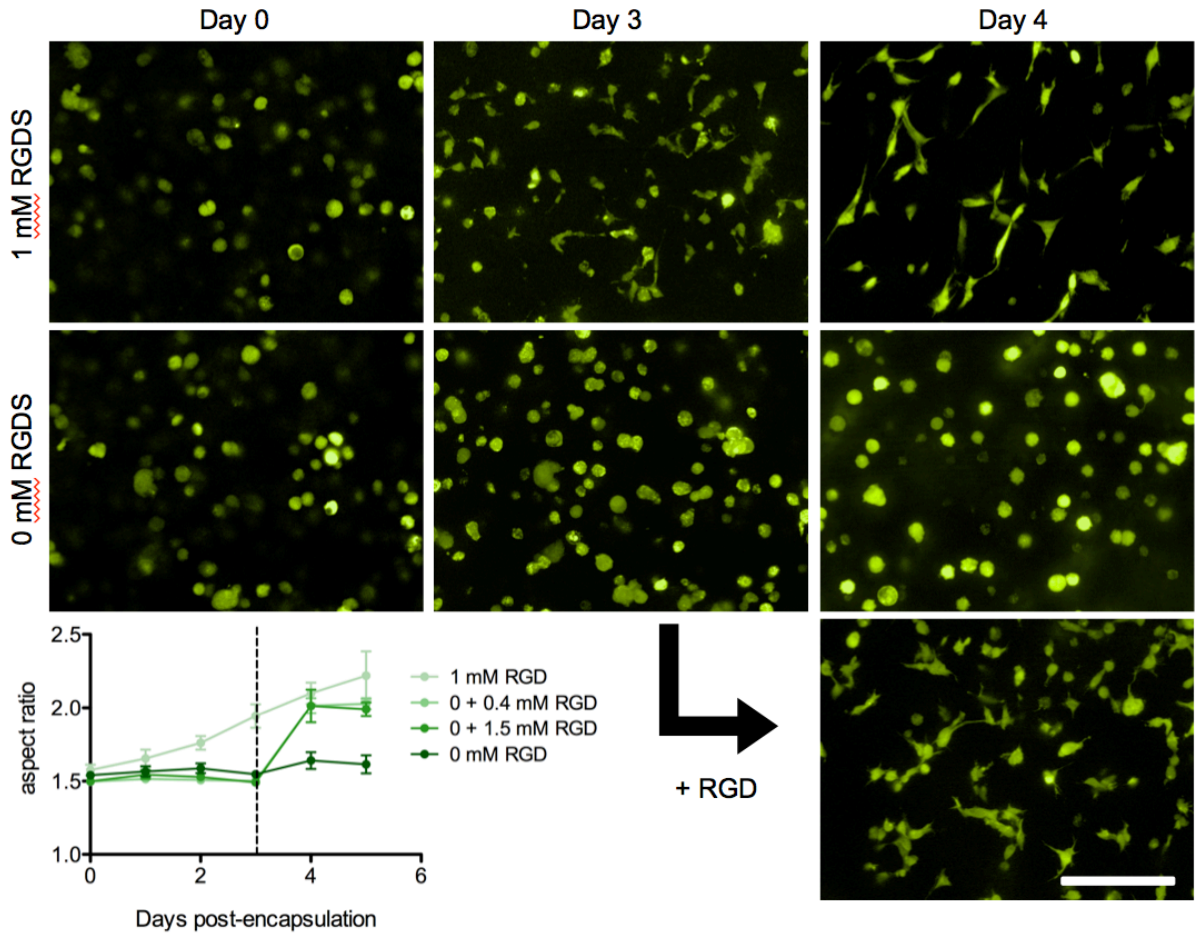

Figure 5.4. Dynamic tethering of adhesive peptides promotes VIC elongation. VICs were encapsulated in PEG hydrogels with or without the RGDS adhesive ligand. In gels with RGDS, VICs were able to spread and elongate within the gel, but VICs encapsulated without RGDS maintained a rounded morphology. Scale bar = 100 μm. The addition of RGDS on day 3 by photoinitiated covalent tethering resulted in VIC elongation after only 24 hours. The graph displays the quantification of the aspect ratio (cell length/width) over 5 days. The dashed line represents the addition of RGDS. Error bars represent +/- SEM, $n \geq 6$.

5.3.3. RGDS-dependent αSMA expression

Expression of αSMA, a hallmark of the myofibroblast phenotype, was also examined by immunostaining samples 7 days after encapsulation (Figure 5.5). When VICs were initially encapsulated in gels with no RGDS, αSMA expression was significantly lower than in VICs encapsulated with 1 mM RGDS. However, the dynamic addition of 1.5 mM RGDS after 3 days

of culture to gels that initially had no RGDS led the VICs to produce as much αSMA as in the gels where RGDS was present throughout the experiment. These results indicate that VIC phenotype is highly dependent on the adhesive ligands present in the extracellular matrix.

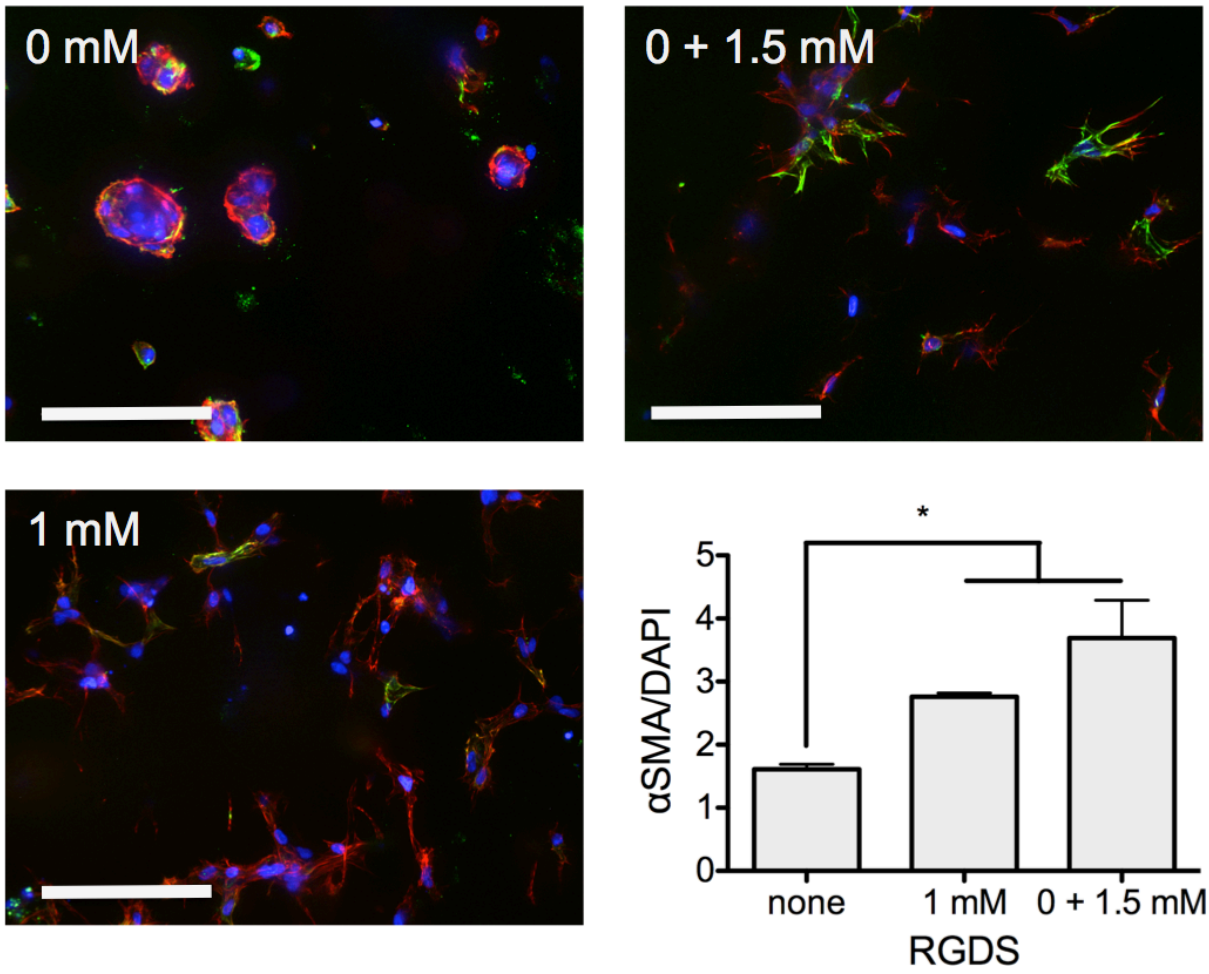

Figure 5.5. VIC αSMA expression is dependent on the presence of adhesive ligands in the extracellular matrix. When VICs were encapsulated in gels containing no RGDS, αSMA expression was significantly lower than in the RGDS-containing gels. When gels that initially contained 0 mM RGDS were then modified with 1.5 mM RGDS, αSMA expression increased to the level seen in gels that containing RGDS throughout the 7 days of the experiment. Nuclei = blue, f-actin = red, αSMA=green. Scale bar = 100 μm. Error bars represent SEM. * $p < 0.05$.

5.4. Discussion

During the progression of fibrotic diseases, including aortic stenosis, cells are exposed to a complex cascade of mechanical and biochemical signals. High-throughput methods are needed to better understand how these signals, both independently and synergistically, direct cell phenotype. While there have been a number of examples of high-throughput cell encapsulation platforms, our approach provides the unique ability to dynamically alter the matrix in which the cells reside.

As expected, VICs required RGDS in order to achieve an elongated morphology (Figure 5.4). Interestingly, VIC spreading and elongation occurred much more rapidly when RGDS was dynamically tethered into the matrix on day 3 than when VICs were initially encapsulated in RGDS-containing gels. This is likely due to VIC remodeling of the local matrix throughout the experiment by secretion of various MMPs to degrade the matrix. In a 3D environment, fibroblast spreading requires both adhesive ligands for the cell to attach to, as well as local degradation of the ECM to provide space for the cell to spread into. Even though VICs encapsulated in gels without RGDS were not able to spread due to the lack of cell-matrix interactions, they were likely still secreting MMPs that were able to cleave some of the crosslinks in the pericellular area. Then, once RGDS was incorporated into the network, the VICs were able to spread at a faster rate.

No differences were observed as a result of the concentration of dynamically tethered RGDS (Figure 5.4). Likely, both of the RGDS concentrations studied (0.4 mM and 1.5 mM) were high enough to present an excess of RGDS ligands compared to the number of available integrin pairs. This is consistent with studies showing an increase in cell migration speed with

increasing RGDS concentration until a threshold is reached, at which point migration speeds plateau[30].

Morphology was not the only aspect of the VIC phenotype that changed in response to the addition of RGDS. Expression of αSMA, a hallmark of the myofibroblast phenotype, was also dependent on RGDS (Figure 5.5). It is unlikely that the rounded VICs in the 0 mM RGDS gels could fully take on the myofibroblast phenotype, as they are not able to spread, attach to the matrix, and generate contractile forces. However, it was not known whether the myofibroblast phenotype was simply functionally inhibited in rounded, constrained VICs due to the restricted morphology or if there were differences in the gene expression levels as well. Quantification of αSMA by immunostaining demonstrated that not only was the αSMA not organized into stress fibers in the 0 mM RGDS condition, but that the total amount of αSMA was lower. After RGDS was tethered into the 0 mM gels, αSMA expression increased. This activation of VICs in response to RGDS, a fibronectin-derived peptide, indicates a possible mechanism that may contribute to valve disease, where increased levels of fibronectin expression have been observed.

Dynamic tethering of the RGDS on day 3 resulted in somewhat higher levels of αSMA than gels that contained RGDS at formation. This may suggest a possible role of temporal modulation of matrix properties in directing VIC phenotype, with a step change in matrix adhesion leading to a more myofibroblast-like phenotype; however, additional experiments would be required to determine whether this is a real effect.

Cellular responses to soluble cues are frequently matrix-dependent. For example, VIC activation in response to soluble delivery of TGF-β1 is dependent of the substrate modulus[31]. The encapsulation platform described here could easily be implemented to study the influence of soluble cues, such as those found in drug candidate libraries, in a more physiologically-relevant

environment. Further, the ability to recapitulate some of the dynamic changes that occur in the ECM throughout disease progression could help identify ranges of disease progression over which a specific drug candidate may be effective. As an example, if a drug could inhibit an integrin-dependent signaling pathway that leads to pathological ECM deposition, combinatorial gel formations representing the range of adhesive ligands present throughout disease progression could be tested to determine an appropriate treatment window.

The high-throughput platform presented here could be particularly useful for the identification of molecules that may regulate cell-matrix interactions or matrix remodeling, as traditional cell-based screens on TCPS would not be able to capture these functions. Since this system has been developed to be compatible with standard protocols for screening drug libraries using robotic liquid handlers, it would be possible to test a large number of molecules. This could help identify potential therapeutics for fibrotic diseases, such as aortic stenosis, in which dysregulation of matrix remodeling plays a critical role in disease progression.

This study has investigated VIC response to a single adhesive ligand, which is derived from fibronectin. While increases in fibronectin expression are observed in patients with aortic stenosis[25], many other ECM proteins may also play an important role in disease progression. To compare the influence of different ECM proteins, adhesive peptides from other disease-associated proteins, such as collagen X[22] or proteoglycans[23], could be sequentially tethered to gels already containing peptides derived from proteins found in healthy valves, such as elastin or collagen I[32].

One benefit of using a thiol-ene reaction for encapsulation of cells within hydrogels is the flexibility that this chemistry provides with respect to the incorporation of additional functionalities. In addition to peptides, whole proteins containing a free thiol could be reacted

into the network. This chemistry is also compatible with a previously developed method for *in situ* stiffening of cell-laden hydrogels[28], which would allow for user-directed modulation of both the biochemical and mechanical matrix properties. Ongoing experiments will investigate the combinatorial effects of stiffness and adhesivity through temporally-controlled tethering of adhesive ligands and matrix stiffening. Ultimately, these dynamic alterations in matrix properties will be in combination with pro-inflammatory cytokines that have been implicated in aortic stenosis, such as TGF-β1 and IL-1β[33,34].

5.5. Conclusions

This work presented a method for high-throughput encapsulation of cells within 3D hydrogel matrices that permit the dynamic addition of ECM cues through the photoinitiated tethering of adhesive peptides. This platform was implemented to study the influence of adhesive ligands on VIC morphology and αSMA expression. VICs were able to spread and elongate in response to RGDS, and the rate of spreading was faster when RGDS was introduced on day 3 rather than during the initial gel formation. αSMA expression was also dependent on adhesive ligands, with a greater intensity of αSMA staining seen in response to addition of RGDS. This study shows the potential for study the influence of matrix cues on cell phenotype, and could be adapted for studies investigating the interplay between soluble cues and matrix properties.

5.6. Acknowledgements

The authors would like to acknowledge support to KMM from an NIH Pharmaceutical Biotechnology Training Grant, support to MES from an NSF Graduate Research Fellowship,

support to SZP from the Discovery Learning Apprenticeship Program, and funding from Howard Hughes Medical Institute (HHMI).

5.7. References

1. Major, J. Challenges and Opportunities in high Throughput Screening: Implications for New Technologies. *J. Biomol. Screen.* **3,** 13–17 (1998).

2. Chambers, K. F., Mosaad, E. M. O., Russell, P. J., Clements, J. A. & Doran, M. R. 3D Cultures of Prostate Cancer Cells Cultured in a Novel High-Throughput Culture Platform Are More Resistant to Chemotherapeutics Compared to Cells Cultured in Monolayer. *PLoS One* **9,** e111029 (2014).

3. Hongisto, V. *et al.* High-Throughput 3D Screening Reveals Differences in Drug Sensitivities between Culture Models of JIMT1 Breast Cancer Cells. *PLoS One* **8,** 1–16 (2013).

4. Elkayam, T., Amitay-Shaprut, S., Dvir-Ginzberg, M., Harel, T. & Cohen, S. Enhancing the drug metabolism activities of C3A--a human hepatocyte cell line--by tissue engineering within alginate scaffolds. *Tissue Eng.* **12,** 1357–1368 (2006).

5. Ceriotti, L. *et al.* Fabrication and characterization of protein arrays for stem cell patterning. *Soft Matter* **5,** 1406 (2009).

6. Anderson, D. G., Putnam, D., Lavik, E. B., Mahmood, T. A. & Langer, R. Biomaterial microarrays: rapid, microscale screening of polymer-cell interaction. *Biomaterials* **26,** 4892–7 (2005).

7. Mih, J. D. *et al.* A multiwell platform for studying stiffness-dependent cell biology. *PLoS One* **6,** 1–10 (2011).

8. Gobaa, S. *et al.* Artificial niche microarrays for probing single stem cell fate in high throughput. *Nat. Methods* **8,** 949–955 (2011).

9. Baker, B. M. & Chen, C. S. Deconstructing the third dimension: how 3D culture microenvironments alter cellular cues. *J. Cell Sci.* **125,** 3015–24 (2012).

10. Meli, L. *et al.* Three dimensional cellular microarray platform for human neural stem cell differentiation and toxicology. *Stem Cell Res.* **13,** 36–47 (2014).

11. Deiss, F. *et al.* A Platform for High-Throughput Testing of the Effect of Soluble Compounds on 3D Cell Cultures. *Anal. Chem.* **85,** 8085–8094 (2013).

12. Tumarkin, E. *et al.* High-throughput combinatorial cell co-culture using microfluidics. *Integr. Biol. (Camb).* **3,** 653–62 (2011).

13. Ranga, A. *et al.* 3D niche microarrays for systems-level analyses of cell fate. *Nat. Commun.* **5,** 1–10 (2014).

14. Celiz, A. D. *et al.* Discovery of a Novel Polymer for Human Pluripotent Stem Cell Expansion and Multilineage Differentiation. *Adv. Mater.* (2015). doi:10.1002/adma.201501351

15. Merryman, W. D. Mechano-potential etiologies of aortic valve disease. *J. Biomech.* **43,** 87–92 (2010).

16. Kessenbrock, K., Plaks, V. & Werb, Z. Matrix Metalloproteinases: Regulators of the Tumor Microenvironment. *Cell* **141,** 52–67 (2010).

17. Hinz, B. Formation and function of the myofibroblast during tissue repair. *J. Invest. Dermatol.* **127,** 526–37 (2007).

18. Bataller, R. & Brenner, D. A. Liver fibrosis. *J Clin Invest.* **115,** 209–18 (2005).

19. Wang, H., Sridhar, B., Leinwand, L. a & Anseth, K. S. Characterization of cell subpopulations expressing progenitor cell markers in porcine cardiac valves. *PLoS One* **8,** e69667 (2013).

20. Rabkin-Aikawa, E., Farber, M., Aikawa, M. & Schoen, F. J. Dynamic and reversible changes of interstitial cell phenotype during remodeling of cardiac valves. *J. Heart Valve Dis.* **13,** 841–7 (2004).

21. Wang, H., Tibbitt, M. W., Langer, S. J., Leinwand, L. A. & Anseth, K. S. Hydrogels preserve native phenotypes of valvular fibroblasts through an elasticity-regulated PI3K/AKT pathway. *Proc. Natl. Acad. Sci.* **110,** 19336–19341 (2013).

22. Wirrig, E. E., Hinton, R. B. & Yutzey, K. E. Differential expression of cartilage and bone-related proteins in pediatric and adult diseased aortic valves. *J. Mol. Cell. Cardiol.* **50,** 561–569 (2011).

23. Hinton, R. B. *et al.* Extracellular matrix remodeling and organization in developing and diseased aortic valves. *Circ. Res.* **98,** 1431–1438 (2006).

24. Stephens, E. H. *et al.* Differential proteoglycan and hyaluronan distribution in calcified aortic valves. *Cardiovasc. Pathol.* **20,** 334–342 (2011).

25. Bossé, Y. *et al.* Refining molecular pathways leading to calcific aortic valve stenosis by studying gene expression profile of normal and calcified stenotic human aortic valves. *Circ. Cardiovasc. Genet.* **2,** 489–98 (2009).

26. Gould, S. T., Darling, N. J. & Anseth, K. S. Small peptide functionalized thiol-ene hydrogels as culture substrates for understanding valvular interstitial cell activation and de novo tissue deposition. *Acta Biomater.* **8,** 3201–9 (2012).

27. Gould, S. & Anseth, K. Role of cell-matrix interactions on VIC phenotype and tissue depostion in 3D PEG hydrogels. *J. Tissue Eng. Regen. Med.* (2013). doi:10.1002/term.1836

28. Mabry, K. M., Lawrence, R. L. & Anseth, K. S. Dynamic stiffening of poly(ethylene glycol)-based hydrogels to direct valvular interstitial cell phenotype in a three-dimensional environment. *Biomaterials* **49,** 47–56 (2015).

29. Fairbanks, B. D. *et al.* A Versatile Synthetic Extracellular Matrix Mimic via Thiol-Norbornene Photopolymerization. *Adv. Mater.* **21,** 5005–5010 (2009).

30. Schwartz, M. P. *et al.* A synthetic strategy for mimicking the extracellular matrix provides new insight about tumor cell migration. *Integr. Biol. (Camb).* **2,** 32–40 (2010).

31. Quinlan, A. M. T. & Billiar, K. L. Investigating the role of substrate stiffness in the persistence of valvular interstitial cell activation. *J. Biomed. Mater. Res. Part A* **087257,** 2474–82 (2012).

32. Chen, J. H. & Simmons, C. A. Cell-matrix interactions in the pathobiology of calcific aortic valve disease: critical roles for matricellular, matricrine, and matrix mechanics cues. *Circ. Res.* **108,** 1510–24 (2011).

33. Jian, B. *et al.* Progression of aortic valve stenosis: TGF-B1 is present in calcified aortic valve cusps and promotes aortic valve interstitial cell calcification via apoptosis. *Ann. Thorac. Surgery,* 457–465 (2003).

34. Kaden, J. J. *et al.* Interleukin-1 beta promotes matrix metalloproteinase expression and cell proliferation in calcific aortic valve stenosis. *Atherosclerosis* **170,** 205–211 (2003).

5.8. Supplementary Information

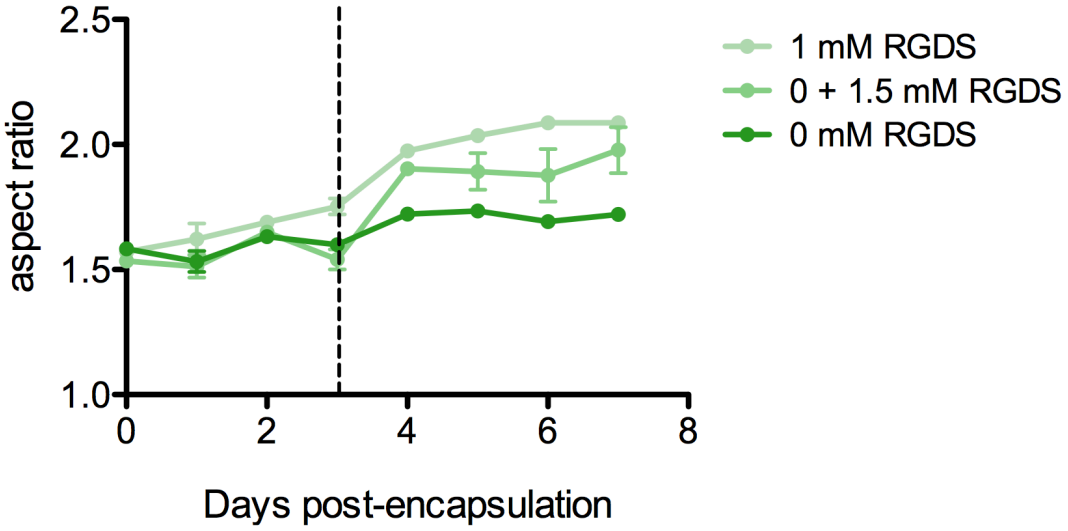

Figure 5.6. In stiffer hydrogels containing 0.875 mM PEG, cell spreading was slower, but VICs elongated in response to addition of RGDS while remaining rounded in gels with no tethered RGDS.

Chapter 6

Conclusions and Recommendations

The activation of valvular interstitial cells (VICs) to the myofibroblast phenotype is a key transition in the development of aortic stenosis. Understanding the VIC fibroblast-to-myofibroblast transition and its reversal is important for several reasons, which include: 1. the potential to identify new pharmacological treatments to prevent or reverse valve disease, 2. improving strategies for tissue engineering heart valves, and 3. providing insights into other fibrotic diseases (e.g., lung, liver, kidney). Valve explants and *in vivo* experiments have provided extensive insight into the changes that occur in the valve during disease progression and genetic contributions to valve disease, but more controlled *in vitro* experiments would help us to understand the primary factors leading to pathological myofibroblast activation and discern the mechanisms by which this transition occurs.

Due to the large number of stimuli that may play a role in VIC activation, highly defined *in vitro* experiments are necessary to elucidate the impact of individual cues. Unfortunately, traditional culture of VICs on stiff plastic plates results in dramatic changes in gene expression levels, as well as activation to the myofibroblast phenotype[1]. A high baseline level of activation makes it difficult, if not impossible, to study the quiescent fibroblast phenotype and the signals that cause these quiescent fibroblasts to become activated. This thesis focused on the

implementation of hydrogel cell culture platforms to recapitulate aspects of the native VIC environment to better understand the fibroblast-to-myofibroblast transition. Collectively, the work presented in this thesis demonstrates the importance of the microenvironment in determining VIC phenotype, and shown that matrix cues alone can be used to direct VIC phenotype.

Poly(ethylene glycol) (PEG)-based matrices can be formed over a wide range of physiologically relevant moduli (e.g., E ~ 0.2 – 100 kPa), and VICs cultured on soft (7 kPa) hydrogels were found to maintain a quiescent fibroblast phenotype *in vitro*[1]. Additionally, peptide-functionalized PEG hydrogels are readily synthesized using a cytocompatible, photoinitated thiol-ene reaction, permitting the encapsulation of cells within materials that allow control of integrin binding, introduction of proteolytically cleavable linkers, and local sequestration of growth factors[2–5]. While PEG macromolecules are associated with high levels of water of hydration that render it relatively bioinert, PEG hydrogels can be easily functionalized with moieties (e.g., peptides, proteins, small molecule drugs) to render them bioactive and illicit specific cellular responses. These characteristics make PEG-based hydrogels an attractive platform to study VIC activation and motivate the use of these hydrogels in this thesis.

In Chapter 3, the influence of the culture microenvironment on VIC phenotype was investigated by quantifying molecular markers of the VICs, such as the percentage of VICs with αSMA stress fibers and the mRNA levels of myofibroblast-associated genes. These measurements were then complemented by a more global characterization of the transcriptional profile. Freshly isolated VICs were compared to three different culture platforms: VICs seeded on TCPS, VICs seeded on (2D) hydrogels, and VICs encapsulated within (3D) hydrogels. On TCPS, most VICs activated to the myofibroblast phenotype as seen by the expression of

organized αSMA stress fibers; however, when cultured on hydrogel surfaces (2D) or embedded within them (3D), less than 10% activation was observed after 48 hours of culture. VICs on TCPS also had the highest level of αSMA mRNA. Interestingly, VICs on 2D hydrogel substrates had higher αSMA expression than VICs encapsulated within the hydrogels, despite similar levels of activation to the myofibroblast phenotype. This finding motivated the transcriptional analysis to better define and provide more detailed insight into differences between the VIC phenotypes that result from variations in microenvironmental conditions.

Microarray data quantifying the mRNA levels of over 20,000 genes revealed that the magnitudes of perturbations in gene expression levels compared to freshly isolated VICs were much greater on TCPS than with hydrogel culture. Many genes influenced by the culture platform were related to functions important in valve disease, such as matrix remodeling, focal adhesions, and cytoskeletal organization and contractility. While both 2D and 3D hydrogel matrices resulted in expression profiles that were more similar to freshly isolated VICs than TCPS, dimensionality was also found to influence the mRNA levels of a number of genes. The VIC functions most influenced by dimensionality (i.e., 2D versus 3D culture) were associated with cell structure and motility, developmental processes, proliferation and differentiation, and transport. It is likely that these biological processes play an important role in the fibroblast-to-myofibroblast transition and in the progression of valve disease, motivating the encapsulation of VICs within 3D hydrogels for the rest of the experiments presented in this thesis. Additionally, these results demonstrate that differences between transcriptional profiles of VIC cultured in 2D versus 3D translates to significantly different responses to matrix stiffness and highlight the important implications of the microarray data in Chapter 3 for the regulation of the fibroblast-to-myofibroblast transition.

In both *in vivo* and *in vitro* studies, there is a strong correlation between aortic valve stiffening and the appearance of elevated numbers of VIC myofibroblasts, highlighting the notion that VICs both respond to and act upon their local environment. This in turn has generated a great deal of interest in deconvoluting the cell-matrix interaction feedback loops that lead to valve disease[6]. In 2D cultures, researchers have shown that systematically increasing the substrate modulus results in increased VIC myofibroblast activation; however, little was known about how VICs responded to stiffness variations in 3D. However, results in Chapter 3 showed clear differences in the transcriptional profile of VICs in 2D and 3D. Further, one would hypothesize that VICs embedded in a 3D environment would interact with the matrix differently (e.g., elevated protease levels, higher levels of cell-matrix interactions). Experiments designed in Chapter 4 sought to quantify the impact of changes in matrix stiffness on VICs embedded in MMP-degradable PEG hydrogels. First, VICs were encapsulated in matrices of varying moduli (E = 0.24 – 12 kPa), and interestingly, αSMA expression decreased with increasing modulus, contrary to findings in 2D systems. However, the coupling of variables in 3D systems can complicate the interpretation of these results. Specifically, since VICs must locally degrade the matrix in order to spread and elongate in 3D, cell morphology is dependent on the crosslinking density, and therefore modulus, of the gel.

To resolve the effects of these two variables, a system for *in situ* stiffening of cell-laden hydrogels was developed. This strategy was implemented to increase matrix modulus after the VICs had achieved an elongated morphology by first encapsulating the VICs and culturing them for several days to allow for local matrix remodeling. After controlling for morphology, a second gel was in situ formed that leading to a step change in the bulk hydrogel modulus. Then, after 2 additional days, VIC myofibroblast activation was measured, and still found to be

inversely proportional to matrix modulus. Essentially, in soft 3D microenvironments, VIC phenotype appeared to be regulated like that observed for valve homeostasis: when the local environment was softer than healthy valve tissue, the VICs became activated to the myofibroblast phenotype, which is associated with matrix remodeling and deposition. At a healthy valve modulus (E ~ 1-2 kPa), the VICs became quiescent. At a stiffer, more "disease-like" modulus, the VICs remained quiescent rather than expressing the pathological myofibroblast phenotype, which could continue to stiffen the matrix. These results suggest that in 3D microenvironments, an additional stimulus is likely necessary to act in combination with matrix stiffness to observe the appearance of the pathogenic VIC behavior. Control experiments revealed that VICs deactivated after stiffening regardless of the enzymatic degradability of the secondary network; however, future experiments should explore later timepoints to determine whether VIC remodeling of the ECM eventually leads to a different phenotype. This could be accomplished by using the same MMP-degradable crosslinker from the initial gel in the secondary network.

Given the extensive range of biochemical and mechanical cues acting upon VICs during disease progression and evolution of the pathogenic myofibroblast phenotype motivates the development of tools to study this plethora of extracellular signals in a systematic manner. In Chapter 5, a high-throughput cell encapsulation method was designed to be compatible with traditional drug screening procedures while also providing the ability to recapitulate the dynamic changes in the ECM that occur during disease progression. This method allowed the creation of arrays of hydrogels with control over matrix modulus, adhesive ligands, gel size, and cell density. These cell-material arrays are compatible with 3D imaging in real time using a high-content confocal microscope to rapidly and quantitatively collect data about cell morphology. Upon

completion of the experiment, these cells can be fixed and stained for proteins of interest. These arrays are also compatible with absorbance and luminescence plate-based assays, including assays to measure luciferase and metabolic activity. As a proof of concept, a fibronectin-derived adhesive ligand, RGDS, was added *in situ* and was found to stimulate VIC spreading at a faster rate than when cells were initially encapsulated with the same ligand, demonstrating the complex interplay between VICs and their ECM. This addition of RGDS also led to an increase in αSMA, indicating a shift towards the myofibroblast phenotype.

In addition to changing the adhesive ligands, future work will include varying the bulk modulus of the hydrogel using the stiffening approach described in Chapter 3 to represent both the mechanical and biochemical changes in the valve matrix that occur in development and disease. The temporal introduction of adhesive ligands and stiffening secondary networks will be varied to investigate how these dynamic changes can lead to reversible or irreversible changes in VIC phenotype. In addition to the quantification of cell morphology and αSMA expression, the percentage of proliferative VICs will be characterized, as proliferation is associated with the pathological activation to the myofibroblast phenotype[7].

While activation can be induced by a myriad of triggers (e.g., inflammation, crosstalk with valve endothelial cells), we hypothesize that persistence of the myofibroblast phenotype likely depends on synergistic effects of both mechanical and chemical stimuli. To test this hypothesis, this high-throughput screening platform should be implemented to create combinatorial arrays varying matrix modulus and soluble factor delivery to study the mechanotransduction and pro-inflammatory cytokine signaling that regulate pathogenic activation of VIC myofibroblast. Cytokines that may be relevant to valve disease progression include TGF-β1, IL-1β, TNF-α, and IL-6. Of these cytokines, TGF-β1 has been the most widely

studied in VICs and is known to promote myofibroblast-like properties[8]. IL-1β is found extensively in human stenotic aortic valves[9] and its signaling leads to expression of MMP-1 and MMP-2, which results in increased cell proliferation and matrix remodeling *in vitro*. Additionally, mice deficient in IL-1 receptor antagonist (IL-1Ra) that negatively regulates IL-1β signal transduction develop aortic stenosis[10]. TNF-α is also present in calcified aortic valves and its expression is induced in response to matrix remodeling[11]. TNF-α leads to calcification of human VICs *in vitro*, but its role in heart-valve fibrosis has not been explored. Finally, IL-6 is expressed in patients with fibrotic aortic valves, and its expression promotes mineralization[12,13]. The study of these cytokines in combination with a range of matrix moduli could uncover the additional stimuli necessary to promote disease-like behavior in 3D cultures.

This high-throughput platform could also be extended to drug screening experiments. This would be a significant improvement over screening VICs seeded on TCPS, because TCPS is so much stiffer than the valve that it may override the effects of the many molecules in the screen. An additional cue, such as the previously discussed cytokines, may be necessary to direct the VICs to a more disease-like phenotype prior to screening. These drug screens could provide useful information about the efficacy of many molecules prior to animal studies. Hits from the drug screen could then be tested in relevant mouse models of aortic stenosis[14].

While soluble biochemical cues can be added to VIC culture, co-cultures with cell types producing these soluble cues may present these molecules in a more physiologically relevant manner. In particular, the valve endothelium is known to play a significant role in the development of aortic stenosis[15], and valvular endothelial cells (VECs) can actively regulate VIC phenotype[16,17]. Endothelial dysfunction is associated with the onset of aortic sclerosis[18]. VECs likely influence VIC phenotype through the secretion of nitric oxide, FGF, endothelin, and

natriuretic peptides[15,16]. VECs could easily be incorporated into the hydrogel culture platforms presented in Chapters 3 and 5 simply by seeding a monolayer of VECs on top of the hydrogels containing VICs. This geometry would be similar to that of the aortic valve, where VICs are found dispersed throughout the tissue while VECs form a monolayer on the surface. This strategy of controlling the spatial proximity during co-culture would also enable signaling between VICs and VECs through nitric oxide or other short-lived molecules.

Our current understanding of the signaling mechanisms involved in VIC response to matrix mechanics is largely based on microarray data measuring the abundance of mRNA transcripts. However, relevant signaling pathways can be difficult to identify through the measurement of mRNA levels alone. Many signal transduction events involve the phosphorylation of a protein or the translocation of a transcription factor to another location within the cell, typically without a change in the total abundance of this protein. One pathway that has been found to regulate stiffness-mediated VIC activation is the PI3K/AKT pathway[1]. When substrate stiffness is reduced, VICs exhibit lower levels of AKT phosphorylation and become deactivated. Further, inhibition of PI3K reduces αSMA expression and prevents VIC activation, even on TCPS. Preliminary data indicates that pAKT localization may also play an important role in AKT-mediated VIC activation, as pAKT is localized to the αSMA stress fibers in VICs seeded on a stiff hydrogel substrate (Figure 6.1). When pAKT was measured in VICs encapsulated within 3D hydrogels, stiffening (as described in Chapter 4) resulted in increased pAKT (Figure 6.2). This experiment did not show a change in pAKT levels in 2D in response to substrate stiffness, possibly due to the small range of moduli tested (0.4 – 13 kPa, compared to the originally investigated range of 7 – 32 kPa). Nonetheless, the trend observed in pAKT in response to 3D hydrogel modulus is consistent with previous 2D results; however, since

encapsulated VICs have higher activation in soft gels, pAKT does not seem to correlate with VIC activation levels.

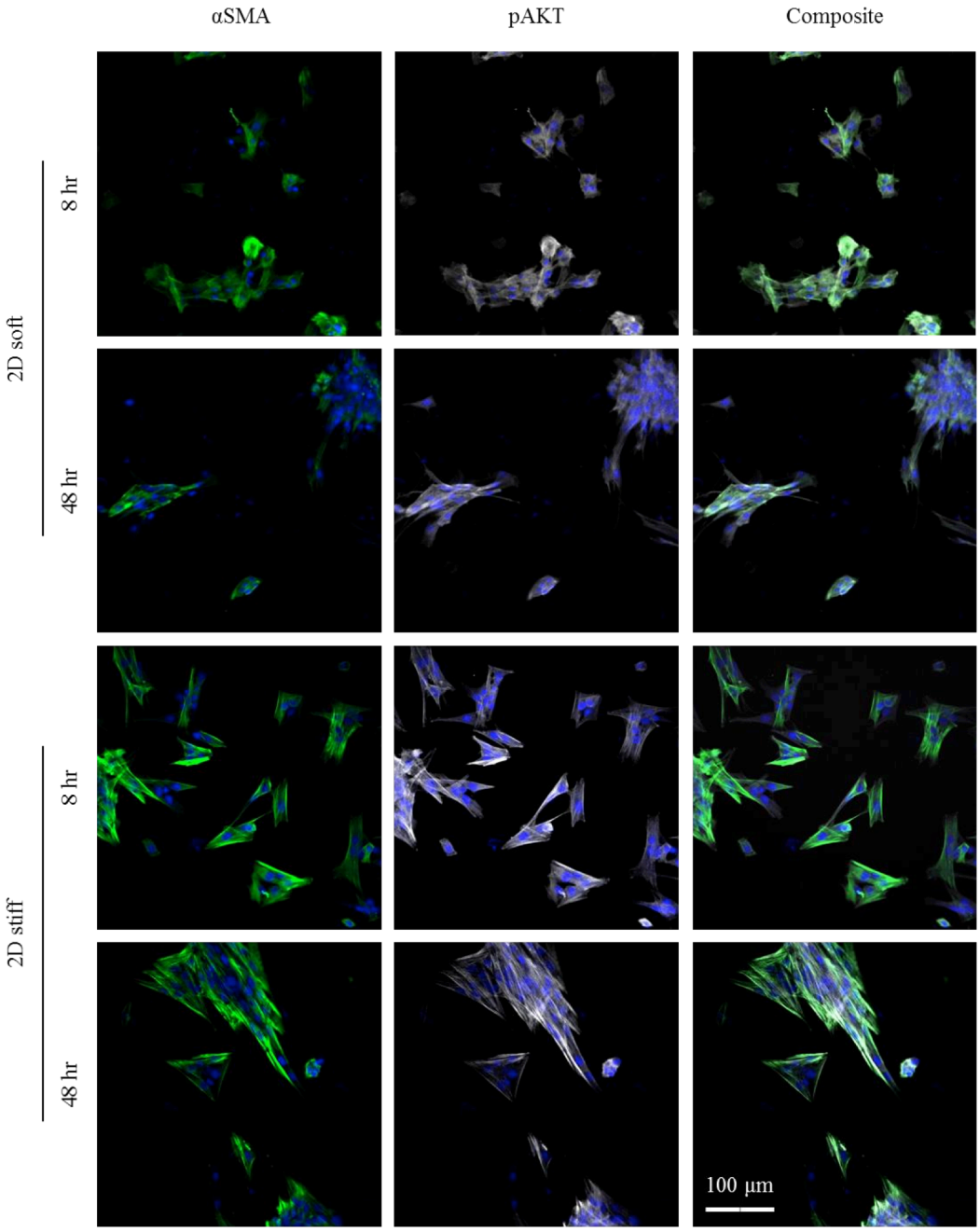

Figure 6.1. VICs on soft and stiff hydrogel substrates were stained for αSMA (green), pAKT (white), and DAPI after 8 and 48 hours of culture. These images show well-defined stress fibers on stiff gels, but not on soft. pAKT appeared to localize to these stress fibers, and remained localized throughout the 48-hour period of study, indicating a possible role for pAKT in VIC activation. In collaboration with Caitlin Jones.

The FAK pathway was also investigated as a possible modulator of the environmental effect of stiffness on VIC αSMA expression, since it localizes to focal adhesions and its expression can vary with environmental stiffness[19,20]. Trends in the levels of pFAK (Figure 6.2) were consistent with previously observed trends of αSMA mRNA levels and VIC activation (Chapters 3 and 4), making this pathway a promising candidate for future study. In addition to the FAK pathway, more pathways of interest could be identified through the use of a protein phosphorylation array to identify which phorphorylated proteins are most influenced by matrix mechanics. A better understanding of the relevant signaling could lead to more promising targets for pharmacological treatments of valve disease.

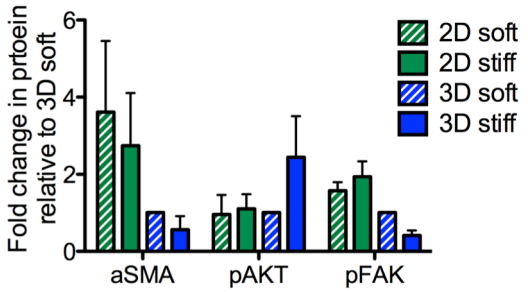

Figure 6.2. Western blots show increase in pAKT after stiffening in 3D and a decrease in pFAK after stiffening. αSMA expression was lower in 3D than in 2D regardless of stiffness. No significant changes in protein levels were observed between stiff and soft 2D conditions, however, this may be due to the small range of moduli tested (0.4 – 13 kPa). In collaboration with Caitlin Jones.

While the materials discussed in this thesis enable the study of synergistic mechanical and biochemical influences, further materials development could lead to the ability to present more complex mechanical cues to the VICs. Materials with the ability to either soften[21] or stiffen (Chapter 4) in response to a user-directed cue (e.g., light) have been developed to study

VIC responses to changes in matrix modulus. While these systems provide useful examples of how VICs may respond to mechanical changes in the valve tissue *in vivo*, progression to valvular stenosis is likely caused by cumulative effects of repeated minor, local injuries. The exploration of this hypothesis *in vitro* necessitates the development of materials that are able to reversibly stiffen *and* soften in response to a cytocompatible cue, such as light. These materials with reversible changes and moduli could lead to insight regarding the reversibility of VIC deactivation in response to stiffening seen in Chapter 4. There are a number of approaches that could be implemented to study reversible changes in the environment. Instead of forming a non-degradable secondary network, cell-laden hydrogels could be stiffened with a network containing an MMP-degradable peptide sequence, which would allow the cells to soften the matrix over time. For a more experimenter-defined approach, a photodegradable moiety could be incorporated into the stiffening network. Then, the hydrogels could be soften to their original modulus by exposure to light.

Another strategy in materials development is the synthesis of supramolecular hydrogels that exhibit changes in modulus depending on the number of interactions between "guest" and "host" functionalities (Figure 6.3). Specifically, hyaluronic acid is functionalized with either azobenzene, the "guest" molecule, or cyclodextrin, the "host". The azobenzene can reversibly associate with the cyclodextrin, forming crosslinks between the hyaluronic acid chains. Irradiation with 365 nm light leads to azobenzene isomerization to the cis conformation, which corresponds to a decrease in the crosslinking density and therefore an overall softening of the hydrogel. The gel can then be stiffened again by reverse isomerization initiated with visible light (400-500 nm). The implementation of this material to study VIC activation could help answer important questions about why VICs become persistently activated to the myofibroblast

phenotype, as seen in disease, rather than reverting to a quiescent phenotype after an injury has been resolved.

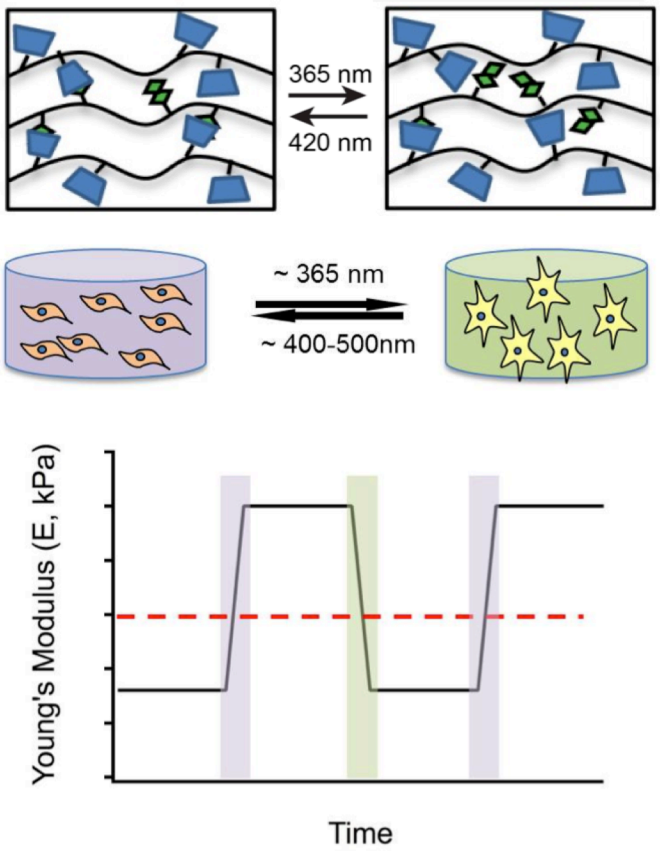

Figure 6.3. Materials with reversible mechanical properties. Guest-host gels can be reversibly softened or stiffened by exposure to 365 nm or 420 nm light, respectively. This system would enable the study of cyclic exposure to changes in modulus. Image courtesy of Dr. Adrianne Rosales.

Another approach to studying the effects of injury and repair on VIC phenotype would be to perform a traditional wound healing assay on a hydrogel substrate. Typically, this would involve physically scraping away a "wound" area in a confluent layer of cells seeded on TCPS and studying how the cells migrate to heal the wound[22]. However, since TCPS is an inherently activating substrate for VICs, this method is unlikely to yield any insight into how the fibroblast-

to-myofibroblast transition is influenced by wound healing. By instead performing this assay on hydrogels, changes in VIC activation levels relative to the proximity to the wound could be measured. Additionally, sequential wounds could be formed to recapitulate the repeated injuries of the valve over time.

In addition to mechanical and biochemical stimuli, genetics also play a significant role in the development of valve disease. Mutations in the NOTCH1 gene have been associated with bicuspid aortic valves and incidence of aortic stenosis[23,24]. To study the interplay of genetic and mechanical influences on the fibroblast-to-myofibroblast transition, cells from genetically modified and control murine valves could be cultured in hydrogels with varying moduli. While the small size of murine aortic valves presents technical challenges for *in vitro* experiments, recent literature has demonstrated the isolation and expansion of Notch-mutated VICs[25]. Studies with these genetically modified murine VICs would help elucidate specific mechanisms by which genetic mutations lead to stenotic valves. Additionally, this strategy could provide a method for testing treatments for a group of patients with a particular genetic mutation.

In this work we have shown the effect of both mechanical and biochemical cues on VIC phenotype, utilizing PEG hydrogels. Gel stiffness was most intensively studied and shown to influence the VIC transcriptional profile and the fibroblast-to-myofibroblast transition. These cell culture platforms will enable better *in vitro* screening of therapeutic agents for treatment of valve disease and more physiologically relevant study of cell biology.

6.1. References

1. Wang, H., Tibbitt, M. W., Langer, S. J., Leinwand, L. A. & Anseth, K. S. Hydrogels preserve native phenotypes of valvular fibroblasts through an elasticity-regulated PI3K/AKT pathway. *Proc. Natl. Acad. Sci.* **110,** 19336–19341 (2013).

2. Fairbanks, B. D. *et al.* A Versatile Synthetic Extracellular Matrix Mimic via Thiol-Norbornene Photopolymerization. *Adv. Mater.* **21,** 5005–5010 (2009).

3. Kloxin, A. M., Kasko, A. M., Salinas, C. N. & Anseth, K. S. Photodegradable hydrogels for dynamic tuning of physical and chemical properties. *Science* **324,** 59–63 (2009).

4. Sridhar, B. V, Doyle, N. R., Randolph, M. a & Anseth, K. S. Covalently tethered TGF-β1 with encapsulated chondrocytes in a PEG hydrogel system enhances extracellular matrix production. *J. Biomed. Mater. Res. A* **102,** 4464–72 (2014).

5. Gould, S. T., Darling, N. J. & Anseth, K. S. Small peptide functionalized thiol-ene hydrogels as culture substrates for understanding valvular interstitial cell activation and de novo tissue deposition. *Acta Biomater.* **8,** 3201–9 (2012).

6. Merryman, W. D. Mechano-potential etiologies of aortic valve disease. *J. Biomech.* **43,** 87–92 (2010).

7. Schoen, F. J. Evolving concepts of cardiac valve dynamics: the continuum of development, functional structure, pathobiology, and tissue engineering. *Circulation* **118,** 1864–80 (2008).

8. Walker, G. A., Masters, K. S., Shah, D. N., Anseth, K. S. & Leinwand, L. A. Valvular myofibroblast activation by transforming growth factor-beta: implications for pathological extracellular matrix remodeling in heart valve disease. *Circ. Res.* **95,** 253–60 (2004).

9. Kaden, J. J. *et al.* Interleukin-1 beta promotes matrix metalloproteinase expression and cell proliferation in calcific aortic valve stenosis. *Atherosclerosis* **170,** 205–211 (2003).

10. Isoda, K., Matsuki, T., Kondo, H., Iwakura, Y. & Ohsuzu, F. Deficiency of interleukin-1 receptor antagonist induces aortic valve disease in BALB/c Mice. *Arterioscler. Thromb. Vasc. Biol.* **30,** 708–715 (2010).

11. Al-Aly, Z. *et al.* Aortic Msx2-Wnt calcification cascade is regulated by TNF-alpha-dependent signals in diabetic Ldlr-/- mice. *Arterioscler. Thromb. Vasc. Biol.* **27,** 2589–2596 (2007).

12. Yu, Z., Seya, K., Daitoku, K. & Motomura, S. Tumor Necrosis Factor- alpha Accelerates the Calcification of Human Aortic Valve Interstitial Cells Obtained from Patients with Calcific Aortic Valve Stenosis via the BMP2-Dlx5. *J. Pharmacol. Exp. Ther.* **337,** 16–23 (2011).

13. Côté, N. *et al.* Angiotensin receptor blockers are associated with reduced fibrosis and interleukin-6 expression in calcific aortic valve disease. *Pathobiology* **81,** 15–24 (2014).

14. Miller, J. D., Weiss, R. M. & Heistad, D. D. Calcific aortic valve stenosis: methods, models, and mechanisms. *Circ. Res.* **108,** 1392–412 (2011).

15. Simmons, C. A. Aortic Valve Mechanics. An Emerging Role for the Endothelium. *J. Am. Coll. Cardiol.* **53,** 1456–1458 (2009).

16. Gould, S. T., Matherly, E. E., Smith, J. N., Heistad, D. D. & Anseth, K. S. The role of valvular endothelial cell paracrine signaling and matrix elasticity on valvular interstitial cell activation. *Biomaterials* **35,** 3596–3606 (2014).

17. El Accaoui, R. N. *et al.* Aortic valve sclerosis in mice deficient in endothelial nitric oxide synthase. *AJP Hear. Circ. Physiol.* **306,** H1302–H1313 (2014).

18. Poggianti, E. *et al.* Disease of the Aortic Valve or Aorta Aortic Valve Sclerosis Is Associated With Systemic Endothelial Dysfunction. **41,** (2003).

19. Paszek, M. J. *et al.* Tensional homeostasis and the malignant phenotype. *Cancer Cell* **8,** 241–254 (2005).

20. Green, J. A. & Yamada, K. M. Three-dimensional microenvironments modulate fibroblast signaling responses. *Adv. Drug Deliv. Rev.* **59,** 1293–8 (2007).

21. Kloxin, A. M., Benton, J. A. & Anseth, K. S. In situ elasticity modulation with dynamic substrates to direct cell phenotype. *Biomaterials* **31,** 1–8 (2010).

22. Gotlieb, A. I., Rosenthal, A. & Kazemian, P. Fibroblast growth factor 2 regulation of mitral valve interstitial cell repair in vitro. *J. Thorac. Cardiovasc. Surg.* **124,** 591–597 (2002).

23. Garg, V. *et al.* Mutations in NOTCH1 cause aortic valve disease. *Nature* **437,** 270–274 (2005).

24. Kathiresan, S. & Srivastava, D. Genetics of human cardiovascular disease. *Cell* **148,** 1242–1257 (2012).

25. Chen, J. *et al.* Notch1 Mutation Leads to Valvular Calcification Through Enhanced Myofibroblast Mechanotransduction. *Arterioscler. Thromb. Vasc. Biol.* 1–10 (2015). doi:10.1161/ATVBAHA.114.305095

Bibliography

Adelöw, C., Segura, T., Hubbell, J. A. & Frey, P. The effect of enzymatically degradable poly(ethylene glycol) hydrogels on smooth muscle cell phenotype. *Biomaterials* **29,** 314–26 (2008).

Aikawa, E. *et al.* Human semilunar cardiac valve remodeling by activated cells from fetus to adult: implications for postnatal adaptation, pathology, and tissue engineering. *Circulation* **113,** 1344–52 (2006).

Al-Aly, Z. *et al.* Aortic Msx2-Wnt calcification cascade is regulated by TNF-alpha-dependent signals in diabetic Ldlr-/- mice. *Arterioscler. Thromb. Vasc. Biol.* **27,** 2589–2596 (2007).

Anderson, D. G., Putnam, D., Lavik, E. B., Mahmood, T. A. & Langer, R. Biomaterial microarrays: rapid, microscale screening of polymer-cell interaction. *Biomaterials* **26,** 4892–7 (2005).

Aragona, M. *et al.* A mechanical checkpoint controls multicellular growth through YAP/TAZ regulation by actin-processing factors. *Cell* **154,** 1047–59 (2013).

Arishiro, K. *et al.* Angiotensin Receptor-1 Blocker Inhibits Atherosclerotic Changes and Endothelial Disruption of the Aortic Valve in Hypercholesterolemic Rabbits. *J. Am. Coll. Cardiol.* **49,** 1482–1489 (2007).

Ayala, P., Lopez, J. I., Ph, D. & Desai, T. A. Microtopographical Cues in 3D Attenuate Fibrotic Phenotype and Extracellular Matrix Deposition : Implications for Tissue Regeneration. *J. Mol. Cell. Cardiol.* **16,** (2010).

Baker, B. M. & Chen, C. S. Deconstructing the third dimension: how 3D culture microenvironments alter cellular cues. *J. Cell Sci.* **125,** 3015–24 (2012).

Baker, C. G. & Campbell, M. The results of valvotomy for aortic stenosis. *Lancet* **267,** 171–175 (1956).

Balachandran, K., Sucosky, P., Jo, H. & Yoganathan, A. P. Elevated cyclic stretch alters matrix remodeling in aortic valve cusps: implications for degenerative aortic valve disease. *Am. J.*

Physiol. Heart Circ. Physiol. **296,** H756–H764 (2009).

Bataller, R. & Brenner, D. A. Liver fibrosis. *J Clin Invest.* **115,** 209–18 (2005).

Benton, J. a, Kern, H. B. & Anseth, K. S. Substrate properties influence calcification in valvular interstitial cell culture. *J. Heart Valve Dis.* **17,** 689–99 (2008).

Benton, J. A. Soluble and microenvironmental factors that modulate myofibroblast and calcific differentiation of valvular interstitial cells. (2009).

Benton, J. A., Fairbanks, B. D. & Anseth, K. S. Characterization of valvular interstitial cell function in three dimensional matrix metalloproteinase degradable PEG hydrogels. *Biomaterials* **30,** 6593–603 (2009).

Benton, J. A., Kern, H. B., Leinwand, L. A., Mariner, P. D. & Anseth, K. S. Statins Block Calcific Nodule Formation of Valvular Interstitial Cells by Inhibiting α -Smooth Muscle Actin Expression. *Arter. Thromb Vasc Biol* 1950–1957 (2009). doi:10.1161/ATVBAHA.109.195271

Bernardini, C. *et al.* Differential expression of nitric oxide synthases in porcine aortic endothelial cells during LPS-induced apoptosis. *J. Inflamm. (Lond).* **9,** 47 (2012).

Birgersdotter, A., Sandberg, R. & Ernberg, I. Gene expression perturbation in vitro--a growing case for three-dimensional (3D) culture systems. *Semin. Cancer Biol.* **15,** 405–12 (2005).

Bossé, Y. *et al.* Refining molecular pathways leading to calcific aortic valve stenosis by studying gene expression profile of normal and calcified stenotic human aortic valves. *Circ. Cardiovasc. Genet.* **2,** 489–98 (2009).

Bouchareb, R. *et al.* Mechanical strain induces the production of spheroid mineralized microparticles in the aortic valve through a RhoA/ROCK-dependent mechanism. *J. Mol. Cell. Cardiol.* (2013). doi:10.1016/j.yjmcc.2013.12.009

Bowler, M. A. & Merryman, W. D. In vitro models of aortic valve calcification: solidifying a system. *Cardiovasc. Pathol.* **24,** 1–10 (2015).

Bryant, S. J. & Anseth, K. S. Hydrogel Scaffolds.

Burdick, J. A. & Anseth, K. S. Photoencapsulation of osteoblasts in injectable RGD-modified PEG hydrogels for bone tissue engineering. *Biomaterials* **23,** 4315–23 (2002).

Butcher, D. T., Alliston, T. & Weaver, V. M. A tense situation: forcing tumour progression. *Nat. Rev. Cancer* **9,** 108–22 (2009).

Butcher, J. T. & Nerem, R. M. Porcine aortic valve interstitial cells in three-dimensional culture: comparison of phenotype with aortic smooth muscle cells. *J. Heart Valve Dis.* **13,** 478–85; discussion 485–6 (2004).

Butcher, J. T. & Nerem, R. M. Valvular endothelial cells and the mechanoregulation of valvular

pathology. *Philos. Trans. R. Soc. Lond. B. Biol. Sci.* **362,** 1445–57 (2007).

Butcher, J. T. & Nerem, R. M. Valvular endothelial cells regulate the phenotype of interstitial cells in co-culture: effects of steady shear stress. *Tissue Eng.* **12,** 905–15 (2006).

Butcher, J. T., Mahler, G. J. & Hockaday, L. A. Aortic valve disease and treatment: the need for naturally engineered solutions. *Adv. Drug Deliv. Rev.* **63,** 242–68 (2011).

Butcher, J. T., Mcquinn, T. C., Sedmera, D., Turner, D. & Markwald, R. R. Transitions in Early Embryonic Atrioventricular Valvular Function Correspond With Changes in Cushion Biomechanics That Are Predictable by Tissue Composition. 1503–1511 (2007). doi:10.1161/CIRCRESAHA.107.148684

Calvo, F. *et al.* Mechanotransduction and YAP-dependent matrix remodelling is required for the generation and maintenance of cancer-associated fibroblasts. *Nat. Cell Biol.* **15,** 637–646 (2013).

Carabello, B. A. Introduction to aortic stenosis. *Circ. Res.* **113,** 179–85 (2013).

Celiz, A. D. *et al.* Discovery of a Novel Polymer for Human Pluripotent Stem Cell Expansion and Multilineage Differentiation. *Adv. Mater.* (2015). doi:10.1002/adma.201501351

Ceriotti, L. *et al.* Fabrication and characterization of protein arrays for stem cell patterning. *Soft Matter* **5,** 1406 (2009).

Chambers, K. F., Mosaad, E. M. O., Russell, P. J., Clements, J. A. & Doran, M. R. 3D Cultures of Prostate Cancer Cells Cultured in a Novel High-Throughput Culture Platform Are More Resistant to Chemotherapeutics Compared to Cells Cultured in Monolayer. *PLoS One* **9,** e111029 (2014).

Chen, J. *et al.* Notch1 Mutation Leads to Valvular Calcification Through Enhanced Myofibroblast Mechanotransduction. *Arterioscler. Thromb. Vasc. Biol.* 1–10 (2015). doi:10.1161/ATVBAHA.114.305095

Chen, J. H. & Simmons, C. A. Cell-matrix interactions in the pathobiology of calcific aortic valve disease: critical roles for matricellular, matricrine, and matrix mechanics cues. *Circ. Res.* **108,** 1510–24 (2011).

Chen, J.-H., Chen, W. L. K., Sider, K. L., Yip, C. Y. Y. & Simmons, C. A. B-Catenin Mediates Mechanically Regulated, Transforming Growth Factor-B1-Induced Myofibroblast Differentiation of Aortic Valve Interstitial Cells. *Arterioscler. Thromb. Vasc. Biol.* **31,** 590–7 (2011).

Choquet, D., Felsenfeld, D. P. & Sheetz, M. P. Extracellular matrix rigidity causes strengthening of integrin-cytoskeleton linkages. *Cell* **88,** 39–48 (1997).

Chrzanowska-Wodnicka, M. & Burridge, K. Rho-stimulated contractility drives the formation of stress fibers and focal adhesions. *J. Cell Biol.* **133,** 1403–15 (1996).

Côté, N. *et al.* Angiotensin receptor blockers are associated with reduced fibrosis and interleukin-6 expression in calcific aortic valve disease. *Pathobiology* **81,** 15–24 (2014).

Cox, T. R. & Erler, J. T. Remodeling and homeostasis of the extracellular matrix: implications for fibrotic diseases and cancer. *Dis. Model. Mech.* **4,** 165–178 (2011).

Cushing, M. C., Liao, J.-T. & Anseth, K. S. Activation of valvular interstitial cells is mediated by transforming growth factor-beta1 interactions with matrix molecules. *Matrix Biol.* **24,** 428–37 (2005).

David Merryman, W. Mechano-potential etiologies of aortic valve disease. *J. Biomech.* **43,** 87–92 (2010).

De Jonge, H. J. M. *et al.* Evidence based selection of housekeeping genes. *PLoS One* **2,** 1–5 (2007).

DeForest, C. a. & Anseth, K. S. Advances in Bioactive Hydrogels to Probe and Direct Cell Fate. *Annu. Rev. Chem. Biomol. Eng.* **3,** 421–444 (2012).

Deiss, F. *et al.* A Platform for High-Throughput Testing of the Effect of Soluble Compounds on 3D Cell Cultures. *Anal. Chem.* **85,** 8085–8094 (2013).

Desmoulière, a, Geinoz, a, Gabbiani, F. & Gabbiani, G. Transforming growth factor-beta 1 induces alpha-smooth muscle actin expression in granulation tissue myofibroblasts and in quiescent and growing cultured fibroblasts. *J. Cell Biol.* **122,** 103–111 (1993).

DiMarco, R. L. *et al.* Engineering of three-dimensional microenvironments to promote contractile behavior in primary intestinal organoids. *Integr. Biol. (Camb).* **6,** 127–42 (2014).

Discher, D. E., Janmey, P. & Wang, Y.-L. Tissue cells feel and respond to the stiffness of their substrate. *Science* **310,** 1139–43 (2005).

Drolet, M., Arsenault, M., Couet, J. & Ms, C. Experimental Aortic Valve Stenosis in Rabbits. *J. Am. Coll. Cardiol.* **1097,** 1211–1217 (2003).

Duan, B., Hockaday, L. A., Kapetanovic, E., Kang, K. H. & Butcher, J. T. Stiffness and adhesivity control aortic valve interstitial cell behavior within hyaluronic acid based hydrogels. *Acta Biomater.* **9,** 7640–50 (2013).

Dupont, S. *et al.* Role of YAP/TAZ in mechanotransduction. *Nature* **474,** 179–83 (2011).

Durbin, A. D. & Gotlieb, A. I. Advances towards understanding heart valve response to injury. *Cardiovasc. Pathol.* **11,** 69–77 (2002).

Edling, C. E. & Hallberg, B. c-Kit-A hematopoietic cell essential receptor tyrosine kinase. *Int. J. Biochem. Cell Biol.* **39,** 1995–1998 (2007).

Eitzman, D. T. *et al.* Bleomycin-induced pulmonary fibrosis in transgenic mice that either lack or

overexpress the murine plasminogen activator inhibitor-1 gene. *J. Clin. Invest.* **97,** 232–237 (1996).

El Accaoui, R. N. *et al.* Aortic valve sclerosis in mice deficient in endothelial nitric oxide synthase. *AJP Hear. Circ. Physiol.* **306,** H1302–H1313 (2014).

El-Hamamsy, I. *et al.* Long-term outcomes after autograft versus homograft aortic root replacement in adults with aortic valve disease: a randomised controlled trial. *Lancet* **376,** 524–531 (2010).

Elkayam, T., Amitay-Shaprut, S., Dvir-Ginzberg, M., Harel, T. & Cohen, S. Enhancing the drug metabolism activities of C3A--a human hepatocyte cell line--by tissue engineering within alginate scaffolds. *Tissue Eng.* **12,** 1357–1368 (2006).

Eriksen, H. a. *et al.* Type I and type III collagen synthesis and composition in the valve matrix in aortic valve stenosis. *Atherosclerosis* **189,** 91–98 (2006).

Fairbanks, B. D. *et al.* A Versatile Synthetic Extracellular Matrix Mimic via Thiol-Norbornene Photopolymerization. *Adv. Mater.* **21,** 5005–5010 (2009).

Fairbanks, B. D., Schwartz, M. P., Bowman, C. N. & Anseth, K. S. Photoinitiated polymerization of PEG-diacrylate with lithium phenyl-2,4,6-trimethylbenzoylphosphinate: polymerization rate and cytocompatibility. *Biomaterials* **30,** 6702–7 (2009).

Farkas, I. J., Szántó-Várnagy, Á. & Korcsmáros, T. Linking proteins to signaling pathways for experiment design and evaluation. *PLoS One* **7,** 1–5 (2012).

Fayet, C., Bendeck, M. P. & Gotlieb, A. I. Cardiac valve interstitial cells secrete fibronectin and form fibrillar adhesions in response to injury. *Cardiovasc. Pathol.* **16,** 203–11 (2007).

Fealey, M. E., Edwards, W. D., Miller, D. V. & Maleszewski, J. J. Unicommissural aortic valves: Gross, histological, and immunohistochemical analysis of 52 cases (1978-2008). *Cardiovasc. Pathol.* **21,** 324–333 (2012).

Fondard, O. *et al.* Extracellular matrix remodelling in human aortic valve disease: The role of matrix metalloproteinases and their tissue inhibitors. *Eur. Heart J.* **26,** 1333–1341 (2005).

Frangogiannis, N. G. Targeting the Transforming Growth Factor (TGF)-β cascade in the remodeling heart: Benefits and perils. *J. Mol. Cell. Cardiol.* (2014). doi:10.1016/j.yjmcc.2014.09.001

Garg, V. *et al.* Mutations in NOTCH1 cause aortic valve disease. *Nature* **437,** 270–274 (2005).

Gelse, K., Pöschl, E. & Aigner, T. Collagens - Structure, function, and biosynthesis. *Adv. Drug Deliv. Rev.* **55,** 1531–1546 (2003).

Gieni, R. S. & Hendzel, M. J. Mechanotransduction from the ECM to the genome: are the pieces

now in place? *J. Cell. Biochem.* **104,** 1964–87 (2008).

Go, A. S. *et al. Heart Disease and Stroke Statistics - 2014 Update: A report from the American Heart Association*. *Circulation* **129,** (2014).

Gobaa, S. *et al.* Artificial niche microarrays for probing single stem cell fate in high throughput. *Nat. Methods* **8,** 949–955 (2011).

Gotlieb, A. I., Rosenthal, A. & Kazemian, P. Fibroblast growth factor 2 regulation of mitral valve interstitial cell repair in vitro. *J. Thorac. Cardiovasc. Surg.* **124,** 591–597 (2002).

Gould, S. & Anseth, K. Role of cell-matrix interactions on VIC phenotype and tissue depostion in 3D PEG hydrogels. *J. Tissue Eng. Regen. Med.* (2013). doi:10.1002/term.1836

Gould, S. T., Darling, N. J. & Anseth, K. S. Small peptide functionalized thiol-ene hydrogels as culture substrates for understanding valvular interstitial cell activation and de novo tissue deposition. *Acta Biomater.* **8,** 3201–9 (2012).

Gould, S. T., Matherly, E. E., Smith, J. N., Heistad, D. D. & Anseth, K. S. The role of valvular endothelial cell paracrine signaling and matrix elasticity on valvular interstitial cell activation. *Biomaterials* **35,** 3596–3606 (2014).

Green, J. A. & Yamada, K. M. Three-dimensional microenvironments modulate fibroblast signaling responses. *Adv. Drug Deliv. Rev.* **59,** 1293–8 (2007).

Grinnell, F., Ho, C., Tamariz, E., Lee, D. J. & Skuta, G. Dendritic Fibroblasts in Three-dimensional Collagen Matrices. **14,** 384–395 (2003).

Gu, L. *et al.* Effect of TGF-beta/Smad signaling pathway on lung myofibroblast differentiation. *Acta Pharmacol. Sin.* **28,** 382–91 (2007).

Gu, X. & Masters, K. S. Regulation of valvular interstitial cell calcification by adhesive peptide sequences. *J. Biomed. Mater. Res. A* **93,** 1620–30 (2010).

Gu, X. & Masters, K. S. Role of the MAPK/ERK pathway in valvular interstitial cell calcification. *Am. J. Physiol. Heart Circ. Physiol.* **296,** H1748–H1757 (2009).

Gu, X. & Masters, K. S. Role of the Rho pathway in regulating valvular interstitial cell phenotype and nodule formation. *Am. J. Physiol. Heart Circ. Physiol.* **300,** H448–58 (2011).

Guvendiren, M. & Burdick, J. A. Stiffening hydrogels to probe short- and long-term cellular responses to dynamic mechanics. *Nat. Commun.* **3,** 792 (2012).

Hahn, M. S., McHale, M. K., Wang, E., Schmedlen, R. H. & West, J. L. Physiologic pulsatile flow bioreactor conditioning of poly(ethylene glycol)-based tissue engineered vascular grafts. *Ann. Biomed. Eng.* **35,** 190–200 (2007).

Harunaga, J. S. & Yamada, K. M. Cell-matrix adhesions in 3D. *Matrix Biol.* **30,** 363–8 (2011).

Hermans, H. *et al.* Statins for calcific aortic valve stenosis: into oblivion after SALTIRE and SEAS? An extensive review from bench to bedside. *Curr. Probl. Cardiol.* **35,** 284–306 (2010).

Hern, D. L. & Hubbell, J. a. Incorporation of adhesion peptides into nonadhesive hydrogels useful for tissue resurfacing. *J. Biomed. Mater. Res.* **39,** 266–76 (1998).

Hinton, R. B. *et al.* Extracellular matrix remodeling and organization in developing and diseased aortic valves. *Circ. Res.* **98,** 1431–1438 (2006).

Hinz, B. Formation and function of the myofibroblast during tissue repair. *J. Invest. Dermatol.* **127,** 526–37 (2007).

Hinz, B. The myofibroblast: paradigm for a mechanically active cell. *J. Biomech.* **43,** 146–55 (2010).

Hongisto, V. *et al.* High-Throughput 3D Screening Reveals Differences in Drug Sensitivities between Culture Models of JIMT1 Breast Cancer Cells. *PLoS One* **8,** 1–16 (2013).

Hoyle, C. E. & Bowman, C. N. Thiol-ene click chemistry. *Angew. Chemie - Int. Ed.* **49,** 1540–1573 (2010).

Huang, D. W., Sherman, B. T. & Lempicki, R. A. Bioinformatics enrichment tools: Paths toward the comprehensive functional analysis of large gene lists. *Nucleic Acids Res.* **37,** 1–13 (2009).

Huang, D. W., Sherman, B. T. & Lempicki, R. A. Systematic and integrative analysis of large gene lists using DAVID bioinformatics resources. *Nat. Protoc.* **4,** 44–57 (2009).

Huang, Y. & Hsu, S. Acquisition of epithelial-mesenchymal transition and cancer stem- like phenotypes within chitosan-hyaluronan membrane-derived 3D tumor spheroids. *Biomaterials* **35,** 10070–10079 (2014).

Humphrey, J. D., Dufresne, E. R. & Schwartz, M. a. Mechanotransduction and extracellular matrix homeostasis. *Nat. Rev. Mol. Cell Biol.* **15,** 802–812 (2014).

Hutcheson, J. D., Setola, V., Roth, B. L. & Merryman, W. D. Serotonin receptors and heart valve disease-It was meant 2B. *Pharmacol. Ther.* **132,** 146–157 (2011).

Iskratsch, T., Wolfenson, H. & Sheetz, M. P. Appreciating force and shape — the rise of mechanotransduction in cell biology. *Nat. Rev. Mol. Cell Biol.* **15,** 825–833 (2014).

Isoda, K., Matsuki, T., Kondo, H., Iwakura, Y. & Ohsuzu, F. Deficiency of interleukin-1 receptor antagonist induces aortic valve disease in BALB/c Mice. *Arterioscler. Thromb. Vasc. Biol.* **30,** 708–715 (2010).

Jian, B. *et al.* Progression of aortic valve stenosis: TGF-B1 is present in calcified aortic valve cusps and promotes aortic valve interstitial cell calcification via apoptosis. *Ann. Thorac. Surgery,* 457–465 (2003).

Johnson, C. M., Hanson, M. N. & Helgeson, S. C. Porcine cardiac valvular subendothelial cells in culture: cell isolation and growth characteristics. *J. Mol. Cell. Cardiol.* **19,** 1185–93 (1987).

Kaden, J. J. *et al.* Interleukin-1 beta promotes matrix metalloproteinase expression and cell proliferation in calcific aortic valve stenosis. *Atherosclerosis* **170,** 205–211 (2003).

Kathiresan, S. & Srivastava, D. Genetics of human cardiovascular disease. *Cell* **148,** 1242–1257 (2012).

Keane, J. F., Bernhard, W. F. & Nadas, A. S. Aortic Stenosis in Infancy. *Circulation* **52,** 1138–1145 (1975).

Kessenbrock, K., Plaks, V. & Werb, Z. Matrix Metalloproteinases: Regulators of the Tumor Microenvironment. *Cell* **141,** 52–67 (2010).

Khetan, S. & Burdick, J. A. Patterning network structure to spatially control cellular remodeling and stem cell fate within 3-dimensional hydrogels. *Biomaterials* **31,** 8228–34 (2010).

Khetan, S. *et al.* Degradation-mediated cellular traction directs stem cell fate in covalently crosslinked three-dimensional hydrogels. *Nat. Mater.* **12,** 458–65 (2013).

Khetan, S., Katz, J. S. & Burdick, J. A. Sequential crosslinking to control cellular spreading in 3-dimensional hydrogels. *Soft Matter* **5,** 1601 (2009).

Kilian, K. a, Bugarija, B., Lahn, B. T. & Mrksich, M. Geometric cues for directing the differentiation of mesenchymal stem cells. *Proc. Natl. Acad. Sci. U. S. A.* **107,** 4872–7 (2010).

Kloxin, A. M., Benton, J. A. & Anseth, K. S. In situ elasticity modulation with dynamic substrates to direct cell phenotype. *Biomaterials* **31,** 1–8 (2010).

Kloxin, A. M., Kasko, A. M., Salinas, C. N. & Anseth, K. S. Photodegradable hydrogels for dynamic tuning of physical and chemical properties. *Science* **324,** 59–63 (2009).

Kural, M. H. & Billiar, K. L. Mechanoregulation of valvular interstitial cell phenotype in the third dimension. *Biomaterials* **35,** 1128–1137 (2013).

Kwan, A. P. L., Cummings, C. E., Chapman, J. A. & Grant, M. E. Macromolecular organization of chicken type X collagen in vitro. *J. Cell Biol.* **114,** 597–604 (1991).

Lieu, H. D. *et al.* Eliminating atherogenesis in mice by switching off hepatic lipoprotein secretion. *Circulation* **107,** 1315–1321 (2003).

Lin, C., Raza, A. & Shih, H. PEG hydrogels formed by thiol-ene photo-click chemistry and their effect on the formation and recovery of insulin-secreting cell spheroids. *Biomaterials* **32,** 9685–9695 (2011).

Lindman, B. R., Bonow, R. O. & Otto, C. M. Current management of calcific aortic stenosis. *Circ. Res.* **113,** 223–37 (2013).

Liu, A. C. & Gotlieb, A. I. Characterization of cell motility in single heart valve interstitial cells in vitro. *Histol. Histopathol.* **22,** 873–82 (2007).

Liu, A. C., Joag, V. R. & Gotlieb, A. I. The emerging role of valve interstitial cell phenotypes in regulating heart valve pathobiology. *Am. J. Pathol.* **171,** 1407–18 (2007).

Liu, F. *et al.* Mechanosignaling through YAP and TAZ drives fibroblast activation and fibrosis. *Am. J. Physiol. - Lung Cell. Mol. Physiol.* **308,** L344–L357 (2015).

Lu, M. *et al.* Integrin alpha8beta1 mediates adhesion to LAP-TGFbeta1. *J. Cell Sci.* **115,** 4641–4648 (2002).

Mabry, K. M., Lawrence, R. L. & Anseth, K. S. Dynamic stiffening of poly(ethylene glycol)-based hydrogels to direct valvular interstitial cell phenotype in a three-dimensional environment. *Biomaterials* **49,** 47–56 (2015).

Mabry, K. M., Payne, S. Z. & Anseth, K. S. Microarray analyses to quantify advantages of 2D and 3D hydrogel culture systems in maintaining the native valvular interstitial cell phenotype. Submitted.

Mabry, K. M., Schroeder, M. E., Payne, S. Z. & Anseth, K. S. Three-dimensional high-throughput cell encapsulation platform to study dynamic changes to the extracellular environment. In preparation.

Mack, M. J. *et al.* 5-year outcomes of transcatheter aortic valve replacement or surgical aortic valve replacement for high surgical risk patients with aortic stenosis (PARTNER 1): a randomised controlled trial. *Lancet* **385,** 2477–2484 (2015).

Major, J. Challenges and Opportunities in high Throughput Screening: Implications for New Technologies. *J. Biomol. Screen.* **3,** 13–17 (1998).

Malkoch, M. *et al.* Synthesis of well-defined hydrogel networks using click chemistry. *Chem. Commun. (Camb).* 2774–2776 (2006). doi:10.1039/b603438a

Masters, K. S., Shah, D. N., Leinwand, L. A. & Anseth, K. S. Crosslinked hyaluronan scaffolds as a biologically active carrier for valvular interstitial cells. *Biomaterials* **26,** 2517–25 (2005).

McCall, J. D. & Anseth, K. S. Thiol-ene photopolymerizations provide a facile method to encapsulate proteins and maintain their bioactivity. *Biomacromolecules* **13,** 2410–7 (2012).

McCall, J. D., Luoma, J. E. & Anseth, K. S. Covalently tethered transforming growth factor beta in PEG hydrogels promotes chondrogenic differentiation of encapsulated human mesenchymal stem cells. *Drug Deliv. Transl. Res.* **2,** 305–312 (2012).

Meli, L. *et al.* Three dimensional cellular microarray platform for human neural stem cell differentiation and toxicology. *Stem Cell Res.* **13,** 36–47 (2014).

Merryman, W. D. & Schoen, F. J. Mechanisms of calcification in aortic valve disease: role of

mechanokinetics and mechanodynamics. *Curr. Cardiol. Rep.* **15,** 355 (2013).

Merryman, W. D. Mechano-potential etiologies of aortic valve disease. *J. Biomech.* **43,** 87–92 (2010).

Messika-Zeitoun, D. *et al.* Aortic valve calcification: determinants and progression in the population. *Arterioscler. Thromb. Vasc. Biol.* **27,** 642–8 (2007).

Mi, H. & Thomas, P. Protein Networks and Pathway Analysis. *Methods Mol. Biol.* **563,** 123–140 (2009).

Mi, H., Muruganujan, A. & Thomas, P. D. PANTHER in 2013: Modeling the evolution of gene function, and other gene attributes, in the context of phylogenetic trees. *Nucleic Acids Res.* **41,** 377–386 (2013).

Mih, J. D. *et al.* A multiwell platform for studying stiffness-dependent cell biology. *PLoS One* **6,** 1–10 (2011).

Miller, J. D. *et al.* Evidence for active regulation of pro-osteogenic signaling in advanced aortic valve disease. *Arterioscler. Thromb. Vasc. Biol.* **30,** 2482–6 (2010).

Miller, J. D. *et al.* Lowering plasma cholesterol levels halts progression of aortic valve disease in mice. *Circulation* **119,** 2693–2701 (2009).

Miller, J. D., Weiss, R. M. & Heistad, D. D. Calcific aortic valve stenosis: methods, models, and mechanisms. *Circ. Res.* **108,** 1392–412 (2011).

Miyake, K., Satomi, N. & Sasaki, S. Elastic modulus of polystyrene film from near surface to bulk measured by nanoindentation using atomic force microscopy. *Appl. Phys. Lett.* **89,** 18–21 (2006).

Moore, S. W., Roca-Cusachs, P. & Sheetz, M. P. Stretchy proteins on stretchy substrates: the important elements of integrin-mediated rigidity sensing. *Dev. Cell* **19,** 194–206 (2010).

Nakayama, Y. *et al.* In-body tissue-engineered aortic valve (Biovalve type VII) architecture based on 3D printer molding. *J. Biomed. Mater. Res. B. Appl. Biomater.* 10–12 (2014). doi:10.1002/jbm.b.33186

O'Brien, K. D. Pathogenesis of calcific aortic valve disease: a disease process comes of age (and a good deal more). *Arterioscler. Thromb. Vasc. Biol.* **26,** 1721–8 (2006).

Ochsner, M., Textor, M., Vogel, V. & Smith, M. L. Dimensionality controls cytoskeleton assembly and metabolism of fibroblast cells in response to rigidity and shape. *PLoS One* **5,** e9445 (2010).

Otto, C. M., Kuusisto, J., Reichenbach, D. D., Gown, a M. & O'Brien, K. D. Characterization of the early lesion of 'degenerative' valvular aortic stenosis. Histological and immunohistochemical

studies. *Circulation* **90,** 844–853 (1994).

Parenteau-Bareil, R., Gauvin, R. & Berthod, F. Collagen-Based Biomaterials for Tissue Engineering Applications. *Materials (Basel).* **3,** 1863–1887 (2010).

Park, C. Y. *et al.* High-throughput screening for modulators of cellular contractile force. *Integr. Biol.* (2015). doi:10.1039/C5IB00054H

Paszek, M. J. *et al.* Tensional homeostasis and the malignant phenotype. *Cancer Cell* **8,** 241–254 (2005).

Peppas, N. A., Hilt, J. Z., Khademhosseini, A. & Langer, R. Hydrogels in Biology and Medicine: From Molecular Principles to Bionanotechnology. *Adv. Mater.* **18,** 1345–1360 (2006).

Poggianti, E. *et al.* Disease of the Aortic Valve or Aorta Aortic Valve Sclerosis Is Associated With Systemic Endothelial Dysfunction. **41,** (2003).

Pontes Soares, C. *et al.* 2D and 3D-organized cardiac cells shows differences in cellular morphology, adhesion junctions, presence of myofibrils and protein expression. *PLoS One* **7,** e38147 (2012).

Quinlan, A. M. T. & Billiar, K. L. Investigating the role of substrate stiffness in the persistence of valvular interstitial cell activation. *J. Biomed. Mater. Res. Part A* **087257,** 2474–82 (2012).

Rabkin-Aikawa, E., Farber, M., Aikawa, M. & Schoen, F. J. Dynamic and reversible changes of interstitial cell phenotype during remodeling of cardiac valves. *J. Heart Valve Dis.* **13,** 841–7 (2004).

Rajamannan, N. M. *et al.* Calcific Aortic Valve Disease: Not Simply a Degenerative Process: A Review and Agenda for Research From the National Heart and Lung and Blood Institute Aortic Stenosis Working Group * Executive Summary: Calcific Aortic Valve Disease - 2011 Update. *Circulation* **124,** 1783–1791 (2011).

Rajamannan, N. M., Gersh, B. & Bonow, R. O. Calcific aortic stenosis: from bench to the bedside--emerging clinical and cellular concepts. *Heart* **89,** 801–5 (2003).

Ranga, A. *et al.* 3D niche microarrays for systems-level analyses of cell fate. *Nat. Commun.* **5,** 1–10 (2014).

Rodriguez, K. J., Piechura, L. M. & Masters, K. S. Regulation of valvular interstitial cell phenotype and function by hyaluronic acid in 2-D and 3-D culture environments. *Matrix Biol.* **30,** 70–82 (2011).

Rodriguez, K. J., Piechura, L. M., Porras, A. M. & Masters, K. S. Manipulation of valve composition to elucidate the role of collagen in aortic valve calcification. *BMC Cardiovasc. Disord.* **14,** 29 (2014).

Rosales, A. M., Mabry, K. M., Nehls, E. M. & Anseth, K. S. Photoresponsive Elastic Properties

of Azobenzene-Containing Poly(ethylene-glycol)-Based Hydrogels. *Biomacromolecules* **16**, 798-806 (2015).

Rosenhek, R. *et al.* Statins but not angiotensin-converting enzyme inhibitors delay progression of aortic stenosis. *Circulation* **110,** 1291–1295 (2004).

Ryan, D. G. Involvement of S100A4 in Stromal Fibroblasts of the Regenerating Cornea. *Invest. Ophthalmol. Vis. Sci.* **44,** 4255–4262 (2003).

Schmidt, D. *et al.* Minimally-invasive implantation of living tissue engineered heart valves: a comprehensive approach from autologous vascular cells to stem cells. *J. Am. Coll. Cardiol.* **56,** 510–20 (2010).

Schoen, F. J. Evolving concepts of cardiac valve dynamics: the continuum of development, functional structure, pathobiology, and tissue engineering. *Circulation* **118,** 1864–80 (2008).

Schoen, F. J. Mechanisms of function and disease of natural and replacement heart valves. *Annu. Rev. Pathol.* **7,** 161–83 (2012).

Schwartz, M. P. *et al.* A synthetic strategy for mimicking the extracellular matrix provides new insight about tumor cell migration. *Integr. Biol. (Camb).* **2,** 32–40 (2010).

Shafi, S. Role of ACE Inhibitors in Atherosclerosis. *Int. J. Biomed. Adv. Res.* **4,** 849–856 (2013).

Sider, K. L. *et al.* Evaluation of a porcine model of early aortic valve sclerosis. *Cardiovasc. Pathol.* **23,** 289–97 (2014).

Simmons, C. A. Aortic Valve Mechanics. An Emerging Role for the Endothelium. *J. Am. Coll. Cardiol.* **53,** 1456–1458 (2009).

Sridhar, B. V, Doyle, N. R., Randolph, M. a & Anseth, K. S. Covalently tethered TGF-β1 with encapsulated chondrocytes in a PEG hydrogel system enhances extracellular matrix production. *J. Biomed. Mater. Res. A* **102,** 4464–72 (2014).

Stephens, E. H. *et al.* Differential proteoglycan and hyaluronan distribution in calcified aortic valves. *Cardiovasc. Pathol.* **20,** 334–342 (2011).

Stewart, B. F. *et al.* Clinical Factors Associated With Calcific Aortic Valve Disease. *J. Am. Coll. Cardiol.* **29,** 630–634 (1997).

Thomas, P. S., Sridurongrit, S., Ruiz-Lozano, P. & Kaartinen, V. Deficient signaling via Alk2 (Acvr1) leads to Bicuspid aortic valve development. *PLoS One* **7,** (2012).

Tibbitt, M. W. & Anseth, K. S. Hydrogels as extracellular matrix mimics for 3D cell culture. *Biotechnol. Bioeng.* **103,** 655–63 (2009).

Tomasek, J. J., Gabbiani, G., Hinz, B., Chaponnier, C. & Brown, R. a. Myofibroblasts and mechano-regulation of connective tissue remodelling. *Nat. Rev. Mol. Cell Biol.* **3,** 349–63

(2002).

Towler, D. A. Molecular and cellular aspects of calcific aortic valve disease. *Circ. Res.* **113,** 198–208 (2013).

Tumarkin, E. *et al.* High-throughput combinatorial cell co-culture using microfluidics. *Integr. Biol. (Camb).* **3,** 653–62 (2011).

Walker, G. A., Masters, K. S., Shah, D. N., Anseth, K. S. & Leinwand, L. A. Valvular myofibroblast activation by transforming growth factor-beta: implications for pathological extracellular matrix remodeling in heart valve disease. *Circ. Res.* **95,** 253–60 (2004).

Wang, H., Haeger, S. M., Kloxin, A. M., Leinwand, L. A. & Anseth, K. S. Redirecting Valvular Myofibroblasts into Dormant Fibroblasts through Light-mediated Reduction in Substrate Modulus. *PLoS One* **7,** e39969 (2012).

Wang, H., Sridhar, B., Leinwand, L. A. & Anseth, K. S. Characterization of cell subpopulations expressing progenitor cell markers in porcine cardiac valves. *PLoS One* **8,** e69667 (2013).

Wang, H., Tibbitt, M. W., Langer, S. J., Leinwand, L. A. & Anseth, K. S. Hydrogels preserve native phenotypes of valvular fibroblasts through an elasticity-regulated PI3K/AKT pathway. *Proc. Natl. Acad. Sci.* **110,** 19336–19341 (2013).

Wei, J. *et al.* The importance of three-dimensional scaffold structure on stemness maintenance of mouse embryonic stem cells. *Biomaterials* **35,** 7724–7733 (2014).

Weind, K. L., Ellis, C. G. & Boughner, D. R. Aortic valve cusp vessel density: Relationship with tissue thickness. *J. Thorac. Cardiovasc. Surg.* **123,** 333–340 (2002).

Weiss, R. M., Miller, J. D. & Heistad, D. D. Fibrocalcific aortic valve disease: Opportunity to understand disease mechanisms using mouse models. *Circ. Res.* **113,** 209–222 (2013).

West, J. L. & Hubbell, J. a. Polymeric Biomaterials with Degradation Sites for Proteases Involved in Cell Migration. *Macromolecules* **32,** 241–244 (1999).

Wipff, P.-J., Rifkin, D. B., Meister, J.-J. & Hinz, B. Myofibroblast contraction activates latent TGF-beta1 from the extracellular matrix. *J. Cell Biol.* **179,** 1311–23 (2007).

Wirrig, E. E., Hinton, R. B. & Yutzey, K. E. Differential expression of cartilage and bone-related proteins in pediatric and adult diseased aortic valves. *J. Mol. Cell. Cardiol.* **50,** 561–569 (2011).

Witt, W., Büttner, P., Jannasch, A., Matschke, K. & Waldow, T. Reversal of myofibroblastic activation by polyunsaturated fatty acids in valvular interstitial cells from aortic valves. Role of RhoA/G-actin/MRTF signalling. *J. Mol. Cell. Cardiol.* **74,** 127–138 (2014).

Wozniak, M. a & Chen, C. S. Mechanotransduction in development: a growing role for contractility. *Nat. Rev. Mol. Cell Biol.* **10,** 34–43 (2009).

Ye, Q. *et al.* Fibrin gel as a three dimensional matrix in cardiovascular tissue engineering. *Eur. J. Cardiothorac. Surg.* **17,** 587–91 (2000).

Yip, C. Y. Y., Chen, J.-H., Zhao, R. & Simmons, C. A. Calcification by valve interstitial cells is regulated by the stiffness of the extracellular matrix. *Arterioscler. Thromb. Vasc. Biol.* **29,** 936–42 (2009).

Yu, Z., Seya, K., Daitoku, K. & Motomura, S. Tumor Necrosis Factor- alpha Accelerates the Calcification of Human Aortic Valve Interstitial Cells Obtained from Patients with Calcific Aortic Valve Stenosis via the BMP2-Dlx5. *J. Pharmacol. Exp. Ther.* **337,** 16–23 (2011).

Zhu, Y., Oganesian, A., Keene, D. R. & Sandell, L. J. Type IIA procollagen containing the cysteine-rich amino propeptide is deposited in the extracellular matrix of prechondrogenic tissue and binds to TGF-β1 and BMP-2. *J. Cell Biol.* **144,** 1069–1080 (1999).